Insulin regulates Energy Homeostasis and Hypoglycemia in the Ventromedial Hypothalamus

Inaugural–Dissertation

zur Erlangung des Doktorgrades

der Mathematisch-Naturwissenschaftlichen Fakultät

der Universität Köln

vorgelegt von

Tim Klöckener

aus Olpe

Köln 2012

Berichterstatter:	**Prof. Dr. Jens C. Brüning**
	Priv-Doz. Dr. F. Thomas Wunderlich
Tag der mündlichen Prüfung:	04.12.2012

Contents

Abbreviations **x**

Abstract **xi**

Zusammenfassung **xii**

1 Introduction **1**

1.1 Obesity 1

1.2 Regulatory Mechanism of Energy Homeostasis 2

1.3 Neuronal Circuits in the Hypothalamus controlling Energy Homeostasis . 3

1.4 The Melanocortin System 5

1.5 Leptin and Leptin Signaling 8

1.6 Leptin Resistance 11

1.7 Insulin and Insulin Signaling 14

1.8 Insulin Resistance 17

1.9 The Ventromedial Hypothalamus and Steroidogenic factor 1 20

1.10 Counter-regulatory Response to Hypoglycemia 21

1.11 Objectives 24

2 Materials and Methods **25**

2.1 Mouse experiments 25

2.1.1 Animal care 25

2.1.2 Experimental mice 25

2.1.3 Food intake and indirect calorimetry 26

2.1.4 Blood collection and determination of glucose levels 26

2.1.5 Analysis of body composition 27

2.1.6 Glucose and insulin tolerance test 27

2.1.7 Leptin sensitivity 27

2.1.8 Fertility assesment . . . 27
2.1.9 Hypoglycemic Clamp studies . . . 28
2.2 Molecular biology . . . 29
2.2.1 Isolation of genomic DNA . . . 29
2.2.2 Quantification of nucleic acids . . . 29
2.2.3 Polymerase chain reaction (PCR) . . . 29
2.2.4 RNA extraction, RT-PCR and quantitative real-time PCR . . . 31
2.3 Cell biology . . . 31
2.3.1 Histological analysis and immunohistochemistry . . . 31
2.3.2 Analysis of PiP_3 accumulation *in situ* . . . 33
2.3.3 Combined *in situ* hybridization and immunohistochemistry . . . 34
2.3.4 Electrophysiology . . . 35
2.3.5 Electron microscopy . . . 35
2.4 Biochemistry . . . 37
2.4.1 Protein extraction . . . 37
2.4.2 Western blot analysis . . . 37
2.4.3 Enzyme-linked immunosorbent assays (ELISA) . . . 38
2.5 Computer analysis . . . 38
2.5.1 Densitometrical analysis . . . 38
2.5.2 Statistical methods . . . 39
2.6 Chemicals and biological material . . . 39

3 Results **42**

3.1 Generation of SF-1 specific insulin receptor knockout mice . . . 42
3.2 Insulin silences VMH SF-1 neurons via K_{ATP} channels . . . 49
3.3 Insulin and leptin responsive SF-1 neurons are distinct sub-populations . . . 50
3.4 Attenuated obesity in SF-$1^{\Delta IR}$ mice upon high-fat diet feeding . . . 52
3.5 Reduced food intake as consequence of increased leptin sensitivity in young SF-$1^{\Delta IR}$ mice . . . 54
3.6 Improved glucose metabolism in SF-$1^{\Delta IR}$ mice upon HFD-feeding . . . 56
3.7 Increased PiP_3 formation in the VMH promotes weight gain . . . 58

3.8 Increased firing frequency of POMC neurons in SF-1$^{\Delta IR}$ males under HFD conditions 62
3.9 Counterregulatory response to hypoglycemia 66

4 Discussion **69**
4.1 Successful generation of SF-1 cell specific insulin receptor knockout mice . 71
4.2 Insulin electrically inhibits SF-1 neurons via K_{ATP} channels 73
4.3 Attenuation of obesity upon SF-1 specific IR deficiency 74
4.4 Improved glucose metabolism in SF-1$^{\Delta IR}$ males on HFD 76
4.5 PiP_3 formation in SF-1 VMH neurons promotes obesity 76
4.6 Unaltered expression of hypothalamic neuropeptides, but increased activity of POMC neurons 78
4.7 Impaired counter-regulatory response to hypoglycemia in SF-1$^{\Delta IR}$ animals 82
4.8 Perspectives 84

List of Figures **87**

List of Tables **88**

Bibliography **89**

Danksagung **120**

Erklärung **121**

Teilpublikationen **122**

Curriculum Vitae **123**

Abbreviations

°C	degree celcius
3′	three prime end of DNA sequence
5′	five prime end of DNA sequence
A	adenosine
aCSF	artificial cerebrospinal fluid
AgRP	agouti-related protein
AKT	protein kinase B
ARC	arcuate nucleus
ATP	adenosine triphosphate
Avertin	tribromoethyl alcohol and *tert*-amyl alcohol
BAT	brown adipose tissue
BMI	body mass index
bp	base pairs
C	cytosine
$CaCl_2$	calcium cloride
cAMP	cyclic adenosine mono-phosphate
cDNA	complementary DNA
CNS	central nervous system
Cre	bacteriophage P1 derived site-specific recombinase (causes recombination)
Da	Dalton
DAPI	4,6-diamidino-2-phenylindole
ddH_2O	double distilled water
DMH	dorsomedial hypothalamic nucleus
DMSO	dimethylsulfoxide

DNA	desoxyribonucleic acid
dNTP	desoxyribonucleotide-triphosphate
e.g.	*exempli gratia*
ECL	enhanced chemoluminiscence
EDTA	ethylendiamine tetraacetate
EGTA	ethylene glycol tetraacetic acid
EIA	enzyme immunoassay
ELISA	enzyme-linked immunosorbent assay
EtBr	ethidium bromide
EtOH	ethanol
fl	loxP flanked
FOXO1	forkhead-O transcription factor 1
g	gram
G	guanine
GABA	γ-aminobutyric acid
GDP	guanosine bisphosphate
GFP	green fluorescent protein
GLUT2	glucose transporter 2
GLUT4	glucose transporter 4
Grb2	growth factor receptor binding protein 2
GTP	guanosine triphosphate
GTT	glucose tolerance test
Gusb	glucuronidase beta
h	hour
H&E	hematoxylin/eosin
H_2O_2	hydrogen peroxide
HCl	hydrochloric acid
HEPES	N-2-hydroxyethylpiperazine-N-2-ethansulfonic acid

HFD	high fat diet
Hprt-1	hypoxanthine guanine phosphoribosyl transferase 1
Hz	Hertz
i.e.	*id est*
icv	intracerebroventricular
IL	interleukin
i.p.	intraperitoneal
IR	insulin receptor
IRES	internal ribosomal entry site
IRS	insulin receptor substrate
ITT	insulin tolerance test
JAK	janus kinase
k	kilo
KCl	potassium chloride
KOH	potassium hydroxide
l	liter
lacZ	gene encoding β-galactosidase
lepR-b	leptin receptor isoform b
LH	lateral hypothalamic nucleus
loxP	recognition site for Cre (locus of x-ing over phage P1)
m	milli
M	molar
MAPK	mitogen-activated protein kinase
MC4R	melanocortin 4 receptor
MCH	melanocyte conentrating hormone
ME	median eminence
$MgCl_2$	magnesium chloride
min	minute

mRNA	messenger RNA
α-MSH	alpha melanocyte-stimulating hormone
Na_2HPO_4	disodium hydrogen phosphate
NaCl	sodium chloride
NaF	sodium fluoride
NAH_2PO_4	monosodium phosphate
$NaHCO_3$	sodium bicarbonate
NaOH	sodium hydroxide
NCD	normal chow diet
NIRKO	neuronal insulin receptor knockout mice
NMR	nuclear magnetic resonance
NPY	neuropeptide Y
ORX	orexin / hypocretin
p-	phospho-
PAGE	polyacrylamide gel electrophoresis
PBS	phosphate buffered saline
PCR	polymerase chain reaction
PDK1	phosphoinositide-dependent protein kinase 1
PFA	paraformaldehyde
PH	pleckstrin homology
PI_3K	phosphoinositide 3-kinase
PiP_2	phosphatidylinositol-(4,5)-bisphosphate
PiP_3	phosphatidylinositol-(3,4,5)-triphosphate
POMC	proopiomelanocortin
PTB	phosphotyrosine binding
PTB1B	protein tyrosine phosphatase 1 B
PTEN	phosphatase and tensin homolog
PVN	paraventricular nucleus

RNA	ribonucleic acid
RNase	ribonuclease
RT	room temperature
rtPCR	reverse transcription polymerase chain reaction
SDS	sodiumdodecylsulfate
sec	second
SEM	standard error of the mean
SH	src homology
SOCS	suppressor of cytokine signaling
STAT	signal transducer and activator of transcription
T2DM	type 2 diabetes mellitus
TAE	tris-acetic acid-EDTA buffer
TE	tris-EDTA buffer
Tris	2-amino-2-(hydroxymethyl)-1,3-propandiole
TWEEN	polyoxethylene-sorbitan-monolaureate
tyr	tyrosine
U	units
V	volt
v/v	volume per volume
VCO_2	volume of produced carbondioxide
VMH	ventromedial nucleus of the hypothalamus
VO_2	volume of consumed oxygen
w/v	weight per volume
WAT	white adipose tissue
WHO	world health organization
x-gal	5-bromo-4-chloro-indolyl-β-D-galactopyranoside
β-gal	β-galactodidase
β-me	β-mercaptoethanol

Abstract

Growing evidence from the last decades intimately links obesity with insulin resistance and type 2 diabetes mellitus as a consequence. Thus, the role of the central nervous system and especially the hypothalamus in the control of energy homeostasis are intensively investigated. The melanocortin system has been identified as a pivotal neurocircuit in this homeostatic process, but many other neuronal populations are similarly involved. Furthermore, the role of insulin as adiposity signal in the control of energy homeostasis has to be further clarified. In particular, steroidogenic factor 1 (SF-1)-expressing neurons of the ventromedial hypothalamus (VMH) control energy homeostasis, but the role of insulin action in these cells remains undefined. This study shows that insulin activates phosphatidylinositol-3-kinase (PI_3K) signaling in SF-1 neurons and reduces firing frequency in these cells by the activation of ATP-dependent potassium (K_{ATP}) channels. These effects were abrogated in mice with Cre-mediated insulin receptor deficiency restricted to SF-1 neurons (SF-$1^{\Delta IR}$ mice). Whereas body weight and glucose homeostasis remained the same in SF-$1^{\Delta IR}$ mice as in controls on a normal chow diet, they were protected from diet-induced leptin resistance, weight gain, adiposity and impaired glucose tolerance. High-fat feeding activated PI_3K signaling in SF-1 neurons of control mice, and this response was attenuated in the VMH of SF-$1^{\Delta IR}$ mice. Mimicking diet-induced overactivation of PI_3K signaling by disruption of the phosphatidylinositol-3,4,5-trisphosphate phosphatase PTEN led to increased body weight and hyperphagia under normal chow diet conditions. Collectively, this study reveals that high-fat diet–induced, insulin-dependent PI_3K activation in VMH neurons contributes to obesity development.

Additionally, insulin was identified as a necessary signal in SF-1 VMH neurons involved in the induction of the counter-regulatory response to hypoglycemia, one of the major limitations for insulin treatment in diabetic patients.

Zusammenfassung

Zunehmende Erkenntnisse der letzten Jahrzehnte konnten zeigen, dass Übergewicht und Insulin Resistenz, mit Typ 2 Diabetes Mellitus als Folge, stark assoziierte Zustände sind. Deshalb werden die Rolle des zentralen Nervensystems und speziell des Hypothalamus in der Kontrolle der Energie Homöostase intensiv erforscht. Das Melanokortin System innerhalb des Hypothalamus wurde als zentrales neuronales Netzwerk für diesen homöostatischen Prozess identifiziert. Die Effekte von Insulin als Sättigungssignal innerhalb des Gehirns waren ebenfalls Gegenstand der Forschung der letzten Jahre. Des weiteren wurden Steroidogenic Factor 1 (SF-1) exprimierende Neuronen innerhalb des ventromedialen Hypothalamus (VMH) als beteiligte Neuronenpopulation in der Kontrolle der Energie Homöostase identifiziert, jedoch wurde die Rolle des Insulinsignalwegs in diesen Zellen bisher noch nicht erforscht. Die vorliegende Arbeit konnte zeigen, dass Insulin in SF-1 Neuronen den Phosphatidylinositol-3-kinase (PI_3K) Signalweg stimuliert und damit die Aktivität dieser Neurone durch das Steuern von ATP-abhängigen Kalium (K_{ATP}) Kanälen herabsetzt. Dieser Effekt war in Mäusen denen der Insulinzezeptor in SF-1 exprimierenden Neuronen fehlt (SF-$1^{\Delta IR}$) nicht mehr vorhanden. Diese Defizienz hatte unter normalen Fütterungsbedingungen keine Auswirkungen, wurden die Mäuse jedoch mit einer fettreichen Diät gefüttert, waren SF-$1^{\Delta IR}$ Tiere zum Teil vor Ernährungsbedingter Gewichtszunahme, Leptinresistenz, Fettleibigkeit und Glukoseintoleranz geschützt. Die Deletion der PI_3K-spezifischen Phosphatidylinositol-3,4,5-trisphosphate Phosphatase PTEN dagegen führte zu Übergewicht und Hyperphagie unter Normal-Futter Bedingungen, da die durch fettreiche Ernährung bedingte Überaktivierung der PI_3K imitiert wird. Zusammenfassend konnte wurde gezeigt, dass die ernährungs-bedingte Überaktivierung der PI_3K in VMH SF-1 Neuronen zur Entwicklung von Übergewicht beiträgt.

Des Weiteren konnte gezeigt werden, dass der Insulinsignalweg in SF-1 Neuronen für die Aktivierung der Leber-spezifischen Glukoneogenese zur Verhinderung von Hypoglykämie, welches eine der Hauptkomplikationen der Insulintherapie darstellt, notwendig ist.

1 Introduction

1.1 Obesity

Energy homeostasis in the body is a tightly regulated process. In order to maintain an adequate body weight, energy intake and energy expenditure are kept in balance. Obesity, in contrast, is the consequence of a sustained positive energy balance. That means to consume more calories than an organism is spending, resulting in excessive storage of lipids in the expanded adipose tissue.

From an evolutionary perspective, obesity is actually a favorable condition. To store energy in the form of adipose tissue in good and plentiful times in order to survive periods of deprivation or starvation has almost exclusively benefits for the organism. Especially for seasonal active animals these energy depots are mandatory and the only way to survive the winter or other deprivation periods.

Also for humans these facts hold true, but the living conditions have changed dramatically in the last centuries. The availability of food has increased due to the industrial revolution and the globalization of our society, resulting in the disappearance of food deprivation (at least in the highly developed countries). Additionally, the energy density of the available food has increased massively over the last decades. In the 1970s in the USA, the average caloric intake per day was 2234 calories. Until 2003 it has raised to 2757 calories per day, an increase of almost 25 percent (Hodan & Buzby, 2005).

Besides, a more sedentary lifestyle in western societies with reduced physical work further contributes to a positive energy balance. As a net effect of the above mentioned factors, the average body mass index (BMI) in Europe and the USA has increased over the last 40 years, resulting in an obesity rate of 40 percent (defined by a BMI of above 30) in the USA and more than 30 percent in Europe (Berghöfer *et al.* , 2008). Worldwide, the total number has risen to 1.4 billion overweight (defined as a BMI above 25) and 200 million obese people (WHO, 2012). This sustained obesity is associated with a risk to develop severe metabolic disorders, such as Type 2 Diabetes Mellitus (T2DM) and cardiovascular

diseases, and it also pre-disposes for other diseases such as cancer, osteoarthritis, non-alcoholic fatty liver disease and obstructive sleep apnea (Dixon, 2010; Mokdad *et al.* , 2003). The overall health costs caused by obesity-associated disorders already exceeded 10 billion € in 2008 and the World Health Organization estimates that every year 2.8 million adults die as a consequence of being obese or overweight (WHO, 2012). Thus, obesity is already considered a pandemic of the 21st century and is a major health burden in the western civilizations.

1.2 Regulatory Mechanism of Energy Homeostasis

In a healthy subject the caloric intake is adjusted and adapted to the amount of used energy and the current storage status of the body. Vice versa, the expended energy is also adapted to the food availability and nutrient status, assuming a regulatory signal from the body, that reflects its energy status to the brain. This has been proposed more than 40 years ago (Coleman, 1973; Coleman & Hummel, 1969), and research in the last decades verified this hypothesis by the discovery of several peripheral hormones involved in this regulatory process (Bataille *et al.* , 1981; Brüning *et al.* , 2000; Kojima *et al.* , 1999; Lacquaniti *et al.* , 2011; Orskov *et al.* , 1994; Tatemoto & Mutt, 1980; Zhang *et al.* , 1994).

One of the major regulators in this homeostatic process is the anorectic hormone leptin. It is mainly produced by adipocytes in the white adipose tissue (Margetic *et al.* , 2002). This hormone reflects the amount of stored energy in the form of fat to the brain, which then integrates this information and adjusts food consumption and energy expenditure to the current needs (Friedman, 1998). However, due to the beforehand mentioned changes in modern lifestyle, in millions of humans these regulatory mechanism fail, resulting in overweight and finally in chronic obesity (Considine *et al.* , 1996).

Upon its discovery, leptin was assumed to be the ultimate cure for obesity (Campfield *et al.* , 1996). But just a few years later the disillusioning discovery was made that obese patients actually have massively increased circulating leptin levels compared to lean patients (Considine *et al.* , 1996), indicating that these obese subjects are leptin resistant (Heymsfield *et al.* , 1999). Thus, except for a very few people carrying a mutation in their endogenous *Leptin* gene, leptin alone is not suitable as therapeutic treatment for obese

humans (Farooqi & O'Rahilly, 2004). But in combination with other peptide hormones, such as Amylin, it is possible to restore leptin sensitivity and hence enable a leptin mediated weight loss (Roth *et al.* , 2008). Although leptin resistance was discovered more than a decade ago, it is still unclear which exact mechanisms or signaling pathways lead to the development of leptin resistance. It has become obvious that both the transport across the blood-brain barrier (BBB) to the brain and the intracellular signaling are impaired (El-Haschimi *et al.* , 2000).

In addition to leptin, various other hormones are involved in this regulatory process, such as insulin and ghrelin. The pancreatic hormone insulin exerts many of its effects in the periphery, but also induces satiety when applied to the central nervous system (CNS) (Blüher *et al.* , 2002; Brüning *et al.* , 1998; Michael *et al.* , 2000; Woods *et al.* , 1979). Furthermore, insulin signaling in the brain plays a crucial role in maintaining energy homeostasis as well as reproduction (Brüning *et al.* , 2000; Hallschmid *et al.* , 2004; Havrankova *et al.* , 1978b; Porte & Woods, 1981; Woods *et al.* , 1979). The best characterized hormone stimulating food intake is ghrelin. It is mainly produced by the stomach and the gut upon nutrient deprivation and likewise signals to the brain, leading to an increase in food intake (Kojima *et al.* , 1999).

Eventually, it is the brain that orchestrates all these different hormonal signals and furthermore draws the appropriate conclusions to adjust feeding and energy expenditure to the current needs.

1.3 Neuronal Circuits in the Hypothalamus controlling Energy Homeostasis

In the beginning of the twentieth century, obesity, as a feature of certain clinical symptoms, was discussed to result from either defects in the pituitary gland or in the CNS, particularly the hypothalamus. The Fröhlich syndrome, a pituitary tumor, was a disease pattern associated with obesity and hypogonadism, that pointed towards the pituitary gland as main regulator of energy homeostasis (Fröhlich, 1901). The experiments of Hetherington and Ranson finally ended this debate when they electrolytically lesioned the hypothalamus of rats stereotactically without affecting the pituitary gland, resulting in

morbidly obese animals (Hetherington & Ranson, 1940). These findings were further defined by other groups in the following decades, using refined lesioning techniques for their experiments. The Ventromedial Nucleus of the Hypothalamus (VMH) was specified as a satiety center, together with the Paraventricular Nucleus (PVN) (Gold, 1973; Stevenson *et al.* , 1950). The VMH-derived signals were believed to be transmitted via the abdominal vagus nerve by sympathetic and parasympathetic innervations to the intestinal tract, verified by the lesioning of the VMH with a simultaneous vagotomy of the abdominal vagus nerve below the diaphragm. The subdiaphragmal vagotomy prevented the effects of the VMH lesioning and the rats stayed lean and normophagic (Inoue & Bray, 1977; Opsahl & Powley, 1974). In contrast, lesions in the Lateral Hypothalamus (LH) led to hypophagia (Anand & Brobeck, 1951).

The role of the LH as feeding center was refined by lesion experiments with kainic acid, but the exact role of certain neuronal populations remained elusive until the 1990s (Grossman *et al.* , 1978; Stricker *et al.* , 1978). With the discovery of the LH specific hormones orexin (ORX) and melanocyte concentrating hormone (MCH), the first neuropeptides were identified that increased their mRNA levels upon fasting (Bittencourt *et al.* , 1992; de Lecea *et al.* , 1998; Sakurai *et al.* , 1998). Injection of these peptides into the brain induced food intake and a knockout of MCH resulted in lean mice when compared to controls, hence establishing the LH as phagic center in the hypothalamus (Qu *et al.* , 1996; Sakurai *et al.* , 1998).

As mentioned earlier, the PVN, the VMH and the adjacent arcuate nucleus (ARC) were defined as possible satiety centers. By systemic injections of toxic glucose analogs, the ARC and the VMH were destroyed, resulting in hyperphagic and obese animals (Debons *et al.* , 1962; Olney & Sharpe, 1969). Due to their location at the median eminence (ME), which serves as the "window" of the BBB that can be passed by larger proteins (Broadwell & Brightman, 1976), neurons in these areas are able to sense hormones and nutrients from the periphery. Furthermore, the ARC and the VMH are in direct proximity of the third ventricle, which exposes them to neuropeptides from the cerebrospinal fluid. The discovery of leptin brought further insights into the hypothalamic regulation of energy homeostasis, as intensive c-Fos immunoreactivity could be observed in the ARC after a

peripheral injection of leptin (Elmquist *et al.* , 1997, 1998b; Van Dijk *et al.* , 1996; Woods & Stock, 1996). Together with the targeted deletion of the melanocortin 4 receptor (MC4R), the discovery of mutations in the MC4R in obese patients, the identification of its ligand α-melanocyte stimulating hormone (α-MSH) and its antagonist agouti-related peptide (AgRP) the ARC was established as primary center in the CNS-mediated regulation of energy homeostasis (Fan *et al.* , 1997; Huszar *et al.* , 1997; Vaisse *et al.* , 1998).

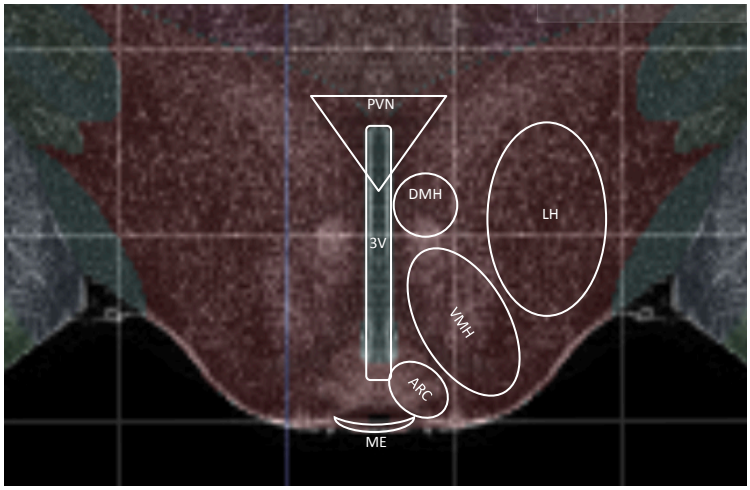

Figure 1.1: Schematic overview of hypothalamic nuclei.
Image taken from Allen mouse brain atlas (Allen institute for brain science, Seattle, USA). Depicted are hypothalamic nuclei that are involved in the regulation of food intake, energy expenditure and substrate utilization. 3V, third ventricle; ARC, arcuate nucleus; DMH, dorsomedial hypothalamic nucleus; LH, lateral hypothalamus; ME, median eminence; PVN, paraventricular nucleus; VMH, ventromedial nucleus of the hypothalamus.

1.4 The Melanocortin System

The melanocortin system is a neurocircuitry that regulates energy balance. Of great importance are neurons that are located in the ARC of the mediobasal hypothalamus (Fan *et al.* , 1997). This region shows a high expression of receptors for various hormones including leptin and insulin and lies in the direct proximity of the third ventricle and the

median eminence, hence exposing it to signals from the cerebrospinal fluid (CSF) and the circulation (Baskin *et al.* , 1993; Broadwell & Brightman, 1976; Elmquist *et al.* , 1998a; Mercer *et al.* , 1996a,b; Obici *et al.* , 2002b; Wang *et al.* , 2002). Access to the latter one is of critical importance for the aforementioned signals from the periphery. Two functionally opposing neuronal populations are located in the ARC, which are the catabolic anorexigenic Pro-opiomelanocortin (POMC) expressing neurons and the anabolic orexigenic Agouti-related Peptide (AgRP) expressing neurons (for review see Butler (2006)). These two neuronal populations are first order neurons. They are able to sense hormones such as leptin, insulin and ghrelin, but are also sensitive to changes in the level of blood glucose and other metabolites and process these signals to other brain areas, leading to an adaptation of thermoregulation, feeding and energy expenditure (Belgardt *et al.* , 2008; Cowley *et al.* , 2001, 2003; Hill *et al.* , 2010; Kim *et al.* , 2000c; Mounien *et al.* , 2010; Nakazato *et al.* , 2001).

POMC is translated as a precursor peptide, which gets cleaved in several steps by cell type-specific pro-hormone convertases into the biologically active alpha-Melanocyte Stimulating Hormone (α-MSH) and other neuropeptides (β-endorphin, β-MSH, γ-MSH and ACTH) (Coll *et al.* , 2004; Millington, 2006). α-MSH can bind to MC4Rs, which are G-protein coupled receptors, and thereby activate the adenylate cyclase, leading to an increase of intracellular cyclic Adenosine Mono-Phosphate (cAMP) (Caruso *et al.* , 2012). The release of α-MSH into the target areas of POMC neurons, such as the paraventricular nucleus (PVN), and the binding to MC4Rs leads to a decreased food intake and an increased energy expenditure (Giraudo *et al.* , 1998; Kim *et al.* , 2000a,b; Wirth *et al.* , 2001). Although the further downstream mechanisms are still under investigation, most likely thyrotropin releasing hormone (TRH) and corticotropin releasing hormone (CRH) producing neurons in the PVN and in the dorsomedial hypothalamus (DMH) play a role in the signal processing and further signal transduction (Kublaoui *et al.* , 2006; Lu *et al.* , 2003; Sarkar *et al.* , 2002). These are brain areas in the direct proximity of the ARC, show a high expression of MC4Rs and have been shown to be projection sites of POMC neurons (Kim *et al.* , 2000a,b). Furthermore, mutations of the MC4R or POMC in humans is highly associated with the development of morbid obesity, highlighting the pivotal role

of POMC neurons and MC4Rs in the regulation of energy homeostasis (Coll *et al.* , 2004; Farooqi *et al.* , 2000; Yeo *et al.* , 1998).

The opposing neuron populations in the ARC are the orexigenic AgRP expressing neurons, that co-express neuropeptide Y (NPY). They inhibit POMC neurons in two different ways. On the one hand, by a direct inhibition of POMC neuron firing activity via inhibitory GABAergic projections on POMC neurons, and on the other hand by an inhibition of MC4Rs on their target neurons by the release of AgRP, which acts as a MC4R antagonist (Aponte *et al.* , 2011; Atasoy *et al.* , 2012; Kim *et al.* , 2000b; Tang-Christensen *et al.* , 2004). The latter mechanism seems to be the more important one, since a mutation in the *agouti* gene, that results in an overexpression, leads to hyperphagic and obese mice (A^y) (Ollmann, 1997). Latest electrophysiological and optogenetics experiments confirmed these findings (Atasoy *et al.* , 2012). In contrast, NPY is expressed abundantly in the brain. It is a potent stimulator of feeding, but its action does not seem to be limited to the ARC and the melanocortin system (Sahu *et al.* , 1988; Stanley *et al.* , 1986).

The important role of POMC and AgRP neurons in the regulation of energy homeostasis has been demonstrated by ablation experiments, where mice, carrying a transgenic Diphtheria Toxin A (DTA)-receptor exclusively on AgRP or POMC neurons, were injected with DTA to ablate these neurons. AgRP neuron ablated mice reduced their food intake dramatically, leading eventually to death by starvation if not rescued by force-feeding (Luquet *et al.* , 2005). In contrast, ablation of POMC neurons results in hyperphagia (Gropp *et al.* , 2005). Other experiments could show that AgRP neurons influence locomotor behavior, e.g. by a constant activation of the Stat3 signaling pathway in AgRP neurons of mice. These mice were leaner due to an increased locomotor activity in the night phase (Mesaros *et al.* , 2008).

Besides the mere physiological effects on feeding and locomotor behavior, recent evidence suggests that the melanocortin system is also connected to higher brain functions, such as reward and addiction related behavior by direct and indirect connections to dopaminergic neurons in the midbrain (Dietrich *et al.* , 2012).

Collectively, the melanocortin system has a pivotal role in the regulation of energy

homeostasis, although higher brain functions, especially in humans, might be able to overrule these signals (figure 1.2).

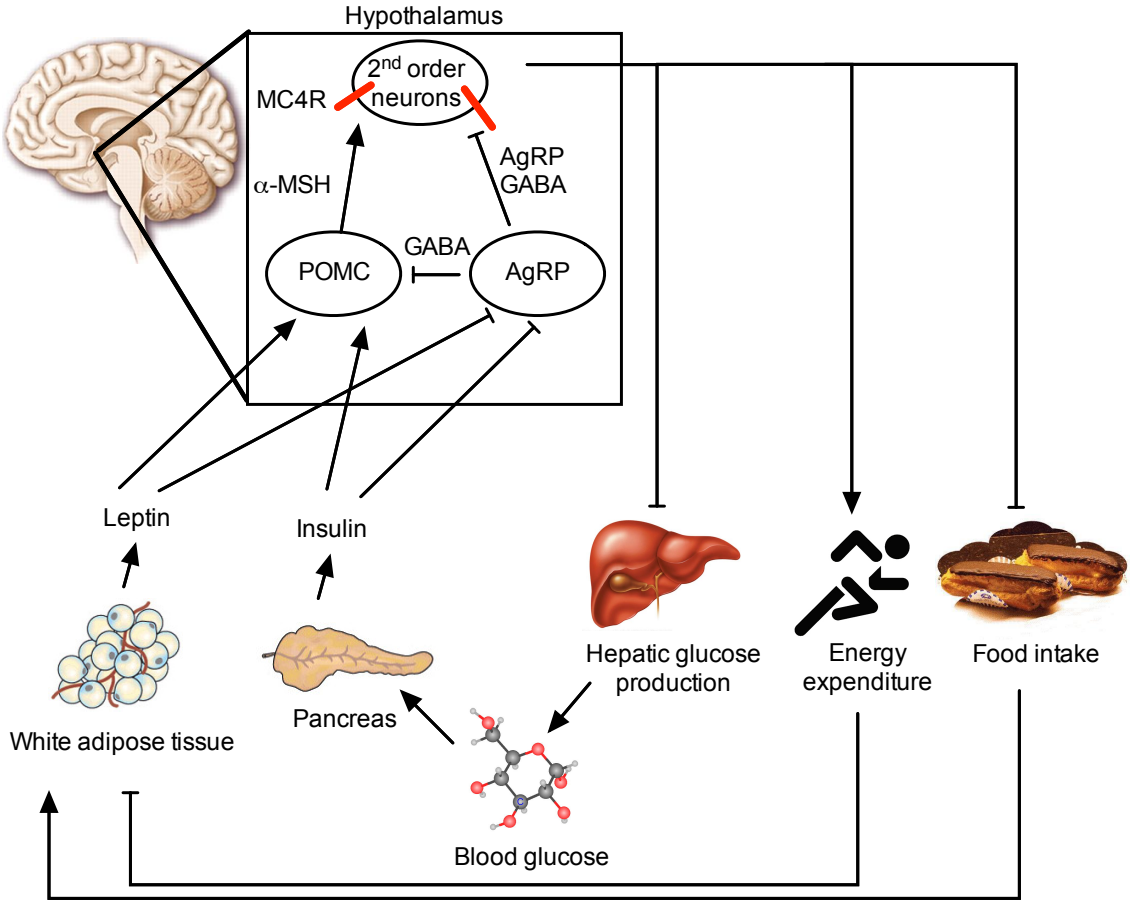

Figure 1.2: Schematic overview of the hypothalamic melanocortin system.
Adiposity signals, such as leptin and insulin are secreted in the periphery and transported across the BBB to first order neurons in the hypothalamus, anorexigenic POMC and orexigenic AgRP neurons. Both insulin and leptin on the one hand increase POMC transcription and firing rate of POMC neurons and on the other hand inhibit AgRP transcription and activity of these neurons. POMC neurons release their neurotransmitter α-MSH, that binds to MC4R on second order neurons (e.g. in the PVN), and thereby stimulates energy expenditure and inhibits food intake and hepatic glucose production. AgRP inhibits POMC neurons in two ways: by direct inhibition of POMC neurons via GABAergic synapses and by GABA and AgRP, a MC4R antagonist, release to second order neurons, leading to increased food intake, elevated hepatic glucose production and reduced energy expenditure.
α-MSH, alpha-melanocyte stimulating hormone; AgRP, agouti-related peptide;
GABA, γ-aminobutyric acid; MC4R, melanocortin 4 receptor; POMC, pro-opiomelanocortin.

1.5 Leptin and Leptin Signaling

Leptin is a 16 kDa peptide hormone, mainly produced in the adipose tissue of mammals and secreted into the circulation in proportion to the body fat content (Frederich *et al.* ,

1995; Maffei *et al.* , 1995). Minimal expression was also reported in the placenta, skeletal muscle, pancreas and some areas of the brain (Bado *et al.* , 1998; Masuzaki *et al.* , 1997).

It was discovered and cloned in 1994 as product of the *obese* gene (Zhang *et al.* , 1994). A homozygous mutation in the *obese* gene leads to severe and morbid obesity amongst the affected animals (Ingalls *et al.* , 1950). In parabiosis experiments, researchers were able to curtail the mutation to a circulating hormone (Coleman, 1973; Coleman & Hummel, 1969; Harris, 1999). When an *ob/ob* mouse was parabiosed to a wildtype mouse, the *ob/ob* mouse lost weight and eventually became lean as the wildtype mouse. The positional cloning led to the discovery of the affected gene and its product leptin (greek: *leptos* = lean) (Zhang *et al.* , 1994).

Leptin signals via its receptor, the leptin receptor (LepR), which belongs to the family of class I cytokine receptors (Chua *et al.* , 1997). As with its ligand, the LepR was also discovered by a spontaneous mutation in mice (Chen *et al.* , 1996; Tartaglia *et al.* , 1995). Mice carrying the mutation were severely diabetic and obese, thus the gene was named *diabetes*. When *db/db* mice were parabiosed to wildtype mice, the wildtype mice starved to death due to the high circulating leptin concentrations derived from the massive amount of adipose tissue in the *db/db* mouse (Coleman, 1973; Coleman & Hummel, 1969; Harris, 1999).

LepRs exist in different isoforms produced by alternative mRNA splicing, but only its long form (LepRb) is able to induce an intracellular signaling cascade (Chen *et al.* , 1996; Chua *et al.* , 1997; Tartaglia, 1997; Tartaglia *et al.* , 1995). As shown in a transgenic complementation experiment, only the LepRb is able to rescue the phenotype of the *db/db* mouse (Kowalski *et al.* , 2001). The role of the other isoforms is still under debate, but they might play a role in the saturable transport across the BBB or in the clearance of leptin from the circulation as soluble receptors (Hileman *et al.* , 2002; Uotani *et al.* , 1999).

When leptin binds to the LepRb, it induces an intracellular signaling cascade via the JAK-STAT pathway (figure 1.3). Upon ligand binding, the receptor associated Janus Kinase (JAK) 2 auto-phosphorylates itself and also phosphorylates the intracellular domain of the receptor at multiple tyrosine residues (p-Tyr), which serve as binding sites for signal transducer and activator of transcription (STAT) proteins (in case of leptin: STAT3)

(Tartaglia, 1997; White *et al.* , 1997). The STAT proteins are thereby phosphorylated, leading to their homo-dimerization, the exposure of a nuclear-localization domain and consequently to the nuclear import, where STAT proteins can bind to the promotor of various genes and exert their function (either repression or activation of transcription) (Banks *et al.* , 2000; Boulton *et al.* , 1995; Lütticken *et al.* , 1994; Stahl & Yancopoulos, 1994). In POMC neurons, leptin induced binding of STAT3 to the promotor of POMC is necessary to activate transcription of the POMC gene and the deletion of STAT3 in POMC neurons results in modest obesity and reduced POMC expression levels (Gao *et al.* , 2004; Xu *et al.* , 2007).

Leptin exerts most, but not all, of its functions in the brain. The deletion of LepRs in the brain leads to severe obesity, but does not reflect the complete phenotype of *ob/ob* or *db/db* mice (Cohen *et al.* , 2001). The transgenic re-expression of LepRb in the brain is sufficient, though, to partially or completely restore fat mass, food intake, reproductivity and glucose tolerance in *db/db* mice, depending on the promotor that was used for the transgene (de Luca *et al.* , 2005; Kowalski *et al.* , 2001). Together with the discovery of the melanocortin system, POMC and AgRP neurons were thought to be the main target for leptin, due to their role as first order neurons. But the deletion of the LepR in POMC neurons resulted only in modest obesity (Balthasar *et al.* , 2004), and the same holds true for the AgRP neuron specific LeprR deficiency (van de Wall *et al.* , 2008). Hence, there must be other neuronal populations that mediate leptin's effect on food intake and energy expenditure, e.g. neurotensin expressing neurons in the LH and dopaminergic neurons in the ventral tegmental area (VTA) (Domingos *et al.* , 2011; Leinninger *et al.* , 2011).

Another gene that is regulated by leptin induced STAT3 signaling is the suppressor of cytokine signaling (SOCS)-3. Its transcription is also induced by the binding of STAT3 to its promotor, but it acts as a negative regulator of JAK-STAT signaling by a competitive binding to the phosphorylated tyrosine residues of JAK2 (Bjorbaek *et al.* , 1998; Endo *et al.* , 1997; Howard *et al.* , 2004). Thus, haploinsufficiency for SOCS-3 or the deletion of SOCS-3 in POMC neurons results in enhanced leptin sensitivity, whereas the overexpression and constitutive activation of STAT3 leads to a constant increase in SOCS-3 expression

and consequently to impaired leptin signaling (Ernst *et al.* , 2009; Howard *et al.* , 2004; Kievit *et al.* , 2006; Munzberg *et al.* , 2004).

In contrast to its action in anorexigenic POMC neurons, leptin signaling in AgRP neurons inhibits the transcription of *AgRP* mRNA but a lack of LepRs in AgRP neurons does not induce any changes in body weight and other metabolic parameters (Mizuno & Mobbs, 1999; Van De Wall *et al.* , 2008).

Leptin binding to its receptor is also able to induce other signaling cascades. Activated JAK2 is also able to phosphorylate insulin receptor substrate (IRS) proteins and therefore induce the PI_3K pathway (Hill *et al.* , 2008; Metlakunta *et al.* , 2011; Xu *et al.* , 2005).

Besides changes on the transcriptional level, leptin is able to induce changes in the electrophysiological activity of neurons via non-specific cation-channels (Cowley *et al.* , 2001). However, this seems to be restricted to specific neuron populations, e.g. the POMC expressing neurons, but also neurons in the VMH (Dhillon *et al.* , 2006).

Taken together, leptin signaling in the brain is mandatory for the maintenance of energy homeostasis, although the exact neuronal populations for leptin's anorectic action still need to be further defined.

1.6 Leptin Resistance

As mentioned before, leptin's ability to reduce food intake and stimulate energy expenditure is heavily impaired in obese subjects (Enriori *et al.* , 2007). Although obese rodents and humans display massively elevated leptin levels in the bloodstream, leptin is not able to induce an intracellular signaling cascade and hence fails to prevent further intake of calories or to induce energy expenditure (Heymsfield *et al.* , 1999). The molecular basis for the development of leptin resistance is still under investigation, but one important factor seems to be the negative regulator of leptin signaling, SOCS-3. Leptin induces the expression of SOCS-3 as a negative feedback loop (Endo *et al.* , 1997; Naka *et al.* , 1997). As demonstrated by Ernst and colleagues, constant activation of STAT3 in POMC neurons leads to a massive increase in SOCS-3 mRNA levels, resulting in impaired leptin signaling in the affected neurons (Ernst *et al.* , 2009). The deletion or knockdown of SOCS-3 and haploinsufficiency results in lean mice, that are resistant to diet-induced obe-

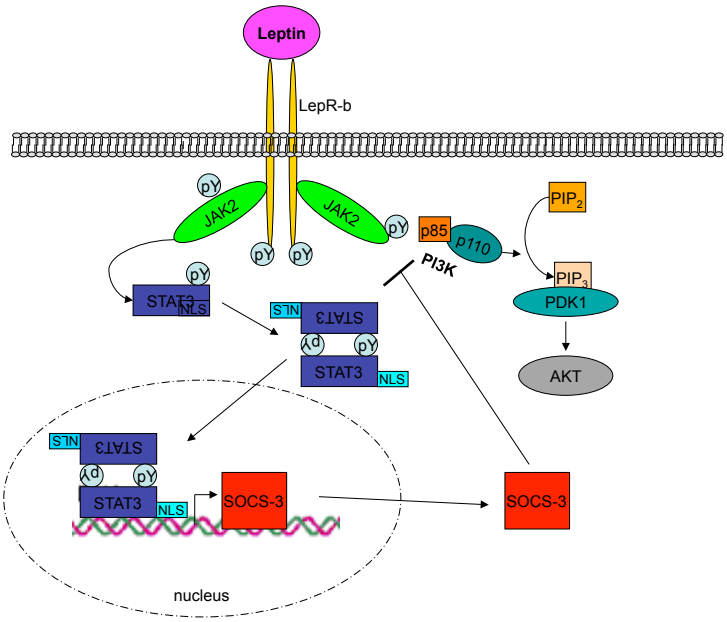

Figure 1.3: Leptin signaling pathway.
Upon leptin binding to LepRb, the associated JAK2 auto-phosphorylates itself and the LepRb at three tyrosine residues. This phospho-tyrosines act as binding site for signal transducer and activator of transcription STAT3, that is also phosphorylated by JAK2 (p-STAT3). p-STAT3 able to dimerize, thereby the NLS gets exposed and the homo-dimers translocate to the nucleus. When bound to its consensus sequence, p-STAT3 is able to induce the transcription of SOCS-3 to inhibit further signaling of LepRb. Activated JAK2 is also able to phosphorylate the PI_3K and thereby activates the PI_3K-pathway.
AKT, protein kinase B; IRS, insulin receptor substrate; JAK2, janus kinase 2; LepRb, leptin receptor isoform b; NLS, nuclear localization signal; PDK1, phosphoinositide dependent kinase 1; PI_3K, phosphatidyl inositol 3 kinase; PiP_2, phosphatidylinositol-(4,5)-bisphosphate; PiP_3, phosphatidylinositol-(3,4,5)-triphosphate, STAT3, signal transducer and activator of transcription 3; SOCS-3, suppressor of cytokine signaling 3.

sity (DIO) (Björnholm *et al.* , 2007; Howard *et al.* , 2004; Liu *et al.* , 2011). Due to the fact that leptin exerts most of its functions in the brain, a neuron specific SOCS-3 knockout already improves the effects of DIO and leads to enhanced leptin sensitivity (Mori *et al.* , 2004). Therefore, it is possible that leptin itself is one of the main contributors to the development of obesity and leptin resistance by its own negative feedback loop.

Another molecule involved in the development of leptin resistance is protein tyrosine phosphatase (PTP)1B, a phosphatase that negatively regulates multiple signaling pathways that are using receptor tyrosine kinases (Haj *et al.* , 2002). PTP1B de-phosphorylates

JAK2 and consequently shuts down further downstream signaling via STAT3. Similar to SOCS-3, neuronal inactivation of PTP1B decreases adiposity and improves leptin sensitivity in mice (Banno *et al.* , 2010; Bence *et al.* , 2006).

The endoplasmatic reticulum (ER) is the main source for newly synthesized proteins, as the folding into the tertiary and quaternary structure is facilitated in this organelle. In states of obesity, a lot of proteins are mis-folded in the ER, leading to an activation of ER stress pathways in order to either re-fold these proteins or to convey them to proteasomal degradation (Blond-Elguindi *et al.* , 1993; Chen *et al.* , 2002). The induction of the unfolded protein response (UPR) activates several kinases as PERK and Ire1, leading to the transcriptional activation of chaperones and the general inhibition of translation (Bernales *et al.* , 2006). If these ER stress pathways are impaired, obesity and leptin resistance are ameliorated (Ogimoto *et al.* , 2006; Ozcan *et al.* , 2009, 2004; Zhang *et al.* , 2008b).

Besides these cell intrinsic mechanisms, the obesity associated activation of immune cells and inflammatory pathways also participate in the attenuation of leptin signaling. Several pro-inflammatory cytokines, such as tumor necrosis factor (Tnf)α and multiple interleukins, have been shown to negatively regulate leptin signaling (Arruda *et al.* , 2011; De Taeye *et al.* , 2007; Denis *et al.* , 2010; Esposito *et al.* , 2003; Kern *et al.* , 2001). The activated kinases c-jun n-terminal kinase (JNK) and inhibitor of nuclear factor kappa-B kinase (IKK) seem to interfere with leptin's ability to decrease food intake, as the global deletion of JNK1 ameliorates obesity (Hirosumi *et al.* , 2002; Velloso *et al.* , 2008; Zhang *et al.* , 2008b). But also nutrients like saturated free fatty acids (FFA) are able to induce inflammatory signaling cascades via toll-like receptors (TLR)2 and 4 (Reyna *et al.* , 2008; Shi *et al.* , 2006; Tsukumo *et al.* , 2007). Kleinridders and colleagues could demonstrate that mice deficient for MyD88, an adaptor molecule used by all TLR isoforms, show improved leptin sensitivity when exposed to high-fat diet (HFD) (Kleinridders *et al.* , 2009).

Although all these factors might contribute to the development of a systemic leptin resistance observed in obese patients and rodents, nutrient derived FFAs are a key factor in the initiation of diet-induced obesity associated inflammation (Cintra *et al.* , 2012).

1.7 Insulin and Insulin Signaling

Beside leptin, insulin is the best characterized hormone in the control of energy homeostasis. Although it was discovered decades before leptin, insulin's action was believed to be limited to the periphery, where its effects were intensively studied. However, towards the end of the seventies, studies indicated that insulin receptors are expressed and that signaling is functional in the brain (Havrankova *et al.* , 1978a,b, 1979).

Insulin was discovered by Banting and Best as a pancreatic extract for the treatment of diabetes (Banting *et al.* , 1922). It is produced by pancreatic β-cells in the Langerhans islets as pre-proinsulin (Steiner *et al.* , 1967). Pre-proinsulin gets processed in two subsequent steps in the ER into the bioactive insulin, as which it is stored in cytoplasmatic secretory vesicles (Davidson *et al.* , 1988; Docherty & Hutton, 1983; Massaglia *et al.* , 1968). To exert its functions in its target organs, insulin is secreted in a tightly controlled process. Upon meal ingestion blood glucose levels rise, leading to a nonspecific import into the β-cells via glucose transporter (GLUT)2. Glucose gets metabolized into ATP via glycolysis and the citric acid-cycle, subsequently leading to the closure of ATP-dependent potassium (K_{ATP}) channels (Ashcroft, 2005). The resulting increase in potassium ions in the cytosol depolarizes the membrane potential and thereby activates voltage-gated calcium channels. This triggers the fusion of secretory insulin vesicles with the plasma membrane (Ashcroft, 2006). Via the blood circulation, insulin is able to reach it target organs; mainly the liver, muscle and adipose tissue, but also the CNS. In the muscle and in adipocytes, insulin leads to the induction of an intracellular signaling cascade, enabling the translocation of an insulin dependent glucose transporter (GLUT4) to the plasma membrane and consequently to an uptake of glucose from the circulation, and further storage in the form of glycogen or fat (Blüher *et al.* , 2002; Brüning *et al.* , 1998; Shepherd & Kahn, 1999). In adipocytes, insulin prevents lipolysis by the transcriptional inhibition of lipases and simultaneously increases lipogenesis (Claycombe *et al.* , 1998; Jaworski *et al.* , 2007; Kershaw *et al.* , 2006; Semenkovich *et al.* , 1989). The major effect of insulin in the liver is to inhibit gluconeogenesis and glycogenolysis to prevent an additional rise in circulating glucose (Cross *et al.* , 1995; Puigserver *et al.* , 2003).

The insulin receptor (IR) is a tetrameric receptor tyrosine kinase that consists of two

α- and two β-subunits, both synthesized by a single gene with 22 exons by proteolytic processing (Kasuga *et al.* , 1982; Ullrich *et al.* , 1985). It exists in two isoforms, IR-A and IR-B, which are generated by alternative splicing of exon 11, from which IR-B is mainly expressed in insulin target tissues (Benecke *et al.* , 1992; Moller *et al.* , 1989; Seino & Bell, 1989).

Upon binding of insulin to the extracellular α-chain of the receptor, the receptor undergoes conformational changes and is thus able to auto-trans-phosphorylate itself at the intracellular β-chains at various tyrosine residues (Kahn *et al.* , 1978). These phosphorylation sites then act as a docking platform for insulin receptor substrate (IRS) proteins that can bind via their phosphotyrosine binding (PTB) domains and in turn become phosphorylated themselves (Eck *et al.* , 1996; Miralpeix *et al.* , 1992; White *et al.* , 1988). Additionally, IRS proteins contain a pleckstrin homology (PH) domain, that interacts with phospholipids and thereby targets IRS proteins to the plasma membrane (Burks *et al.* , 1997, 1998; Jacobs *et al.* , 2001). Of the five known IRS isoforms, IRS 1 and 2 seem to be the most important ones in the transmission of the insulin signaling cascade (Lavan *et al.* , 1997a,b; Sun *et al.* , 1991, 1995).

Activated IRS proteins are able to induce several downstream signaling pathways, but the best characterized in respect to energy homeostasis is the phosphoinositide-3-kinase (PI_3K) pathway. The PI_3K can bind to the phosphorylated tyrosine residues of the IRS proteins with its rous sarcoma virus (Src)-homology (SH) 2 domain (Lavan *et al.* , 1992), leading to a de-inhibition of the regulatory subunit p85 and thereby an activation of the catalytic subunit p110 (Lavan & Lienhard, 1993; Myers *et al.* , 1992, 1994a). The activated PI_3K is able convert phosphaditylinositol-(3,4)-bisphosphate (PiP_2) into phosphaditylinositol-(3,4,5)-triphosphate (PiP_3), which acts as a second messenger at the plasma membrane (Myers *et al.* , 1993; Skolnik *et al.* , 1991; Whitman *et al.* , 1988). This is counteracted by the negative regulator of the PI_3K pathway, the phosphatase and tensin homolog (PTEN). PTEN de-phosphorylates PiP_3 back to PiP_2, thereby negatively regulating the signaling pathway (Maehama & Dixon, 1998). PiP_3 recruits of the phosphadityinositol dependent kinase 1 (PDK1) to the plasma membrane, which induces further downstream signaling, consequently leading to the phosphorylation and activation of

the proteinkinase B (AKT). AKT is then able to phosphorylate, among others, the transcription factor forkhead box protein O1 (FOXO1) (Alessi *et al.* , 1997a,b; Anderson *et al.* , 1998; Casamayor *et al.* , 1999; Currie *et al.* , 1999; Pullen *et al.* , 1998). FOXO1 is a transcription factor that is exported from the nucleus upon phosphorylation, gets ubiquitylated in the cytoplasm and finally degraded by the 26S proteasome (Huang & Tindall, 2007; Lin *et al.* , 1997; Ogg *et al.* , 1997). In POMC neurons, FOXO1 and STAT3 have overlapping binding sites at the POMC promotor where FOXO1 inhibits, and STAT3 activates, transcription of the POMC gene. Therefore both insulin and leptin signaling in POMC neurons is necessary to fully activate transcription of POMC (Belgardt *et al.* , 2008). In AgRP neurons FOXO1 and STAT3 have opposite effects. FOXO1 acts as activator and STAT3 as suppressor of the transcription of AgRP (Kitamura *et al.* , 2006).

The PI_3K pathway serves as a convergence point of both leptin and insulin signaling. Therefore it is difficult to curtail the effects of the PI_3K pathway to either leptin or insulin. Current results indicate that different isoforms of the PI_3K might be responsible for either leptin's or insulin's effect on the downstream signaling (Hill *et al.* , 2008, 2009), whereas for certain functions, especially in the brain, both are necessary to fully induce the PI_3K pathway (Koch *et al.* , 2010).

Beside the PI_3K pathway, insulin is also able to activate the MAPK pathway. Phosphotyrosine residues on IRS proteins act as a binding platform for the growth factor receptor-bound protein (Grb), that thereby activates the MAPK pathway (Myers *et al.* , 1994b; Skolnik *et al.* , 1993). In contrast to the PI_3K pathway, the MAPK pathway is considered to be more important in cell survival, proliferation and growth (figure 1.4) (Skolnik *et al.* , 1993; Wada *et al.* , 1998).

The importance of insulin signaling in the control of energy homeostasis is highlighted by multiple publications over the last decades. The specific deletion of IRs in the skeletal muscles reflects the symptoms of T2DM, showing that most of the glucose uptake is insulin dependent (Brüning *et al.* , 1998). A similar phenotype was reported in mice lacking IRs in hepatocytes. These mice displayed severe hyperglycemia and systematic insulin resistance (Michael *et al.* , 2000). On the contrary, the adipose tissue specific knockout of the IR is protected against the development of obesity and consequently against T2DM,

showing that insulin is a critical factor in the differentiation and expansion of adipocytes (Blüher *et al.* , 2002; Kershaw *et al.* , 2006).

Besides these effects in peripheral tissues, insulin action in the brain is of great importance in the control of energy homeostasis and reproduction. The neuron specific insulin receptor knockout (NIRKO) mouse is slightly obese and shows hypothalamic hypogonadism (Brüning *et al.* , 2000). Furthermore, insulin signaling in the brain has critical functions in the control of adipogenesis (Koch *et al.* , 2008; Scherer *et al.* , 2011). Further experiments allowed a deeper look into insulin's action in the brain. By knocking out the IR in hypothalamic neuron populations, Könner and colleagues could show that insulin signaling in AgRP, but not in POMC neurons is necessary to suppress hepatic glucose production (Könner *et al.* , 2007). In POMC neurons, insulin signaling is needed to fully activate the transcription of POMC, shown by the deletion of PDK1 (Belgardt *et al.* , 2008). On the other hand, hyperactivation of the insulin pathway by a deletion of the phosphatase PTEN also results in overweight mice, leading to the hypothesis that insulin is able to silence POMC neurons via K_{ATP} channels (Plum *et al.* , 2006).

1.8 Insulin Resistance

The association of obesity with T2DM has been recognized over the last decades and resistance to the hormone insulin is one of the hallmarks in the progression of T2DM (Brüning *et al.* , 1997; Kahn, 1994a; Reaven, 1995). In initial and mild states of insulin resistance, the pancreatic β-cells are able to compensate the increased demand for insulin by an increased production and secretion of insulin. But insulin resistance is, if not treated, a progressing disorder leading to further demands of insulin to maintain euglycemia (Martin *et al.* , 1992). This results in hyperplasia and increased secretion activity of the insulin producing β-cells, that eventually collapse (Parsons *et al.* , 1992; Pipeleers, 1992). Subsequently, insulin fails to suppress hepatic glucose production and to induce glucose uptake into muscle tissue and adipocytes, hence resulting in severely elevated blood glucose levels and finally in T2DM (Kahn, 1994b). Furthermore, T2DM predisposes for associated diseases such as diabetic retinopathy, hypertension, angiopathy and

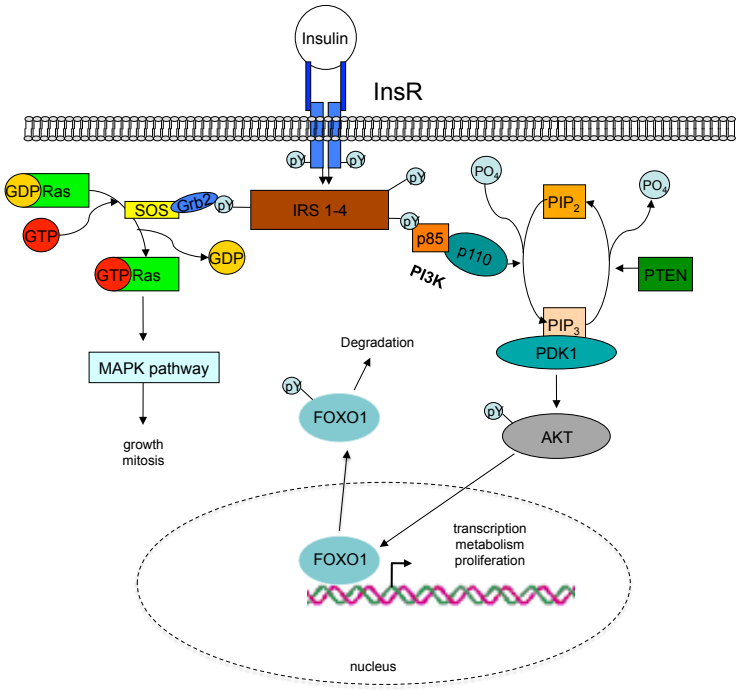

Figure 1.4: Insulin signaling pathway.
Binding of insulin leads to a conformational change of the IR, ending in activation of the intrinsic kinase ability. After auto-phosphorylation of the IR, IRS proteins bind to the phosphorylated residues by their SH2 domains, and are themselves phosphorylated by the IR. Grb binds via its SH2 domain, eliciting activation of the Ras-Raf-MAPK signalling pathway, which mediates some of insulin's effects on growth. Phosphorylation of IRS proteins allows binding of p85, the regulatory subunit of the PI_3K complex. This de-inhibits p110, the catalytic subunit of PI_3K, which subsequently phosphorylates the membrane lipid PiP_2 to generate PiP_3. PiP_3 accumulation in turn will recruit and allow binding of both PDK1 and AKT via their PH domains. After co-localisation induced by PiP_3 binding, PDK1 phosphorylates and thereby activates AKT, which mediates most of insulin's effect on glucose and glycogen metabolism, as well as activating protein translation and gene transcription.
AKT, protein kinase B; FOXO1, forkhead-O transcription factor 1; Grb, growth factor receptor bound; IR, insulin receptor; IRS, insulin receptor substrate; MAPK, mitogen-activated protein kinase; PDK1, phosphoinositide dependent kinase 1; PI_3K, phosphoinositide 3-kinase; PiP_2, phosphatidylinositol-(4,5)-bisphosphate; PiP_3, phosphatidylinositol-(3,4,5)-triphosphate, STAT3, signal transducer and activator of transcription 3; Ras, Rat sarcoma protein; Sos, son of sevenless

neuropathy (Gastaldelli *et al.* , 2000; Reaven, 1995; Semenkovich, 2006; van Leiden *et al.* , 2002).

The full clinical manifestation of insulin resistance occurs only in rare monogenic disorders, such as Donohue or Rabson-Mendenhall syndrome. In these syndromes insulin resistance is caused by mutations or polymorphisms in insulin signaling molecules, such as AKT, PI_3K or IRS proteins that impair the signaling downstream of the IR (Semple *et al.*

, 2011). But in the vast majority of patients, the exact molecular mechanisms underlying insulin resistance are not fully understood.

Obesity is associated with a chronic low-grade inflammatory state, indicated by elevated levels of pro-inflammatory cytokines such as Tnf-α and IL-6 in the blood circulation and in the white adipose tissue (WAT) (Hotamisligil *et al.* , 1993; Wellen & Hotamisligil, 2005). These inflammatory cytokines induce intracellular stress-signaling cascades that lead to the activation of effector kinases such as JNK and IKK, that are able to inhibit insulin signaling by an inhibitory phosphorylation at serine residues of IRS proteins (Cai *et al.* , 2005; Hirosumi *et al.* , 2002; Hotamisligil *et al.* , 1996; Shoelson *et al.* , 2003). Serine phosphorylation of the IRS protein inhibits downstream signaling as it prevents the binding of IRS proteins to the IR by their PTB domain (Aguirre *et al.* , 2000, 2002; Paz *et al.* , 1997). Consequently, the inhibition of inflammation or the deletion of the effector kinases improves insulin sensitivity (Belgardt *et al.* , 2010; Hirosumi *et al.* , 2002; Sabio *et al.* , 2008, 2009, 2010). But not only inflammatory cytokines are able to activate stress-signaling cascades. It has been shown that ER stress, beside impairing leptin's action, is also able to induce insulin resistance via the unfolded-protein response (Bailly-Maitre *et al.* , 2010; Ozcan *et al.* , 2009, 2004; Zhang *et al.* , 2008b). Futhermore, FFAs, that are elevated in the circulation upon HFD-feeding, have been shown to induce intracellular JNK signaling via toll-like receptors (TLR) 2 and 4. Hence, deletion of TLR4 improves insulin sensitivity in muscle tissue of diet-induced obese mice (Davis *et al.* , 2009; Radin *et al.* , 2008; Shi *et al.* , 2006). But FFAs are also able to activate via diacylglycerols protein kinase C (PKC) isoforms that have been shown to interfere with insulin signaling by serine phosphorylation of IRS proteins (Bandyopadhyay *et al.* , 2005; Benoit *et al.* , 2009). Another mechanism of FFA-induced insulin resistance is the activation of protein phosphatase 2A (PP2A), that is able to de-phosphorylate AKT (Galbo *et al.* , 2011). Also the aforementioned unspecific phosphatase PTP1B is activated by FFAs and inflammation and impairs insulin signaling by de-phosphorylation of IRS proteins (Galbo *et al.* , 2011). Consistently, PTP1B knockout mice are protected against diet-induced insulin resistance (Elchebly *et al.* , 1999).

Beside FFA, ceramides, a class of sphingolipids, are also implicated in the develop-

ment of insulin resistance, possibly again by activating JNK and IKK (Chavez & Summers, 2012).

1.9 The Ventromedial Hypothalamus and Steroidogenic factor 1

The Ventromedial Hypothalamus (VMH) was for a long time considered to be the most important satiety center in the brain. By either lesion experiments, leading to increased food intake and obesity, or by electrical stimulation, leading to anorexia, the importance of this nucleus in the regulation of energy homeostasis was demonstrated (Aravich & Sclafani, 1983; Boyle, P. C. & Keesey, 1975; Hetherington & Ranson, 1940; Leibowitz *et al.* , 1981; Olney & Sharpe, 1969; Stevenson *et al.* , 1950). Researchers used the model of hypothalamic obesity for their investigations, which resulted from a lesioned VMH (Anand & Brobeck, 1951; Brobeck, 1946).

Upon the discovery of the melanocortin system, the VMH was neglected by most researchers. Imprecise techniques and a lack of knowledge about the neurons in the ARC were considered to be the reason of the phenotype in hypothalamic obesity (probably the ARC was also lesioned in addition to the VMH). The VMH was then believed to be a possible projection target for POMC or AgRP neurons in the regulatory metabolic neurocircuitry that further process the melanocortin derived neuroendocrine signals (Fu & van den Pol, 2008).

This view changed when the orphan receptor *Steroidogenic Factor 1* (SF-1) was discovered to be expressed in the VMH (Ikeda *et al.* , 1994). Initial experiments revealed a lethal phenotype in mice with a whole body knockout due to a failure in the development of the adrenal glands (Sadovsky *et al.* , 1995). But when these mice were rescued by a transplantation of adrenal glands, they developed severe obesity due to an absent VMH (Majdic *et al.* , 2002). These results established SF-1 as a marker for the VMH.

In initial studies by Dhillon and colleagues in 2006, a transgenic mouse with the Cre recombinase under the control of the SF-1 promotor was created. They could show that the Cre is expressed predominantly in the VMH with minor expression in the adrenal gland, testis and pituitary gland. Using this transgenic mouse to delete the leptin receptor specifically in VMH neurons revealed a direct role for leptin to regulate the elec-

trophysiological activity of these neurons. Interestingly, the authors were able to show that the effect of leptin signaling in the VMH is independent of leptin action on POMC neurons. Whereas the single deletion of LepRs on POMC and SF-1 neurons led to only modest obesity, the deletion of LepRs on both neuron populations caused severe obesity, reflecting the sum of the weight gain observed in the individual deletion of the receptor in the respective neurons (Bingham *et al.* , 2008; Dhillon *et al.* , 2006).

Furthermore, the same group could show that glutamatergic output of SF-1 expressing neurons was mandatory for normal body weight regulation. Mice lacking the glutamate transporter *VGLUT2* in SF-1 neurons, leading to an impaired glutamate release, also showed an increase in body weight and modest hyperphagia (Tong *et al.* , 2007b). These findings correspond with the results of Sternson and colleagues, who were able to show, by a combination of uncaging experiments in the VMH together with electrophysiological recordings of ARC POMC and AgRP neurons, that unidentified VMH neurons build excitatory hotspots on POMC neurons (Sternson *et al.* , 2005). This further highlights the role of SF-1 expressing neurons in the homeostatic mechanism of melanocortin regulated body weight control.

1.10 Counter-regulatory Response to Hypoglycemia

Apart from being involved in the regulation of energy homeostasis, VMH neurons also play a role in the detection and counter-regulation of hypoglycemia, one of the major limitations in the treatment of type 1 and 2 diabetes patients with insulin (Borg *et al.* , 1994; Cryer *et al.* , 2003).

Due to the fact that the brain uses glucose as the major (and almost exclusive) fuel, it is very sensitive to a drastic fall of blood glucose concentrations (Cryer *et al.* , 2003). Therefore, powerful neuroendocrine and autonomic counter-regulatory mechanisms protect the brain against severe hypoglycemia (Cryer, 2008). This is achieved by the release of epinephrine, norepinephrine, corticosterone and glucagon into the circulation, leading to an increase of hepatic glucose production and an inhibition of peripheral glucose uptake (figure 1.5) (Cryer *et al.* , 2003; Dagogo-Jack *et al.* , 1993; Heller & Cryer, 1991). But the

mechanism how the brain senses hypoglycemia and how the appropriate release of the aforementioned hormones is facilitated is still under investigation.

The first evidence pointing towards the involvement of the VMH in the counter-regulatory response to hypoglycemia (CRR) came from VMH-lesioned rats that showed an impaired CRR (Borg *et al.* , 1994). This was verified by either glucose infusion into the VMH or the induction of local glucopenia in the VMH (Borg *et al.* , 1997, 1999, 1995). Furthermore, both glucose excited (GE) but also glucose inhibited (GI) neurons were found within the VMH (Song *et al.* , 2001). Thus, glucose sensing in the VMH has a pivotal role in the induction of CRR (Kang *et al.* , 2006; Levin *et al.* , 2004). Several factors are involved in VMH's glucose sensing and hence the induction of CRR. AMP-activated protein kinase (AMPK) plays a central role since activation of AMPK with 5-aminoimidazole-4-carboxamide (AICAR) amplifies the hormonal CRR (McCrimmon *et al.* , 2006). Similarly, the K_{ATP} channels, that are key mediators of glucose stimulated insulin release from pancreatic β-cells, are implicated in the mechanism of glucose sensing. Mice deficient for the regulatory subunit of K_{ATP} channels, Kir6.2, show an impaired CRR (Miki *et al.* , 2001). But also nitric oxide (NO) is necessary for glucose sensing and the induction of CRR. AMPK is able to phosphorylate and thereby activate the neuronal nitric oxide synthase (nNOS), leading to the production of NO that can signal via soluble guanylyl cyclase (sGC). Blockade of any of these steps leads to a loss of glucose sensing ability (Canabal *et al.* , 2007; Murphy *et al.* , 2009).

Insights into insulin's role in the induction of CRR is derived from experiments in neuronal insulin receptor knockout (NIRKO) mice. These mice displayed an impaired CRR when exposed to insulin induced hypoglycemia, caused by an impaired glucagon release from α-cells in the pancreas (Fisher *et al.* , 2005).

Further evidence for the involvement of VMH and especially SF-1 neurons was provided by Tong and colleagues who could show that glutamate release from SF-1 neurons is necessary for the induction of the CRR. Both insulin induced hypoglycemia and fasting, but also local glycopenia mediated CRRs were blunted in mice lacking VGLUT2 in SF-1 neurons, again caused by an impaired release of glucagon and epinephrine into the circulation (Tong *et al.* , 2007a).

Finally it could been shown that a lack of IRs in the brain leads to a reduced expression of the glucose transporter GLUT4 in the brain, particularly in the VMH, leading to a defect in glucose sensing of those neurons. This resulted again in reduced levels of epinephrine secreted from the adrenal gland and thus to an impaired CRR (Diggs-Andrews *et al.* , 2010).

Although both insulin signaling and VMH neurons are key factors in the CRR, it is still unclear whether SF-1 neurons represent the central glucose sensing neurons in the VMH, mediating insulin's effect in the counter-regulation against hypoglycemia.

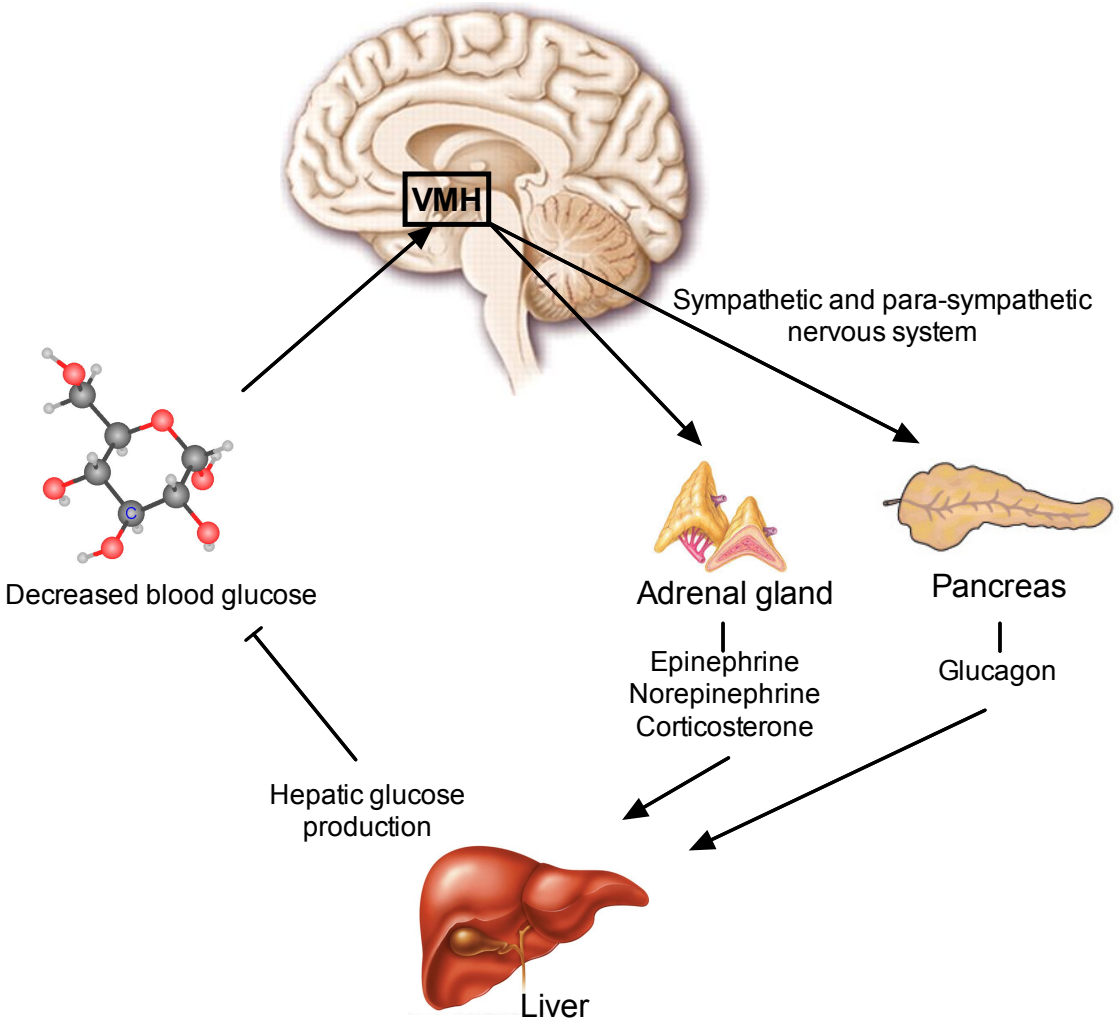

Figure 1.5: Schematic overview of the counter-regulatory response to hypoglycemia.
The brain, especially the ventromedial hypothalamus (VMH), senses decreasing blood glucose concentrations and triggers the release of epinephrine, norepinephrine and corticosterone from the adrenal glands and the secretion of glucagon from pancreatic α-cells via the sympathetic and para-sympathetic nervous system These hormones increase the hepatic glucose production to counter-regulate the hypoglycemia.

1.11 Objectives

The role of the VMH as important hypothalamic nucleus in the control of energy homeostasis is well established. Likewise, insulin's action in distinct neuronal populations as a regulator of peripheral glucose production has been intensively studied, e.g. in POMC and AgRP neurons (Könner *et al.* , 2007), further refining the results of Brüning and colleagues (Brüning *et al.* , 2000). Additionally, the NIRKO mouse used in the latter publication has been further studied with respect to the counter-regulatory response to hypoglycemia (CRR), establishing insulin as key factor in the induction of the CRR. The identification of steroidogenic factor 1 (SF-1) as a marker for the VMH and the subsequent creation of a mouse line, using the SF-1 promotor to drive the expression of the Cre recombinase, allowed further insight into the role of leptin signaling in the VMH in control of energy homeostasis (Dhillon *et al.* , 2006; Zhang *et al.* , 2008a), but also into the role of SF-1 expressing neurons in the induction of CRR (Tong *et al.* , 2007a). Hence, the SF-1 Cre mouse line is a new tool that enables a detailed investigation of insulin signaling in the VMH.

Due to the importance of the VMH in the regulation of body weight maintenance, as shown in lesion experiments, SF-1 neurons might be a target for insulin in the CNS. Thus, the aim of this study was to create mice that specifically lack the insulin receptor (IR) in SF-1 neurons (SF-1$^{\Delta IR}$) and to investigate the effect of lacking insulin signaling on SF-1 neurons in terms of energy homeostasis and glucose metabolism. To over-activate the insulin signaling pathway, mice were generated lacking the phosphatase PTEN (SF-1$^{\Delta PTEN}$; by Dr. Bengt F. Belgardt) and both PTEN and IR simultaneously (SF-1$^{\Delta IR:PTEN}$). Moreover, the role of insulin signaling in SF-1 neurons in the CRR was analyzed by exposing the mice to hypoglycemic-hyperinsulinemic clamp studies.

2 Materials and Methods

2.1 Mouse experiments

General mouse handling was performed according to Silver (1995)

2.1.1 Animal care

Care of all animals was within institutional animal care committee guidelines. All animal procedures were conducted in compliance with protocols and approved by local government authorities (Bezirksregierung Köln, Cologne, Germany) and were in accordance with NIH guidelines. Animals were housed in groups of 3 - 5 mice per cage at an ambient temperature of 22 - 24°C and kept at a 12-hour light / 12-hour dark cycle. Animals were either fed normal chow diet (NCD; Teklad Global Rodent 2018; Harlan) containing 53.5% carbohydrates, 18.5% protein, and 5.5% fat (12% of calories from fat) or a high-fat diet (HFD; C1057; Altromin) containing 32.7% carbohydrates, 20% protein, and 35.5% fat (55.2% of calories from fat). Animals had *ad libitum* access to water and food at all times. Food was only withdrawn if required for an experiment. Body weight was measured once a week; body length (naso-anal length) was measured after sacrificing. Mice were sacrificed by lethal CO_2 anesthesia.

2.1.2 Experimental mice

SF-1 Cre$^{tg/wt}$ mice (Dhillon *et al.* , 2006) were mated with IR$^{fl/fl}$ mice (Brüning *et al.* , 1998) to generate SF-1 Cre$^{tg/wt}$;IR$^{fl/fl}$ animals (SF-1$^{\Delta IR}$) with IR$^{fl/fl}$ animals as control. SF-1$^{\Delta IR}$ were further bred to PTEN$^{fl/fl}$ mice (Suzuki *et al.* , 2001) to generate SF-1 Cre$^{tg/wt}$;IR$^{fl/fl}$:PTEN$^{fl/fl}$, that lack both IR and PTEN in SF-1 expressing cells (SF-1$^{\Delta IR:\Delta PTEN}$) with the respective SF-1 Cre negative animals as control. For immunohistochemistry (IHC) experiments and electrophysiological recordings SF-1$^{\Delta IR}$ were mated with either Z/eG or RosaArte1 mice (SF-1$^{GFP:\Delta IR}$ and SF-1$^{lacZ:\Delta IR}$) (Novak *et al.* , 2000; Seibler *et al.* , 2003). As controls, SF-1 Cre$^{tg/wt}$ animals were also bred to Z/eG and

RosaArte1 mice to generate SF-1^{GFP} and SF-1^{lacZ}. For electrophysiology experiments in POMC neurons, transgenic mice with GFP under control of the *Pomc* promotor (POMC^{GFP}) (Cowley *et al.* , 2001) were mated with SF-1$^{\Delta IR}$ to generate POMC^{GFP}:SF-1$^{\Delta IR}$, that express GFP in POMC neurons but lack the IR in SF-1 neurons. SF-1 Cre negative animals served as controls(POMC^{GFP};IR$^{fl/fl}$), further named POMC^{GFP}.

2.1.3 Food intake and indirect calorimetry

Daily food intake was calculated as the average intake of NCD or HFD from custom made food racks within the time stated. Mice were acclimated to the food intake settings for at least five days. Weight of the racks was determined daily. Calorimetry measurements were performed in a PhenoMaster System (TSE systems, Bad Homburg, Germany and CLAMS, Oximax Windows 4.00, Columbus Instruments, Columbus, OH, USA), which allows measurement of metabolic performance and activity-monitoring by an infrared light-beam frame (TSE systems). Mice were placed at room temperature (22 °C–24 °C) in 7.1-l chambers of the PhenoMaster open circuit calorimetry. Mice were allowed to adapt to the chambers for at least 48 hours. Food and water were provided *ad libitum* in the appropriate devices and measured by the build-in automated instruments. Locomotor activity and parameters of indirect calorimetry were measured for at least the following 48 hr. Presented data are average values obtained in these recordings.

2.1.4 Blood collection and determination of glucose levels

Tail bleeding was performed as described before (Silver, 1995). Blood glucose values were determined from whole venous blood using an automatic glucose monitor (GlucoMen; A. Menarini Diagnostics, Florence, Italy). Venous blood samples were stored on ice for 15 minutes and subsequently centrifuged at 13.000 rpm for 20 minutes. Resulting serum was stored at -20°C. For collection of plasma, EDTA (1.6 mg/1ml serum) was added to prevent clotting. Determination of blood glucose levels and collection of blood samples from control and various conditional knockout mice were performed side-by-side in the morning to avoid intra-group deviations due to circadian variations.

2.1.5 Analysis of body composition

Body fat content was measured *in vivo* by nuclear magnetic resonance using a minispec mq7.5 (Bruker Optik, Ettlingen, Germany). Radiofrequency pulse sequences are transmitted into mouse tissue, which are retransmitted by hydrogen atoms in the tissue, the signals of which are detected by the minispec. Amplitude and duration of these signals are related to properties of the material.

2.1.6 Glucose and insulin tolerance test

For glucose tolerance tests (GTT), mice were fasted overnight for 16h. After determination of fasted blood glucose levels, each animal received an intraperitoneal injection of 20% glucose solution (10ml/kg body weight). Blood glucose was determined 15, 30, 60 and 120 min after injection. For insulin tolerance tests (ITT), each random fed animal received an intraperitoneal injection of 0.75U/ml insulin-solution (0,75U/kg body weight) after determination of random fed blood glucose concentration. Blood glucose was determined 15, 30, 60 min after injection, and blood glucose concentrations were calculated relative to starting blood glucose levels.

2.1.7 Leptin sensitivity

Intracerebroventricular cannulas were implanted as previously described (Brown *et al.* , 2006), except that the lateral ventricle was targeted using coordinates located using a brain atlas (coordinates were bregma 1.0 mm lateral, 0.2 mm caudal and 2.0 mm ventral). After one week recovery and an overnight fast, mice were injected with 2 μl artificial cerebrospinal fluid (aCSF). Food intake was measured 4 and 8 h later. After a 7 d break, 5 μg mouse leptin (NHPP) in 2 μl was injected and food intake was measured 4 and 8 h later. On the basis of the notion that SF-1$^{\Delta IR}$ mice are protected from HFD-induced obesity, data were analyzed by unpaired, one-tailed Student's *t*-test.

2.1.8 Fertility assesment

IR$^{fl/fl}$ (control) and SF-1$^{\Delta IR}$ males were mated with SF-1$^{\Delta IR}$ and control females, respectively. Litter frequency and mean litter size were analyzed for at least four litters.

Additionally, testes and ovaries were examined for morphological abnormalities. Therefore, testes and ovaries of 20 week old animals were dissected, fixed overnight in 4% formaldehyde and then embedded for paraffin sections. Subsequently, 7μm thick sections were deparaffinized and stained using haematoxylin and eosin (H&E) for general histology. Images were taken with a Leica DM 1000 LED (Leica Microsystems, Wetzlar, Germany).

2.1.9 Hypoglycemic Clamp studies

Catheter implantation

At the age of 12 weeks, female and male mice were anesthetized by i.p. injection of avertin (240 mg/kg) and adequacy of the anesthesia was ensured by the loss of pedal reflexes. A micro-renathane catheter (MRE 025; Braintree Scientific Inc.) was inserted into the right internal jugular vein, advanced to the level of the superior *vena cava*, and secured in the proximal part of the vein with 4-0 silk; the distal part of the vein was occluded with 4-0 silk. After irrigation with physiological saline solution, the catheter was filled with heparin solution and sealed at the distal end. The catheter was subcutaneously tunneled, thereby forming a subcutaneous loop, and exteriorized at the back of the neck. Cutaneous incisions were closed with a 4-0 silk suture and the free end of the catheter was attached to the suture in the neck as to permit the retrieval of the catheter on the day of the experiment. Mice were intraperitoneally injected with 1 ml of saline containing 15 μg/g body weight of Tramal and placed on a heating pad in order to facilitate recovery.

Hypoglycemic-hyperinsulinemic Clamp experiment

After 7 days of recovery, only mice that had regained 90% of their preoperative weight were studied. After a 5-h fast, awake mice were placed in a tail-restraint apparatus, and after an adjustment period, a 200 μl blood sample was collected from the tail tip. Separated plasma was stored for basal metabolite and hormone determinations, while erythrocytes were resuspended in saline and re-infused to avoid volume depletion. After basal sampling, regular human insulin (Novo Nordisk, Bagsvaerd, Denmark) diluted in saline with 0.1% BSA (Sigma) was infused (200 mU*kg^{-1} bolus and 20 mU*kg^{-1} *min^{-1})

at time zero. Blood samples ($\sim$ 2.2 μl) were drawn at 10 min intervals to measure blood glucose (B-Glucose Analyzer; Hemocue). Extreme care was taken with the glucose infusion (20% glucose; DeltaSelect) to gradually lower glycemia and match groups for levels of hypoglycemia ($\sim$ 50 mg*dl^{-1}). No seizure activity was noted. A 200 μl blood sample was drawn at the end of the 120 min hypoglycemic clamp for metabolite and hormone assays.

2.2 Molecular biology

Standard methods in molecular biology were performed according to the protocols in Sambrook & Russell (2001), if not mentioned afterwards.

2.2.1 Isolation of genomic DNA

Mouse tail biopsies were incubated overnight in lysis buffer (100mM Tris pH 8.5, 5mM EDTA, 0.2% (w/v) SDS, 0.2M NaCl, 500mg/ml Proteinase K) in a thermoshaker (Eppendorf, Hamburg, Germany) at 55°C. After removal of tissue debris, DNA was precipitated by adding an equivalent volume of 2-Propanol (100%) and centrifuged at 13000 rpm for 15 minutes. After washing with 70% (v/v) ethanol and subsequent centrifugation, the DNA pellet was dried and redissolved in TE buffer

2.2.2 Quantification of nucleic acids

DNA and RNA concentrations were quantified by measuring the sample absorption at 260 nm and 280 nm with a NanoDrop ND-1000 UV-Vis spectrophotomoter (Peqlab, Erlangen, Germany). An optical density of 1 corresponds to approximately 50 μg/ml of double stranded DNA and to 38 μg/ml of RNA. A ratio greater than 2 of absorptions at 260 nm (DNA/RNA) divided by the absorption at 280 nm (protein) was used as an index of purity of DNA/RNA.

2.2.3 Polymerase chain reaction (PCR)

PCR was used to detect loxP flanked exons and various transgenes with primers described in table 2.1. Reactions were performed in a Thermocycler iCycler PCR machine

(BioRad, München, Germany) or in a Peltier Therman Cycler PTC-200 (MJ Research, Waltham, USA). All amplifications were performed in a total reaction volume of 25 μl containing a minimum of 50ng template DNA, 25pmol of each primer, 25μM dNTP mix, polymerase buffer and 1 U of polymerase. Standard PCR programs started with 5 minutes (min) of denaturation at 95°C, followed by 35 cycles consisting of denaturation at 95°C for 45 seconds (sec), annealing at oligonucleotide-specific temperatures for 30 sec and elongation at 72°C for 30 sec, and a final elongation step at 72°C for 5 min.

Table 2.1: PCR primers

Primer	**Sequence**	**Annealing site / function**	**Orientation**
SF-1 Cre1	GGTCAGCCTAATTAGCTCTGT	*Ghrelin* control	sense
SF-1 Cre2	GATCTCCAGCTCCTCCTCTGTC	*Ghrelin* control	antisense
SF-1 Cre3	TGCGAACCTCATCACTCGTTGCAT	*Sf-1* promotor	sense
SF-1 Cre4	CTGAGCTGCAGCGCAGGGACAT	Cre	antisense
IR-5′	GATGTGCACCCCATGTCTG	*Insr* floxed exon	sense
IR-3′	CTGAATAGCTGAGACCACAG	*Insr* floxed exon	antisense
IR-Δ	GGGTAGGAAACAGGATGG	*Insr* deletion	sense
PTEN-5′	CTCCTCTACTCCATTCTTCCC	*Pten* floxed exon	sense
PTEN-3′	ACTCCCACCAATGAACAAAC	*Pten* floxed exon	antisense
LacZ1	AAAGTCGCTCTGAGTTGTTATC	endogenous *Rosa26* locus	sense
LacZ2	GATATGAAGTACTGGGCTCTT	endogenous *Rosa26* locus	antisense
LacZ3	GACAAACCACAACTAGAATGC	transgenic lacZ allele	antisense
Z/eG1	CAGGAACTCCAGCAGGACCATG	Z/eG transgene	sense
Z/eG2	CTGGTCGAGCTGGACGGCGACG	Z/eG transgene	antisense
POMC-GFP1	TGGCTCAATGTCCTTCCTGG	*Pomc* promotor	sense
POMC-GFP2	CACATAAGCTGCATCGTTAAG	enogenous *Pomc*	antisense
POMC-GFP3	CAGGAACTCCAGCAGGACCATG	GFP	antisense

2.2.4 RNA extraction, RT-PCR and quantitative real-time PCR

Tissue samples were homogenized in Trifast (Peqlab, Erlangen, Germany) using an Ultra Turrax homogenizer (IKA, Staufen, Germany). Subsequent purification of total RNA was conducted according to the Trifast protocol by Peqlab. When exon-spanning probes were not available to quantify RNA expression of target genes, on-column DNA digestion was performed (RNAse-free DNAse, Qiagen, Hilden, Germany). 200ng RNA was reverse-transcribed into cDNA using the Eurogentec RT KIT (Eurogentec, Belgium). For quantitative real-time PCR, 100ng cDNA was amplified using Taqman Universal PCR-mastermix, NO AmpERASE UNG with Taqman assay on demand kits (Applied Biosystems, Foster City, USA) as shown in table 2.2. Relative expression of genes was adjusted for total RNA content by glucuronidase (GUSB) and hypoxyanthine guanine phosphoriboysl transferase (HPRT) 1 RNA. Real-time PCR analysis was performed on an ABI-PRISM 7700 Sequence detector (Applied Biosystems, Foster City, USA). Assays were linear over 4 orders of magnitude.

Table 2.2: Real-time PCR probes

Gene	Catalogue Nr.	Gene	Catalogue Nr.
Agrp	Mm00435874_ml	*Bdnf*	Mm01334042_m1
Cart	Mm00489086_m1	*Fshb*	Mm00433361_m1
Gh	Mm01258409_g1	*Gusb*	Mm00446953_m1
Hprt	Mm03024075_m1	*Lh*	Mm00656868_g1
Npy	Mm00445771_m1	*Pomc*	Mm00435874_m1
Sf-1	Mm00446826_m1	*Tshb*	Mm03990915_g1

2.3 Cell biology

2.3.1 Histological analysis and immunohistochemistry

SF-1 Cre mice were mated with RosaArte1 mice or Z/EG mice to generate SF-1^{lacZ} and SF-1^{GFP} mice which served as controls for the immunohistochemistry studies

(Novak *et al.* , 2000; Seibler *et al.* , 2003). SF-1$^{\Delta IR}$ mice were mated with RosaArte1 mice to generate SF-1$^{\Delta IR:lacZ}$ mice which lack IR in SF-1 expressing cells but express lacZ in these cells.

Mice were anesthetized and transcardially perfused with physiologic saline solution followed by 4% paraformaldehyde (PFA) in 0.1 M phosphate buffered saline (PBS; pH 7.4). The brains were dissected, post- fixed in 4% PFA at 4°C, transferred to 20% sucrose for 6 h and frozen in tissue freezing medium. Then, 25 μm thick free-floating coronal sections were cut through the ARC using a freezing microtome (Leica, Germany). The sections were collected in PBS/azide (pH 7.4) and washed extensively to remove cryoprotectant. Subsequently, the sections were treated with 0.3% H2O2 in PBS for 20 min to quench endogenous peroxidase activity. Following pretreatments, the sections were processed using the Renaissance® TSATM Fluorescence Systems Tyramide Signal Amplification Kit (PerkinElmerTM) according to manufacturer's guidelines (primary antibody: rabbit anti-lacZ, #55976; Cappel; secondary antibody: goat anti-rabbit peroxidase labeled, Vector Laboratories).

For visualization of GFP expression after Cre-recombination, SF-1^{GFP} mice were anesthetized and transcardially perfused with physiologic saline solution followed by 4% paraformaldehyde. Brains were dissected and post-fixed in 4% PFA at 4°C, transferred to 20% sucrose for 6 h and frozen in tissue freezing medium. Then, 25 μm thick free-floating coronal sections were cut through the mediobasal hypothalamus using a freezing microtome (Leica, Gemrany). The sections were washed, pretreated with 0.3% H2O2, blocked with PBT/azide containing 3% donkey serum, and incubated overnight with primary antibody (anti-GFP rabbit serum, 1:10.000 in blocking solution; A6455 from Invitrogen/Molecular Probes). Incubation with secondary antibody (anti-rabbit IgG biotin, 1:500; 711-065-152 from Jackson ImmunoResearch) was followed by an additional incubation with the VECTASTAIN Elite ABC kit (Vector Laboratories) for 1 h and visualization with 0.4% DAB/0.01% H2O2. Afterwards the sections were mounted onto gelatin-coated slides and covered with glycerin.

To determine the efficiency of IR deletion, SF-1^{lacZ} control and SF-1$^{\Delta IR:lacZ}$ KO reporter were fasted over night, anesthetized, and intravenously injected with either saline or 5U

of human regular insulin (NovoNordisc) for 10 or 20 min. Mice were then perfused transcardially with physiologic saline solution; brains were dissected, frozen in tissue freezing medium (Jung Tissue Freezing MediumTM) and sectioned in 7 μM thick slices on a cryostat (Leica, Germany). Tissues were stained with galactosidase (#55976; Cappel) and PIP3 (#Z-G345; Echelon, FITC) and double fluorescence immunostaining was performed as previously described (Plum *et al.* , 2006).

All slides were photographed through a Zeiss Axioskop equipped with a Zeiss AxioCam for acquisition of digital images using Spot Advanced 3.0.3 software (Zeiss, Jena, Germany).

2.3.2 Analysis of PiP_3 accumulation *in situ*

For quantitative analysis of PiP_3 levels in SF-1 neurons on NCD, a total of 13851 LacZ-positive neurons was counted in VMH slices of SF-1^{lacZ} control mice injected with saline, (n = 2; 891 SF-1 neurons), 10 min insulin-stimulated control mice (n = 3, 1859 SF-1 neurons), 20 min insulin-stimulated control mice (n = 2, 1637 SF-1 neurons), SF-$1^{\Delta IR}$ mice injected with saline (n = 3; 1735 SF-1 neurons), 10 min insulin-stimulated SF-$1^{\Delta IR}$ mice (n = 3, 1586 SF-1 neurons) and 20 min insulin-stimulated SF-$1^{\Delta IR}$ mice (n = 3, 1701 SF-1 neurons). For quantitative analysis of PiP_3 levels in SF-1 neurons on HFD, a total of 4502 LacZ-positive neurons was counted in VMH slices of control mice injected with NaCl, (n = 4; 2524 SF-1 neurons) and SF-$1^{\Delta IR}$ mice injected with NaCl (n = 3; 1978 SF-1 neurons). The amount of PiP_3 was classified either as low (immunoreactive cytoplasmatic dots/sprinkles in the proximity of the nucleus at background levels, i.e., 4 or fewer dots, no cloudy aspect, no confluent areas), moderate (dots/sprinkles at levels above background, i.e., more than 4 dots, cloudy aspect), or high (numerous dots/sprinkles, cloudy with confluent areas). Slides were viewed through a Zeiss Axioskop equipped with a Zeiss AxioCam for acquisition of digital images. Neurons positive for β-gal were counted and marked digitally to prevent multiple counts, and PiP_3 immunoreactivity was rated as previously described (Könner *et al.* , 2007) using Zeiss AxioVision version 4.2 imaging software. Results were calculated as percentage of SF-1 expressing neurons, which show the respective PiP_3 levels.

2.3.3 Combined *in situ* hybridization and immunohistochemistry

For *in situ* hybridization combined with immunohistochemistry, series of 8μm coronal sections of freshly frozen brains were sliced using a cryostat, thaw-mounted onto RNase-free slides and stored at -80 °C until processing. Locked Nucleic Acid (LNA) RNA probe detecting exon 4 of the insulin receptor gene (*Insr*) labeled at the 5′ and 3′ end with digoxigenin was supplied by Exiqon (Vedbaek, Denmark). For *in situ* hybridization, brain sections containing the VMH were fixed onto slides in 4% ice-cold PFA in PBS. Acetylation (5 μl*ml^{-1} acetic anhydride in 0.1 M triethanolamine) reduced nonspecific background signals. In an initial step (prehybridization), the slides were immersed in hybridization buffer (50% (w/v) deionized formamide, Denhardt's solution, 500 μg*ml^{-1} salmon sperm DNA, 500 μg*ml^{-1} tRNA) for 2.5 h at 48 °C to block nonspecific binding. Hybridization was performed for at least 6 h at 48 °C in hybridization buffer containing 10% (w/v) dextran sulfate. Washes with increasing stringency were then performed. To further remove unbound LNA probe, the brain slices were subjected to RNase A (0.5 μl*ml^{-1}) digestion. In addition, to block nonspecific staining, slices were treated with 3% (v/v) H_2O_2 in Tris-buffered saline and tyramide blocking solution. Specifically bound probe was detected using a digoxigenin antibody coupled to peroxidase with cyanine-3 fluorophore–tyramide. After in situ hybridization, immunohistochemistry for detection of β-galactosidase-positive neurons was performed as described (Belgardt *et al.* , 2008). Finally, slides were covered with DAPI Mounting Shield (Vector Laboratories) to visualize neurons. Images were taken using a Zeiss Meta Confocal microscope (Zeiss, Jena, Germany).

Quantification of the IR signal was performed with ImageJ (US National Institutes of Health) by converting the cyanine-3 fluorophore–tyramide signal into gray scale and measuring mean gray values of the VMH in SF-1^{lacZ} and SF-1$^{\Delta IR:lacZ}$ mice, using the β-galactosidase signal as marker for the VMH. During these measurements, the area was kept constant by using the "specify ROI" plug-in.

2.3.4 Electrophysiology

Mice were anesthetized with halothane (B4388; Sigma-Aldrich) and decapitated. Coronal slices (250 - 300 μm) containing the VMH and the ARC were cut with a vibrating microtome (HM-650 V; Thermo Scientific) under cold (4 °C), carbogenated (95% O_2 and 5% CO_2), glycerol-based modified artificial cerebrospinal fluid (GaCSF) (Ye *et al.* , 2006). GaCSF contained (in mM) 250 glycerol, 2.5 KCl, 2 $MgCl_2$, 2 $CaCl_2$, 1.2 NaH_2PO_4, 10 HEPES, 21 $NaHCO_3$, 5 glucose, adjusted to pH 7.2 with NaOH.

If not mentioned otherwise, during the recordings the slices were continuously superfused with carbogenated aCSF at a flow rate of 2 ml*min^{-1}. aCSF contained (in mM) 125 NaCl, 2.5 KCl, 2 $MgCl_2$, 2 $CaCl_2$, 1.2 NaH_2 PO_4, 21 $NaHCO_3$, 10 HEPES, and 5 glucose adjusted to pH 7.2 with NaOH. Patch-clamp recordings were performed at 22 - 24 °C with an EPC10 patch-clamp amplifier (HEKA). Data were sampled at intervals of 100 μs (10 kHz) and low-pass filtered at 2 kHz with a four-pole Bessel filter. Whole-cell capacitance was determined by using the capacitance compensation (C-slow) of the EPC10. Cell input resistances were calculated from voltage responses to hyperpolarizing current pulses. The calculated liquid junction potential (14.6 mV) between intracellular and extracellular solution was not compensated.

2.3.5 Electron microscopy

12 week old mice were anesthetized and perfused transcardially with saline followed by Somogyi-Takagi fixative containg 4% paraformaldehyde and 0.8% glutaraldehyde in 0.1 M phosphate buffer. A tissue block containing the VMH and the ARC was dissected from each brain. 50 μm thick vibratome sections were cut and thoroughly washed in 0.1 M phosphate buffer (PB). To eliminate unbound aldehydes, sections were incubated in 1% sodiumborohydride for 15 min, and then rinsed in PB. Next, sections were incubated in rabbit anti-GFP (Molecular Probes Inc., Eugene, OR) (dilution 1 : 1000 in PB) for 24 h at room temperature. Subsequently, sections were incubated in biotinylated goat anti- rabbit immunoglobulin (dilution 1 : 250; Vector Laboratories, Burlingame, CA, USA) at room temperature. After washing in PB, sections were placed in avidin-biotin-complex (ABC Elite Kit, Vector Labs) for 2 h at RT. The tissue-bound peroxidase was

visualized by a diaminobenzidine reaction. After the immunostaining, the sections were osmicated (15 min in 1% osmic acid in PB), and dehydrated in increasing ethanol concentrations. During the dehydration, 1% uranyl-acetate was added to the 70% ethanol to enhance ultrastructural membrane contrast. Dehydration was followed by flat-embedding in Araldite. Ultrathin sections were cut on a microtome, collected on Formvar-coated single-slot grids and analyzed with a Tecnai 12 Biotwin (FEI Company) electron microscope. The quantitative analysis of synapse numbers was performed in a double-blind fashion on electron micrographs from mice of different experimental groups. To obtain a complementary measure of axo-somatic synaptic number, unbiased for possible changes in synaptic size, the disector technique was used. On consecutive 90-nm-thick sections, the average projected height of the synapses was determined and about 30% of this value was used as the distance between the disectors. On the basis of this calculation, the number of axo-somatic synapses was counted from 7 perikaryal profiles in two consecutive serial sections roughly 270 nm apart (the "reference" and "look-up" sections) from each tissue block. In order to increase the sampling size, the procedure was repeated in such a way that the reference and look-up sections were reversed. The numbers of symmetrical, asymmetrical and total contacts were collected independently from serial sections. Synapse characterization was performed at 20000 magnification, while all quantitative measurements were performed on electron micrographs at a magnification of 11000. Symmetric and asymmetric synapses were counted on all selected neurons only if the pre- and/or postsynaptic membrane specializations were clearly seen and synaptic vesicles were present in the presynaptic bouton. Asymmetric synapses are formed by axons that contain large vesicles and excitatory neurotransmitters (i.e. primarily glutamate; excitatory synapses). In contrast, symmetric synapses have presynaptic axons with small synaptic vesicles that contain the inhibitory transmitter GABA. The presynaptic and postsynaptic densities of these synapses are approximately of equal thickness (inhibitory synapses). Synapses with neither clearly symmetric nor asymmetric membrane specializations were excluded from the assessment. The plasma membranes of selected cells were outlined on photomicrographs and their length was measured with the help of a chartographic wheel. Plasma membrane length values measured in the individual

animals were added and the total length was corrected to the magnification applied. The synaptic counts were expressed as numbers of synapses on a membrane length unit of 100 μm.

2.4 Biochemistry

2.4.1 Protein extraction

Shock-frozen tissues were thawed and homogenized in lysis buffer (50 mM HEPES (pH 7.4), 1% Triton X-100, 0.1 M NaF, 10 mM EDTA, 50 mM NaCl, 10 mM Na_3O_4V, 0.1% SDS, 10 μg/ml Aprotinin, 2 mM Benzamidine, 2 mM PMSF) using a Ultrathurrax homogenizer (IKA Werke, Staufen, Germany). Particulate matter was removed by centrifugation for 1 h at 4°C. The supernatant was transferred to a new reaction tube and protein concentrations were determined by measuring the sample absorption at 280 nm with a NanoDrop ND-1000 UV- Vis Spectrophotometer (Peqlab, Erlangen, Germany). Proteins that contain tryptophane, tyrosine residues or cysteine-cysteine disulphide bonds absorb in the UV range of 280 nm. Subsequently, protein extracts were diluted to 10 mg/ml with lysis buffer and 4 x SDS sample buffer (125 mM Tris- HCl (pH 6.8), 5% SDS, 43.5% glycerol, 100 mM DTT, and 0.02% bromphenol blue), incubated at 95°C for 5 min and stored at -80°C.

2.4.2 Western blot analysis

Frozen protein extracts were thawed at 95°C for 5 min, then separated on 10% (v/v) SDS polyacrylamide gels and semi-dry blotted onto PVDF membranes (Bio-Rad, München, Germany). Membranes were then incubated with 1% blocking reagent (Roche, Mannheim, Germany) for 1 h at RT or overnight at 4°C. Subsequently, primary antibodies (table 2.3) diluted in 0.5% blocking solution were applied for 1 h at RT or overnight at 4°C. PVDF membranes were then washed three times for 15 min with 1 x TBS/1%Tween. After 1 h incubation at RT with the respective secondary antibodies, membranes were washed three times for 15 min with 1 x TBS/1%Tween, incubated for 1 min in Pierce ECL Western Blotting Substrate (Perbio Science, Bonn, Germany), sealed in a plastic bag and exposed

to chemiluminescence films (Amersham, Braunschweig, Germany). Films were developed in an automatic developer (Kodak, Stuttgart, Germany).

Table 2.3: Primary western blot antibodies

Antigen	Catalogue Nr.	Distributor	Dilution
β-actin	#A5441	Sigma Aldrich, Seelze, Germany	1:10000
α-tubulin	#T6074	Sigma Aldrich, Seelze, Germany	1:5000
IR-β	sc-711	Cell signaling, Danvers, USA	1:500

2.4.3 Enzyme-linked immunosorbent assays (ELISA)

Serum insulin, leptin and testosterone, as well as plasma corticosterone, epinephrine and norepinephrine concentrations were measured by ELISA according to manufacturer's guidelines (Mouse Leptin ELISA, Mouse/Rat Insulin ELISA, Crystal Chem, Downers Grove, USA; Corticosterone Enzyme Immunoassay Kit, Assay Designs Inc., Ann Arbor, USA; Epinephrine EIA, Norepinephrine EIA, DRG Instruments, Heidelberg, Germany). For evaluation of glucagon plasma levels, an radioimmunoassay (RIA) was performed according to manufacturer's guidelines Glucagon RIA Kit, #GL-32K, LINCO Research, St.Charles, USA).

2.5 Computer analysis

2.5.1 Densitometrical analysis

Protein expression was assessed by Western blot analysis and bands were measured in intensity per mm2 using the Quantity One Software (Bio-Rad, München, Germany). After background subtraction, each sample was normalized to an internal loading control. Average protein expression of control mice was set to 100% and compared to protein expression of knockout animals unless stated otherwise.

2.5.2 Statistical methods

Data sets were analyzed for statistical significance using a two-tailed unpaired student's t-test. All p values below 0.05 were considered significant. All displayed values are means $\pm$ S.E.M.. * $p \leq 0.05$; ** $p \leq 0.01$; *** $p \leq 0.001$ versus controls.

2.6 Chemicals and biological material

Size markers for agarose gel electrophoresis (Gene RulerTM DNA Ladder Mix) and for SDS-PAGE (Page RulerTM Prestained Protein Ladder Mix) were obtained from MBI Fermentas, St. Leon-Rot, Germany. RedTaq DNA Polymerase and 10x RedTaq buffer were purchased from Sigma-Aldrich, Seelze, Germany. All chemicals used in this work are listed in table 1 and all enzymes used in this work are listed in tables 2.4, 2.5 and 2.6. Solutions were prepared with double distilled water.

Table 2.4: Chemicals 1

Chemical	Supplier
β-mercaptoethanol	Applichem, Darmstadt, Germany
ϵ-aminocaproic acid	Sigma-Aldrich, Seelze, Germany
0.9% saline (sterile)	Delta Select, Pfullingen, Germany
2,2,2-Tribromoethanol (Avertin)	Sigma-Aldrich, Seelze, Germany
2-Methyl-2-Butanol	Sigma-Aldrich, Seelze, Germany
Acetic acid	Merck, Darmstadt, Germany
Acetone	KMF Laborchemie, Lohmar, Germany
Acrylamide	Roth, Karlsruhe, Germany
Agarose	Peqlab, Erlangen, Germany
Agarose (Ultra Pure)	Invitrogen, Karlsruhe, Germany
Ammonium Acetate	Merck, Darmstadt, Germany
Ammoniumpersulfat (APS)	Sigma-Aldrich, Seelze, Germany
Aprotinin	Sigma-Aldrich, Seelze, Germany
Avidin Biotin Complex-Vectastain Elite	Vector, Burlingame, USA

Table 2.5: Chemicals 2

Chemical	Supplier
Bacillol	Bode Chemie, Hamburg, Germany
Barium hydroxide	Sigma-Aldrich, Seelze, Germany
Benzamidine	Sigma-Aldrich, Seelze, Germany
Bovine serum albumin (BSA)	Sigma-Aldrich, Seelze, Germany
Bromphenol blue	Merck, Darmstadt, Germany
Calcium chloride	Merck, Darmstadt, Germany
Chloroform	Merck, Darmstadt, Germany
Desoxy-ribonucleotid-triphosphates (dNTPs)	Amersham, Freiburg, Germany
Diaminobenzidin (DAB)	Dako, Kopenhagen, Denmark
Dimethylsulfoxide (DMSO)	Merck, Darmstadt, Germany
di-Natriumhydrogenphosphat	Merck, Darmstadt, Germany
Enhanced chemiluminescence (ECL) Kit	Perbio Science, Bonn, Germany
Ethanol, absolute	Applichem, Darmstadt, Germany
Ethidium bromide	Sigma-Aldrich, Seelze, Germany
Ethylendiamine tetraacetate (EDTA)	Applichem, Darmstadt, Germany
Forene (isoflurane)	Abbot GmbH, Wiesbaden, Germany
Glucose 20%	DeltaSelect, Pfullingen, Germany
Glycerol	Serva, Heidelberg, Germany
Glycine	Applichem, Darmstadt, Germany
Halothane	Sigma-Aldrich, Seelze, Germany
HEPES	Applichem, Darmstadt, Germany
Hydrochloric acid (37%)	KMF Laborchemie, Lohmar, Germany
Hydrogen peroxide	Sigma-Aldrich, Seelze, Germany
Insulin	Novo Nordisk, Bagsvaerd, Denmark
Isopropanol (2-propanol)	Roth, Karlsruhe, Germany
Kaisers Glycerin Gelatine	Merck, Darmstadt, Germany

Table 2.6: Chemicals 3

Chemical	Supplier
Leptin, recombinant	NHPP, Torrence, USA
Magnesium chloride	Merck, Darmstadt, Germany
Methanol	Roth, Karlsruhe, Germany
Nitrogen (liquid)	Linde, Pullach, Germany
Octenisept	Schülke & Mayr, Norderstedt, Germany
Paraformaldehyde (PFA)	Sigma-Aldrich, Seelze, Germany
Phenylmethylsulfonylfluoride (PMSF)	Sigma-Aldrich, Seelze, Germany
Phosphate buffered saline (PBS)	Gibco BRL, Eggenstein, Germany
Potassium chloride	Merck, Darmstadt, Germany
Potassium hydroxide	Merck, Darmstadt, Germany
Sodium acetate	Applichem, Darmstadt, Germany
Sodium chloride	Applichem, Darmstadt, Germany
Sodium citrate	Merck, Darmstadt, Germany
Sodium dodecyl sulfate	Applichem, Darmstadt, Germany
Sodium fluoride	Merck, Darmstadt, Germany
Sodium heparin (Liquemin)	Roche, Grenzach-Wyhlen, Switzerland
Sodium hydroxide	Applichem, Darmstadt, Germany
Sodium orthovanadate	Sigma-Aldrich, Seelze, Germany
Sucrose	Applichem, Darmstadt, Germany
Tetramethylethylenediamine (TEMED)	Sigma-Aldrich, Seelze, Germany
Tissue Freezing Medium	Jung, Heidelberg, Germany
Tramadolhydrochlorid (Tramal)	Grünenthal, Aachen, Germany
Trishydroxymethylaminomethane (Tris)	Applichem, Darmstadt, Germany
Triton X-100	Applichem, Darmstadt, Germany
Tween 20	Applichem, Darmstadt, Germany
Vectashield Mounting Medium with DAPI	Vector, Burlingame, USA
Western Blocking Reagent	Roche, Mannheim, Germany
Zinc sulfate	Sigma-Aldrich, Seelze, Germany

3 Results

3.1 Generation of SF-1 specific insulin receptor knockout mice

To investigate the role of insulin signaling in SF-1 neurons in the VMH in the CNS mediated control of energy homeostasis, transgenic mice that express the Cre recombinase under control of the SF-1 promotor (Dhillon *et al.* , 2006) were crossed with mice with loxP-site flanked exon 4 of the insulin receptor gene (Brüning *et al.* , 1998) (figure 3.1).

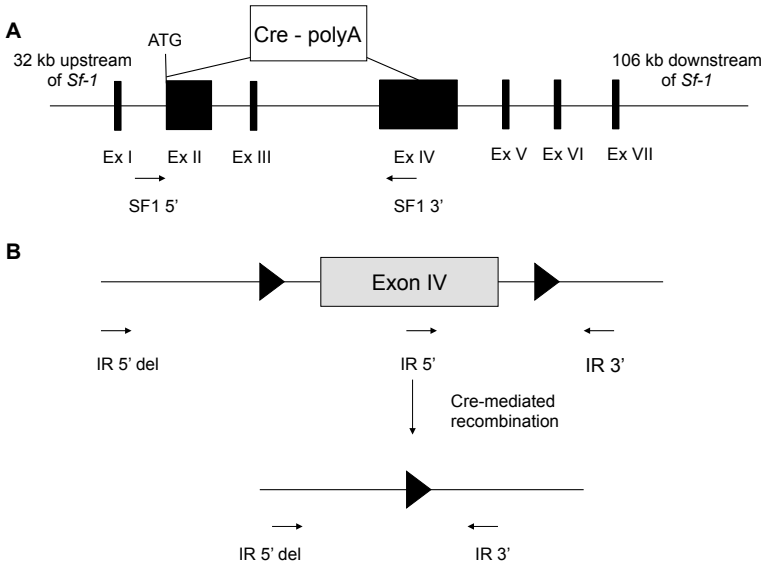

Figure 3.1: Scheme of SF-1 Cre mediated recombination of the insulin receptor allele.
(A) Transgenic SF-1 Cre construct generated by Dhillon *et al.* (2006). ***(B)*** Exon 4 of the insulin receptor flanked by loxP-sites. Cre mediated recombination leads to the excision of exon 4, which results in a frameshift mutation and thereby introduces a pre-mature stop codon. This results in severely truncated insulin receptor mRNA, which is degraded by the nonsense-mediated decay mechanism in the Cre-expressing cells (Brüning *et al.* , 1998). Depicted by arrows are the PCR primers used for genotyping of the alleles, triangles represent loxP-sites.

In cells, that express the Cre recombinase, exon 4 of the *insulin receptor* gene is excised, leading to a pre-mature stop-codon. The severely truncated *insulin receptor* mRNA is then degraded by nonsense-mediated decay mechanisms. Even if the nonsense-mediated

decay fails and remaining mRNA is translated, the lack of the transmembrane domain will lead to a non-functional receptor.

To confirm the VMH-specific expression of the SF-1 Cre transgene, these mice were also crossed to RosaArte1 and Z/eG mice (Novak *et al.* , 2000; Seibler *et al.* , 2003). Due to the fact that SF-1 gene expression is also reported in the adrenal gland, pituitary gland and testis, IHC was performed using the aforementioned reporter strains to visualize the magnitude of expression in this tissues. Figure 3.2 shows massive recombination in the VMH (3.2 A), but little expression was also seen in the cerebral cortex (not shown). In the pituitary gland, GFP positive cells were found, although to a much lesser extend (3.2 B). Furthermore, in the cortex of the adrenal gland (3.2 C) and in Sertoli cells in the testis (3.2 D) of SF-1^{GFP} mice little Cre expression was observed.

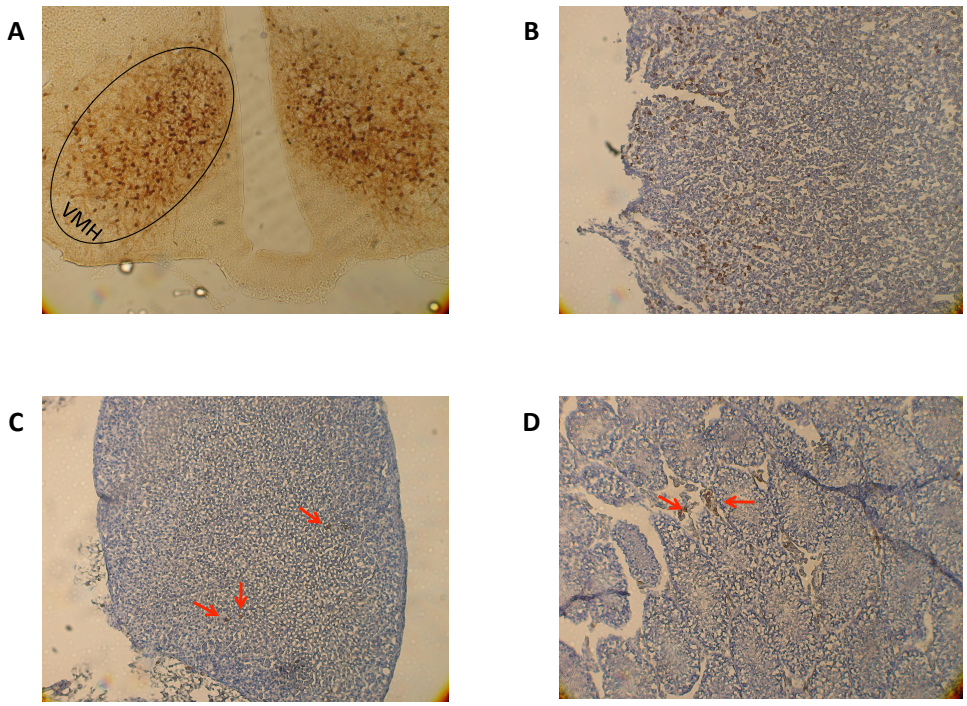

Figure 3.2: Immunohistochemistry using peroxidase-coupled GFP antibodies to visualize Cre expression in SF-1^{GFP} mice in the brain and peripheral organs. β-galactosidase was stained in SF-1^{lacZ} and SF-1$^{lacZ:\Delta IR}$ mice and positive neurons were counted.
(A) GFP expression in the VMH of SF-1^{GFP} mice. ***(B)*** GFP expression in the pituitary gland.
(C) GFP expression in the adrenal gland. ***(D)*** GFP expression in the testis.

Due to the fact that expression of endogenous *Sf-1* is reported in several peripheral tis-

sues (Parker *et al.* , 2002), western blot analysis was performed of metabolically relevant tissues to exclude any effects of IR deletion in peripheral organs. As shown in figure 3.3, no major alterations were observed in the expression levels of the IR between control and SF-1$^{\Delta IR}$ mice. Although the SF-1 Cre is mainly expressed in the VMH of the hypothalamus, IR protein levels did not differ in whole-hypothalamus and the same holds true for peripheral organs and the pituitary gland, where no or little Cre expression was observed or reported.

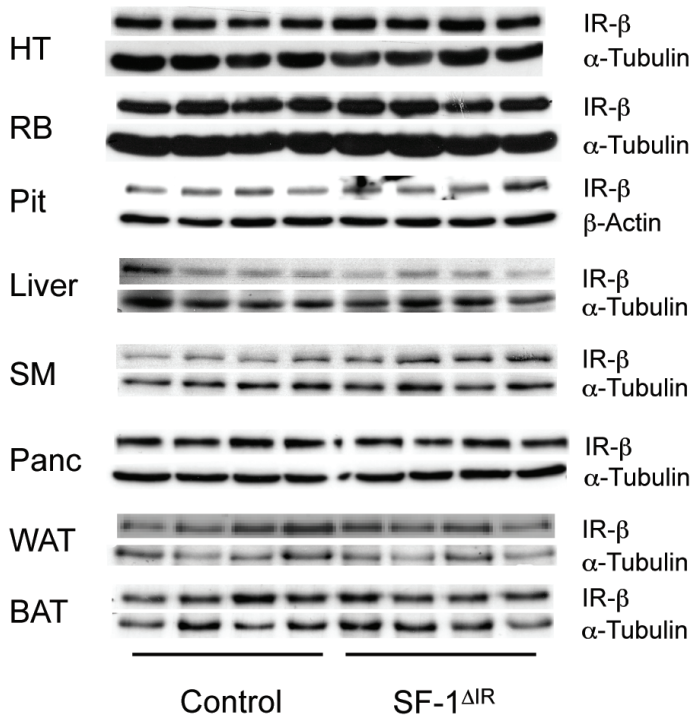

Figure 3.3: Western blot analysis of brain and peripheral tissue lysates from control and SF-1$^{\Delta IR}$ mice for the β-subunit of the IR and α-tubulin or β-actin as loading control.
BAT, brown adipose tissue; HT, hypothalamus; Pit, pituitary gland; Panc, pancreas; RB, remaining brain without the hypothalamus; SM, skeletal muscle; WAT, white adipose tissue.

Owing to the expression pattern of the SF-1 Cre in the hypothalamus, the pituitary gland, Sertoli cells in testis and in Leydig cells of ovaries of SF-1$^{\Delta IR}$ animals (Ikeda *et al.*

, 1994), the reproductive ability of both SF-1$^{\Delta IR}$ males and females was assessed by the evaluation of breeding success. To this end, male and female SF-1$^{\Delta IR}$ animals were bred with the respective control IR$^{fl/fl}$ mice and average litter size and average litter frequency were analyzed. As shown in figure 3.4A and B, neither average litter size nor average litter frequency differed between the genotypes.

Furthermore, quantitative real-time PCR analysis was performed on pituitary gland cDNA to investigate the effect of IR deficiency in the VMH on key hormones of the hypothalamic-pituitary-gonadal (HPG) axis. Hence, the expression levels of follicle-stimulating hormone (*Fsh*β), luteinizing hormone (*Lh*β), thyroid-stimulating hormone (*Tsh*β) and growth hormone (*Gh*) were determined. Figure 3.4C indicates no differences in the expression levels of pivotal hormones of the HPG axis between control and SF-1$^{\Delta IR}$ male mice. This was further confirmed by the analysis of free triiodothyronine (T_3) levels in the serum of control and SF-1$^{\Delta IR}$ males, where no alteration were detectable (3.4D). Thus, the IR deficiency of SF-1 neurons did not affect fertility or the HPG axis.

As the IR shares a high homology with the insulin-like growth factor 1 receptor (IGF-1R) and shares a high homology to other receptor tyrosine-kinases, there are no appropriate antibodies available for the detection of the IR with IHC methods. Thus, *in situ* hybridization (ISH) was performed on hypothalami of control SF-1^{lacZ} and SF-1$^{lacZ:\Delta IR}$ animals. The *in situ* probe was designed against the exon 4 of the *insulin receptor* gene for being able to distinguish between control and SF-1$^{\Delta IR}$ genotypes. Additionally, the exon 4 encodes for a subunit of the ligand-binding domain of the IR, therefore providing highest specificity for the *in situ* probe (red). The analyzed sections were co-stained against β-galactosidase to visualize SF-1 Cre expressing neurons (green) and with DAPI to visualize the nuclei of the surrounding neurons (blue). Figure 3.5A shows representative sections of control and SF-1$^{lacZ:\Delta IR}$ brain slices. Subsequently, the *insulin receptor* mRNA signal was quantified in SF-1$^{lacZ:\Delta IR}$ compared to controls using ImageJ (NIH), verifying the successful deletion of the *insulin receptor* gene (figure 3.5B).

To address if the deficiency for the IR in SF-1$^{\Delta IR}$ mice also translates into functional down-regulation of the PI_3K pathway, immunohistochemistry (IHC) staining for the second messenger of the PI_3K pathway, PiP_3, were performed. To this end mice were either

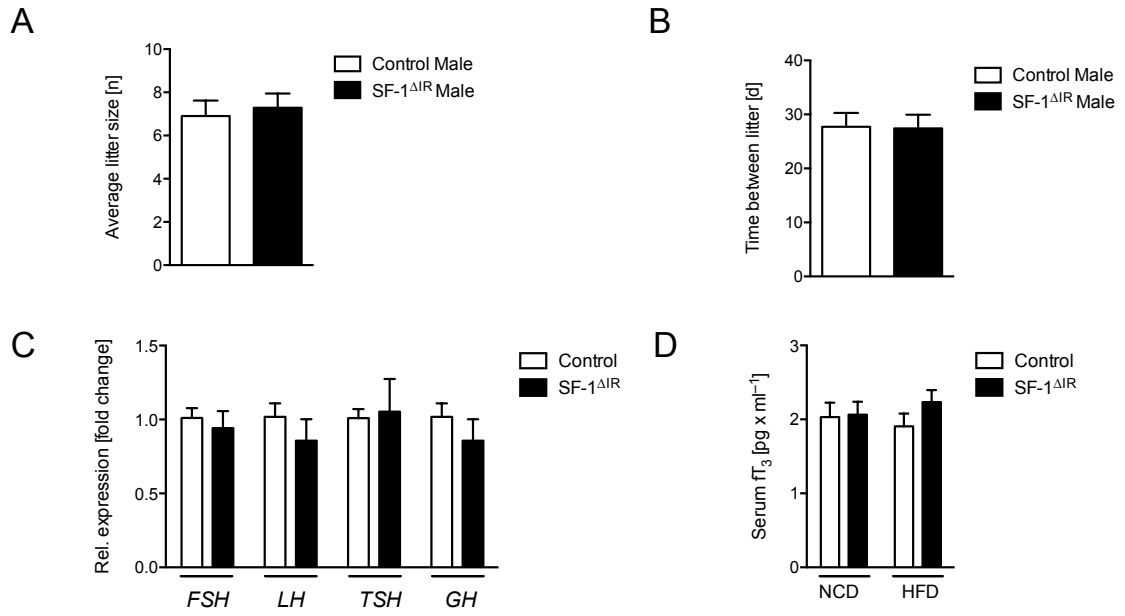

Figure 3.4: Fertility and function of the HPG axis was investigated in control and SF-1$^{\Delta IR}$ knockout animals.
(A) Average littersize of breedings with male control (n = 3, 10 litters) and SF-1$^{\Delta IR}$ (n = 3, 14 litters). ***(B)*** Average time between litter of breedings with control (n = 3, 10 litters) and SF-1$^{\Delta IR}$ (n = 3, 14 litters). ***(C)*** Quantitative real-time PCR analysis for expression levels of follicle-stimulating hormone (*Fshβ*), luteinizing hormone (*Lhβ*), thyroid-stimulating hormone (*Tshβ*) and growth hormone (*Gh*) in pituitary gland cDNA of control (n = 6) and SF-1$^{\Delta IR}$ knockout (n = 6) males. ***(D)*** Free triiodothyronine (T_3) levels in the serum of control (n = 20) and SF-1$^{\Delta IR}$ (n = 20) males.
Displayed values are means ± S.E.M..

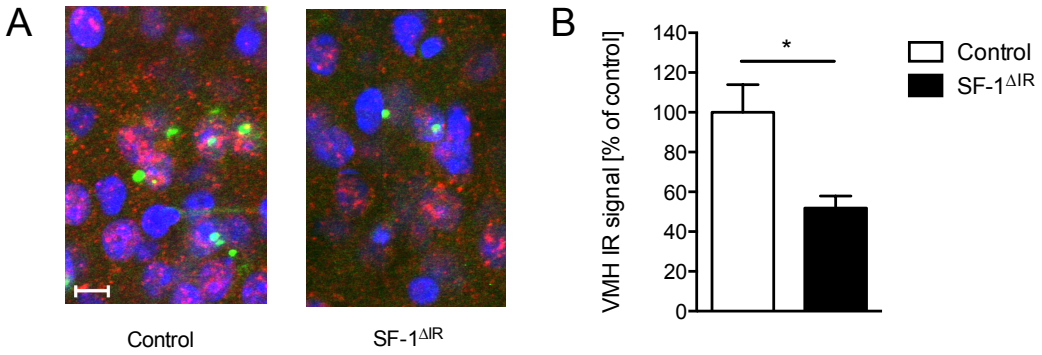

Figure 3.5: *In situ* hybridization (ISH) against *Insulin receptor* mRNA in control (SF-1^{lacZ}) and SF-1$^{lacZ:\Delta IR}$ animals. The ISH probe was designed against the exon 4 of the *insulin receptor* gene that is deleted upon Cre mediated recombination and thus will not detect remaining mRNA of the *insulin receptor*. Exon 4 encodes for a subunit of the ligand binding domain, hence providing a high specificity.
(A) Representative sections of controls and SF-1$^{\Delta IR}$ brain slices. *Insulin receptor* mRNA (red), anti-*β*-galactosidase immuno staining (green) and counterstaining for nuclei with DAPI (blue). Scale bar, 10 μm. ***(B)*** Quantification of the VMH *InsR* mRNA signal normalized to controls.
Displayed values are means ± S.E.M.; *, $p \leq 0.05$.

injected with saline into the *vena cava inferior*, or stimulated for 10 or 20 min with 5U of human insulin. After the stimulation, both control (SF-1^{lacZ}) and SF-$1^{lacZ:\Delta IR}$ mice were transcardiacally perfused with PBS and subsequently stained for PiP_3 and β-galactosidase as marker for Cre-mediated recombination. PiP_3 levels were analyzed as described in Könner *et al.* (2007).

As shown in figure 3.6A, 56% of the SF-1 neurons in SF-1^{lacZ} mice showed low PiP_3 levels when injected with saline (35% showed moderate PiP_3 and 9% high levels). Upon 10 min of insulin stimulation, 57% of SF-1 neurons shifted to moderate PiP_3 levels, whereas only 19% remained on a low level and already 24% even showed high PiP_3 accumulation around the nucleus. When mice were finally stimulated for 20 min with 5U of insulin the majority of SF-1 neurons displayed high (43%) or moderate (44%) PiP_3 levels and only 13% remained on a low level. Prolonged insulin stimulation resulted in a shift towards higher PiP_3 levels in SF-1 neurons of SF-1^{lacZ} animals.

In contrast to SF-1^{lacZ} control mice, the shift towards higher PiP_3 levels was completely abolished in SF-$1^{lacZ:\Delta IR}$ mice, that lack the IR on SF-1 neurons. Figure 3.6B indicates that neither 10 min nor 20 min insulin stimulation resulted in a shift towards high or even moderate PiP_3 levels. Baseline PiP_3 levels after saline injection were mainly low (83% of SF-1 neurons low) and even after insulin stimulation for 10 min (86% low) or 20 min (81% low), no activation of PiP_3 formation could be observed.

Figure 3.6C upper panel shows representative images of control SF-1^{lacZ} and SF-$1^{lacZ:\Delta IR}$ knockout brain slices, injected with saline or either stimulated for 10 min or 20 min with 5U of human insulin, respectively. In the lower panel, exemplary images for PiP_3 levels of neurons with low, moderate or high levels are depicted. PiP_3 is visualized in red, β-galactosidase in green and counterstaining for the nuclei with DAPI is shown in blue.

Due to the fact that insulin and especially the PI_3K signaling pathway are survival signals for cells, number of SF-1 neurons was investigated in control SF-1^{lacZ} and SF-$1^{lacZ:\Delta IR}$ males. As depicted in figure 3.6D, numbers of β-gal positive neurons did not differ between the genotypes.

Taken together, Cre mediated recombination was verified in the VMH, pituitary gland, adrenal gland and testis of SF-1^{GFP} reporter animals (figure 3.2A - D). Besides, scattered

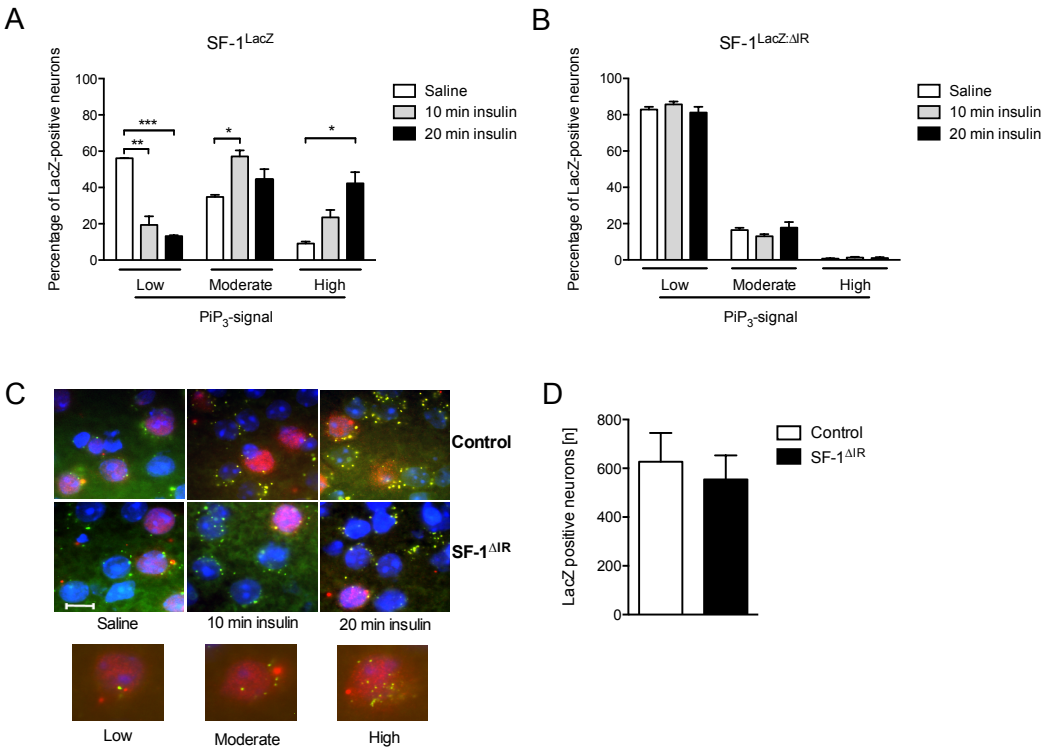

Figure 3.6: Double immunohistochemistry (IHC) staining for PiP_3 levels and β-galactosidase as marker for Cre-positive neurons in saline injected, 10 min or 20 min insulin-stimulated SF-1^{lacZ} control and SF-$1^{lacZ:\Delta IR}$ knockout animals.
(A) Quantification of PiP_3 levels in saline treated (n = 2; 891 SF-1 neurons), 10 min (n = 3, 1859 SF-1 neurons) or 20 min (n = 2, 1637 SF-1 neurons) insulin-stimulated SF-1^{lacZ} control animals. Displayed are percentages of neurons showing the respective PiP_3 levels for each stimulus. ***(B)*** Quantification of PiP_3 levels in saline treated (n = 3; 1735 SF-1 neurons), 10 min (n = 3, 1586 SF-1 neurons) or 20 min (n = 3, 1701 SF-1 neurons) insulin-stimulated SF-$1^{lacZ:\Delta IR}$ knockout animals. Displayed are percentages of neurons showing the respective PiP_3 levels for each stimulus. ***(C)*** *Upper panel* Representative images of PiP_3 formation in the VMH of SF-1^{lacZ} reporter and SF-$1^{lacZ:\Delta IR}$ knockout mice. Scale bar, 10 μm. *Lower panel* PiP_3 immunoreactivity magnitudes as described in Material & Methods. PiP_3 (green), β-galactosidase (red) and DAPI (blue). ***(D)*** Numbers of SF-1 neurons in VMH slices of SF-1^{lacZ} and SF-$1^{lacZ:\Delta IR}$ mice.
Displayed values are means $\pm$ S.E.M.; *, $p \leq 0.05$; ***, $p \leq 0.001$.

Cre expression was also observed in the spleen and ovaries (personal observation). Despite this expression pattern of the SF-1 Cre, no alterations in IR protein expression could be observed in brain lysates and metabolically relevant peripheral organs (figure 3.3). Furthermore, the number of SF-1 Cre positive neurons was not affected by the Cre-mediated IR deficiency (3.6D). Likewise, fertility was unchanged between control and SF-$1^{\Delta IR}$ mice and the functionality of the HPG axis was confirmed (figure 3.4). However, SF-1 Cre mediated recombination results in a reduced expression of *insulin receptor* mRNA, proven by *in situ* hybridization (figure 3.5). That the reduced expression also

translates into a efficient downregulation of the PI_3K pathway was verified using immunohistochemical stainings for the second messenger in this pathway, PiP_3 (figure 3.6).

3.2 Insulin silences VMH SF-1 neurons via K_{ATP} channels

Using SF-1^{GFP} mice, the effects of insulin stimulation on the electrophysiological properties were studied. To determine the insulin responsiveness of SF-1 neurons and SF-1 neurons that lack the insulin receptor (SF-$1^{GFP:\Delta IR}$ neurons), perforated patch clamp recordings were performed to ensure the integrity of intracellular components (figure 3.7A). Basic biophysical properties such as whole-cell capacitance, membrane potential, firing rate and input resistance were not significantly different between SF-1 neurons of the two genotypes (table 3.1).

Table 3.1: Electrophysiological parameters of SF-1 neurons in SF-1^{GFP} and SF-$1^{GFP:\Delta IR}$ mice.

	Whole-cell capacitance (pF)	Firing rate (Hz)	Membrane potential (mV)	Input resistance (GΩ)
SF-1^{GFP}	12.5 ± 1.0	3.5 ± 0.5	-46.8 ± 1.0	1.24 ± 0.12
	(n = 14)	(n = 13)	(n = 14)	(n = 14)
SF-$1^{GFP:\Delta IR}$	16.5 ± 1.8	2.9 ± 0.5	-48.5 ± 1.7	1.51 ± 0.24
	(n = 12)	(n = 9)	(n = 12)	(n = 11)

Insulin inhibited 43% (6 of 14) of the SF-1^{GFP} neurons (figure 3.7C) recorded from the medio-basal VMH, where most of the insulin-stimulated PiP_3 formation was detectable. In the subset of insulin-responsive neurons, the membrane potential significantly hyperpolarized upon insulin stimulation from -48.2 ± 0.7mV to -54.1 ± 1.7mV ($n = 6$; $p < 0.05$; figure 3.7D) and the firing rate was significantly reduced from 2.2 ± 0.5 Hz to 0.7 ± 0.5 Hz ($n = 5$; $p < 0.05$; figure 3.7D). Application of the specific K_{ATP} channel antagonist tolbutamide along with insulin resulted in the recovery of membrane potential and firing rate to control values (figure 3.7D). In contrast, none of the SF-$1^{GFP:\Delta IR}$ neurons were inhibited by insulin (0 of 12; figure 3.7C). Of note, insulin induced excitation in one of the SF-1GFP neurons and two of the SF-$1^{GFP:\Delta IR}$ neurons. Taken together, our results indi-

cate that insulin modulates the biophysical properties in a subset of SF-1 VMH neurons in a similar manner as it does for POMC neurons in the ARC.

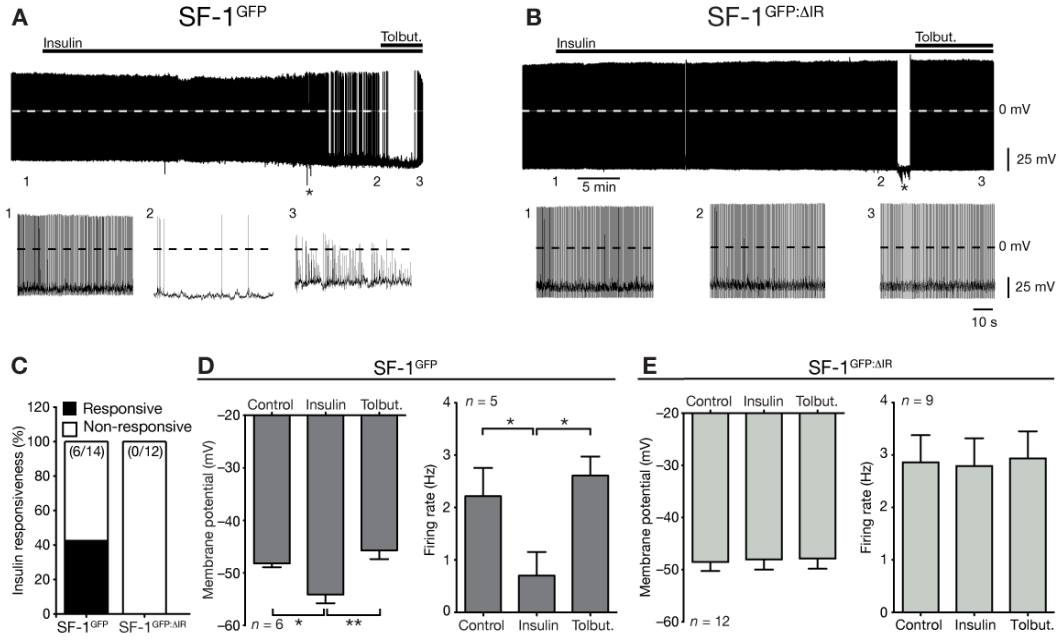

Figure 3.7: Perforated patch-clamp recordings were performed of GFP positive neurons from SF-1^{GFP} and SF-1$^{GFP:\Delta IR}$ mice.
(A) Representative recording trace of an identified insulin-responsive SF-1-positive neuron in a hypothalamic slice from an SF-1^{GFP} mouse before and during addition of 200 nM insulin, followed by application of 200 μM tolbutamide (tolbut.). ***(B)*** Representative recording trace of an identified SF-1-positive a neuron from a SF-1$^{GFP:\Delta IR}$ mouse before and during addition of 200 nM insulin, followed by application of 200 μM tolbutamide. ***(C)*** Percentage of insulin-responsive SF-1 neurons from SF-1^{GFP} mice and SF-1$^{GFP:\Delta IR}$ mice. ***(D)*** *Left panel* Membrane potential of identified SF-1 neurons in hypothalamic slices from SF-1^{GFP} before and during application of 200 nM insulin, followed by addition of 200 μM tolbutamide (n = 6 neurons per group). *Right panel* Firing frequency of identified SF-1 neurons in hypothalamic slices from SF-1^{GFP} mice before and during application of 200 nM insulin, followed by addition of 200 μM tolbutamide (n = 5 neurons per group). ***(E)*** *Left panel* Membrane potential of identified SF-1 neurons from SF-1$^{GFP:\Delta IR}$ mice before and during application of 200 nM insulin, followed by addition of 200 μM tolbutamide (n = 12 neurons per group). *Right panel* Firing frequency of identified SF-1 neurons from SF-1$^{GFP:\Delta IR}$ mice before and during application of 200 nM insulin, followed by addition of 200 μM tolbutamide (n = 9 neurons per group).
Displayed values are means $\pm$ S.E.M.; *, $p \leq 0.05$; **, $p \leq 0.01$; ***, $p \leq 0.001$.

3.3 Insulin and leptin responsive SF-1 neurons are distinct sub-populations

To address whether leptin-regulated SF-1 VMH neurons and insulin-regulated SF-1 VMH neurons might segregate into distinct populations, whole-cell patch clamp electrophysi-

ological recordings from identified SF-1 VMH neurons were performed with individual or sequential application of leptin and insulin (tables 3.2, 3.3 and 3.4). Experiments were performed in collaboration with Joel K. Elmquist and Kevin W. Williams. Tables are adapted from Klöckener *et al.* (2011).

Table 3.2: Responses of SF-1 neurons to leptin and insulin.

	Leptin	Insulin
Depolarized	8 (11.4%)	0 (0%)
Hyperpolarized	14 (20.0%)	5 (13.2%)
No response	48 (68.6%)	33 (86.8%)
Total	70 (100%)	38 (100%)

This analysis revealed that SF-1 VMH neurons that depolarized upon leptin stimulation did not decrease firing frequency upon subsequent insulin stimulation and that 3 of 21 neurons, which did not respond to leptin, hyperpolarized upon subsequent insulin stimulation (table 3.3).

Table 3.3: Responses of SF-1 neurons to sequential leptin and insulin double application.

		Leptin 1st	
		Depolarized	No response
Insulin 2nd	Hyperpolarized	0	3
	No response	2	18
	Total	2	21

Moreover, 1 of 16 neurons that did not to respond to insulin depolarized upon subsequent leptin treatment, and 5 of 16 neurons that did not respond to insulin hyperpolarized upon subsequent leptin application (table 3.4).

Collectively, these experiments provide evidence that leptin and insulin responses of SF-1 VMH neurons are likely to segregate, probably representing two distinct neuronal populations.

Table 3.4: Responses of SF-1 neurons to sequential insulin and leptin double application.

		Insulin 1st
		No response
Leptin 2nd	Depolarized	1
	Hyperpolarized	5
	No response	10
	Total	16

3.4 Attenuated obesity in SF-1$^{\Delta IR}$ mice upon high-fat diet feeding

To investigate the effect of insulin receptor deficiency in VMH SF-1 neurons on energy homeostasis, control (IR$^{fl/fl}$) and SF-1$^{\Delta IR}$ were fed either a normal-chow (NCD) or a high-fat diet (HFD) for 16 weeks after weaning. Under NCD conditions, no alterations could be observed in the body weight of control and SF-1$^{\Delta IR}$ males (figure 3.8A triangles) and females (personal observation). Accordingly, neither total body fat content nor epigonadal fat pad weight did differ between the genotypes on NCD in male (figure 3.8B and C) and female mice (personal observation).

Upon HFD feeding, male control mice showed significantly increased body weight after 3 weeks when compared to control males fed a NCD. In contrast, HFD-fed SF-1$^{\Delta IR}$ males were completely protected against the high-fat diet induced weight gain until 14 weeks of age. Only from 15 weeks of age on, a difference was observed between NCD-fed controls and SF-1$^{\Delta IR}$ fed a HFD, whereas SF-1$^{\Delta IR}$ on HFD remained significantly lighter when compared to HFD-fed controls (figure 3.8A). In line with this findings, SF-1$^{\Delta IR}$ males fed a HFD displayed reduced epigonadal fat pad weight and total body fat content measured by nuclear magnetic resonance spectography as compared to HFD-fed control males at the age of 20 weeks (figure 3.8B, C).

To confirm that the lower body weight results from reduced adiposity, serum leptin levels were measured in 8 and 20 weeks old control and SF-1$^{\Delta IR}$ males, both fed NCD and HFD. As shown in figure 3.9A, leptin levels are significantly lower in HFD fed SF-1$^{\Delta IR}$

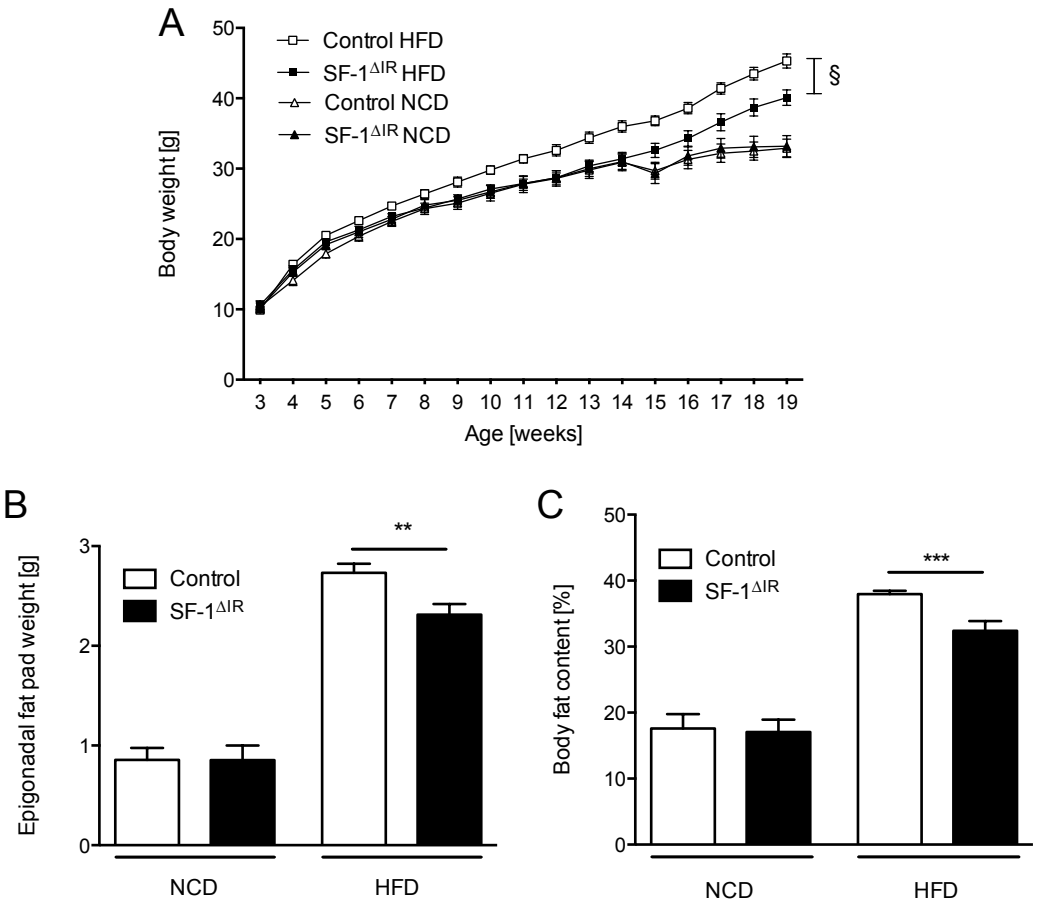

Figure 3.8: SF-1$^{\Delta IR}$ are protected against HFD- induced weight gain.
(A) Average body weight curve of control and SF-1$^{\Delta IR}$ fed either normal chow diet (NCD) or high-fat diet (HFD) over the period of 16 weeks (n > 15 per genotype and diet). ***(B)*** Average epigonadal fat pad weight of control and SF-1$^{\Delta IR}$ animals on NCD and HFD at the age of 20 weeks (n > 15 per genotype and diet). ***(C)*** Average total body fat content of control and SF-1$^{\Delta IR}$ animals on NCD and HFD at the age of 20 weeks (n > 15 per genotype and diet).
Displayed values are means $\pm$ S.E.M.; *, $p \leq 0.05$; **, $p \leq 0.01$; ***, $p \leq 0.001$; §, $p \leq 0.01$ for the body weight curve.

males compared to controls, both at 8 and 20 weeks of age. To examine the expansion of the epigonadal white adipose tissue (WAT), sections of WAT were analyzed according to the size of the adipocytes. As shown in figure 3.9B and C, the average size of adipocytes in 20 week old SF-1$^{\Delta IR}$ males was decreased in comparison to control animals on HFD.

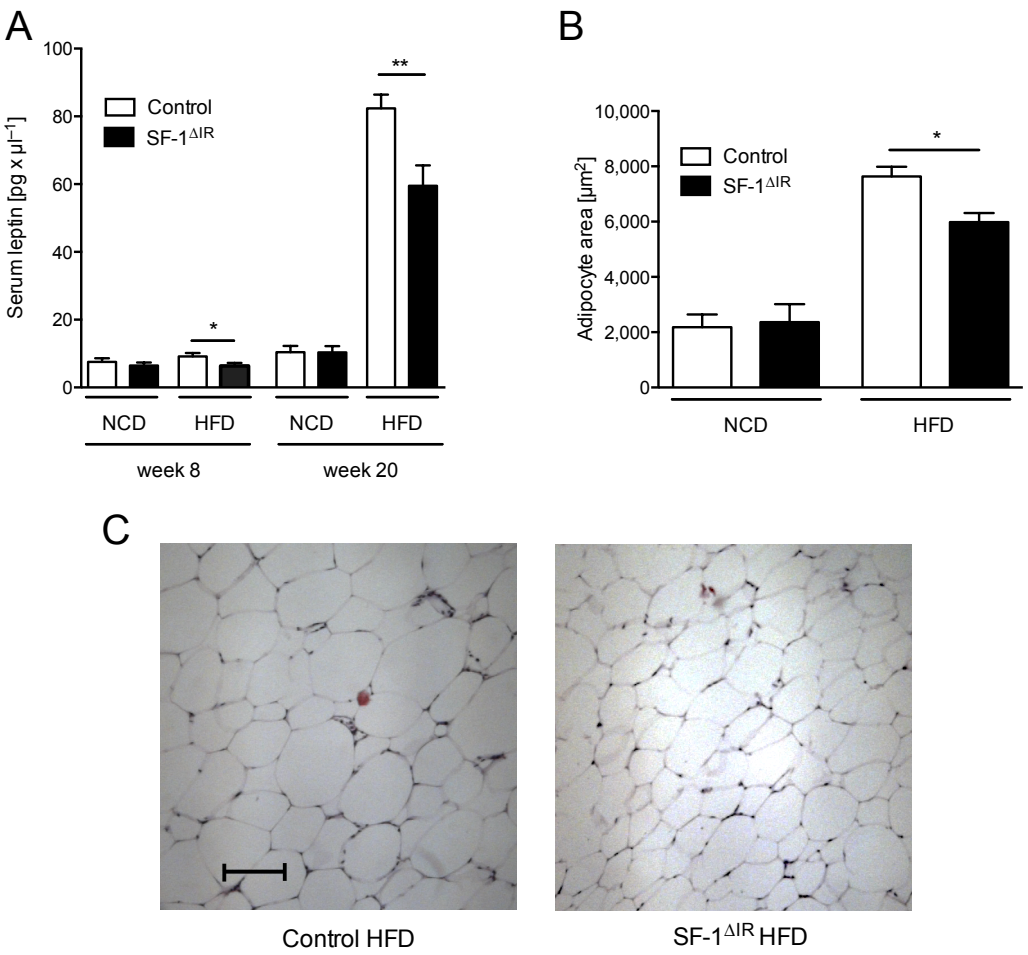

Figure 3.9: Reduced adiposity in HFD-fed SF-1$^{\Delta IR}$ males.
(A) Average serum leptin levels of control and SF-1$^{\Delta IR}$ fed either NCD or HFD at the age of 8 and 20 weeks (n > 15 per genotype and diet). ***(B)*** Average size of adipocytes in the epigonadal white adipose tissue (WAT) of control and SF-1$^{\Delta IR}$ animals on NCD and HFD at the age of 20 weeks (n > 3 per genotype and diet). ***(C)*** Representative images of H&E stained sections from WAT of control and SF-1$^{\Delta IR}$ on HFD at the age of 20 weeks. Scale bar, 100 μm.
Displayed values are means $\pm$ S.E.M.; *, $p \leq 0.05$; **, $p \leq 0.01$.

3.5 Reduced food intake as consequence of increased leptin sensitivity in young SF-1$^{\Delta IR}$ mice

As alterations in energy homeostasis can be caused by food intake, energy expenditure or both, it was investigated if these factors are altered by the ablation of the IR in SF-1 neurons in the VMH. To this end, young (6 - 7 weeks of age) and older (12 - 13 weeks) control and SF-1$^{\Delta IR}$ males on HFD were analyzed for daily caloric intake, O_2 consumption and CO_2 production by means of indirect calorimetry. This analysis revealed that

young SF-1$^{\Delta IR}$, that did not differ in body weight from controls, showed no alterations in O_2 consumption, CO_2 production or food intake (figure 3.10).

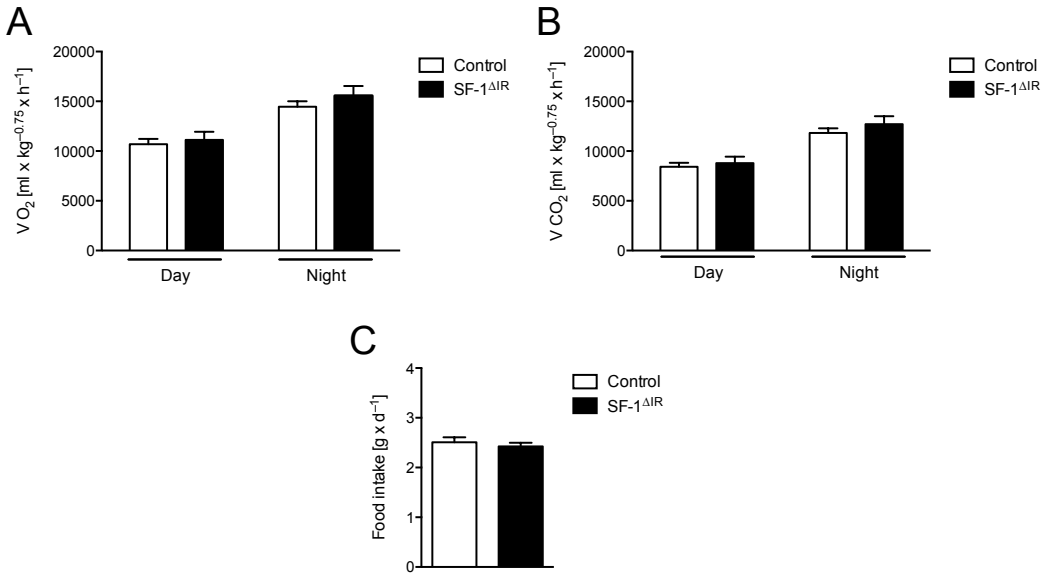

Figure 3.10: Unaltered energy expenditure and food intake of 6 to 7 week old control and SF-1$^{\Delta IR}$ males on HFD measured by indirect calorimetry.
(A) Average O_2 consumption normalized to lean mass of control and SF-1$^{\Delta IR}$ on HFD at the age of 6 to 7 weeks (n > 16 per genotype). ***(B)*** Average CO_2 production normalized to lean mass of control and SF-1$^{\Delta IR}$ on HFD at the age of 6 to 7 weeks (n > 16 per genotype). ***(C)*** Average food intake per day of control and SF-1$^{\Delta IR}$ on HFD at the age of 6 to 7 weeks (n > 16 per genotype). Displayed values are means $\pm$ S.E.M..

In contrast, older SF-1$^{\Delta IR}$ males showed a significantly decreased absolute food intake when compared to controls (figure 3.11C), whereas both O_2 consumption and CO_2 production remained unchanged when normalized to lean mass (figure 3.11A and B). However, if the food intake was normalized for the alterations in body weight, no obvious changes were detected anymore.

In line with the previous findings, neither locomotor activity nor respiration rate were altered in HFD-fed SF-1$^{\Delta IR}$ at both ages (personal observation).

To address whether the decreased body weight and absolute food intake in older SF-1$^{\Delta IR}$ males results from alterations in leptin's ability to reduce food intake, 7 to 8 week old HFD-fed controls and SF-1$^{\Delta IR}$ males were fasted overnight. Subsequently, they were injected with either artificial cerebrospinal fluid (aCSF) or 5 μg leptin intracerebroventricularly (icv) and food intake was monitored for 8 hours. Of note, animals used for this study did not display any differences in body weight. As depicted in figure 3.12, leptin

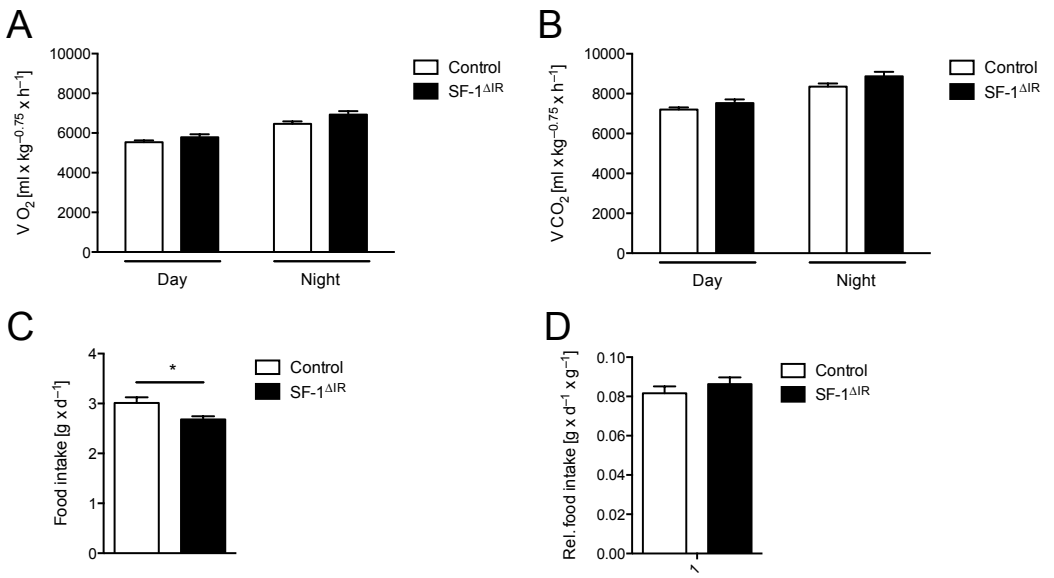

Figure 3.11: Unaltered energy expenditure and food intake of 12 to 13 week old control and SF-1$^{\Delta IR}$ males on HFD measured by indirect calorimetry.
(A) Average O_2 consumption normalized to lean mass of control and SF-1$^{\Delta IR}$ on HFD at the age of 13 to 14 weeks (n > 14 per genotype). ***(B)*** Average CO_2 production normalized to mass of control and SF-1$^{\Delta IR}$ on HFD at the age of 13 to 14 weeks (n > 14 per genotype). ***(C)*** Average absolute food intake per day of control and SF-1$^{\Delta IR}$ on HFD at the age of 12 to 13 weeks (n > 14 per genotype). ***(D)*** Average daily food intake normalized for body weight of control and SF-1$^{\Delta IR}$ on HFD at the age of 12 to 13 weeks (n > 14 per genotype).
Displayed values are means $\pm$ S.E.M.; *, $p \leq 0.05$.

was able to reduce food intake significantly further in SF-1$^{\Delta IR}$ males when compared to controls.

These results indicate an increased leptin sensitivity in SF-1$^{\Delta IR}$ mice, already before the onset of changes in body weight and absolute food intake.

3.6 Improved glucose metabolism in SF-1$^{\Delta IR}$ mice upon HFD-feeding

Previously, it could be shown that insulin's action in the CNS regulates peripheral glucose homeostasis (Koch *et al.* , 2008; Könner *et al.* , 2007; Obici *et al.* , 2002a; Pocai *et al.* , 2005), what is attenuated in conditions of diet-induced obesity (Belgardt *et al.* , 2010; Kleinridders *et al.* , 2009). Hence, intraperitoneal (i.p.) glucose tolerance tests and insulin tolerance tests were performed in 15 week old control and SF-1$^{\Delta IR}$ animals under NCD conditions and furthermore blood glucose levels and serum insulin concentrations were

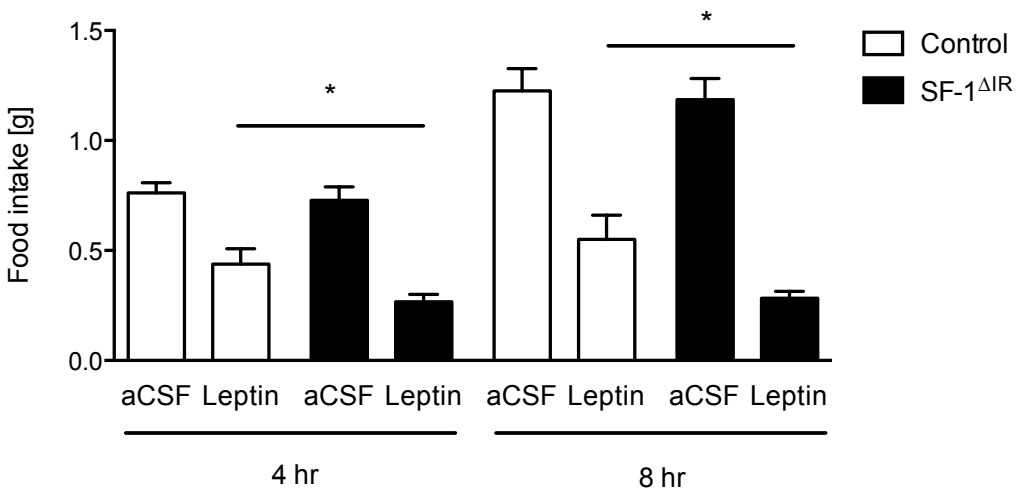

Figure 3.12: 7 to 8 week old, body weight matched, control and SF-1$^{\Delta IR}$ males on HFD were starved over night and subsequently intracerebroventricularly injected with either artificial cerebrospinal fluid (aCSF) or 5 μg leptin. Food intake was then monitored for 8 hours after re-feeding (n > 5 per genotype).
Displayed values are means $\pm$ S.E.M.; *, $p \leq 0.05$ in an unpaired, one-tailed student's t-test.

determined. The analysis revealed no alterations upon insulin receptor deficiency in the VMH on glucose homeostasis in both genotypes (figure 3.13).

Thus, the lack of insulin receptors on SF-1 neurons in the VMH does not alter peripheral glucose metabolism under NCD conditions.

When control and SF-1$^{\Delta IR}$ mice were exposed to HFD feeding, SF-1$^{\Delta IR}$ males revealed an improved glucose metabolism. Whereas blood glucose levels remained unchanged (figure 3.14A), insulin levels were significantly lower in SF-1$^{\Delta IR}$ males (figure 3.14B) at the age of 20 weeks. Moreover, both insulin sensitivity and glucose tolerance were improved at 15 and 16 weeks of age (figure 3.14C and D). Although fasted and random-fed blood glucose did not differ, SF-1$^{\Delta IR}$ males on HFD showed an improved insulin stimulated glucose clearance from the circulation upon injection with human insulin (figure 3.14C). Furthermore, SF-1$^{\Delta IR}$ males also showed an improved glucose clearance from the bloodstream after an i.p. injection of glucose (figure 3.14D).

Under NCD-conditions, insulin receptor deficiency does not alter peripheral glucose metabolism. Neither blood glucose levels, serum insulin concentrations, insulin stimulated glucose uptake nor glucose clearance from the circulation revealed any differences between the genotypes. Upon HFD-feeding, blood glucose values did not differ, too,

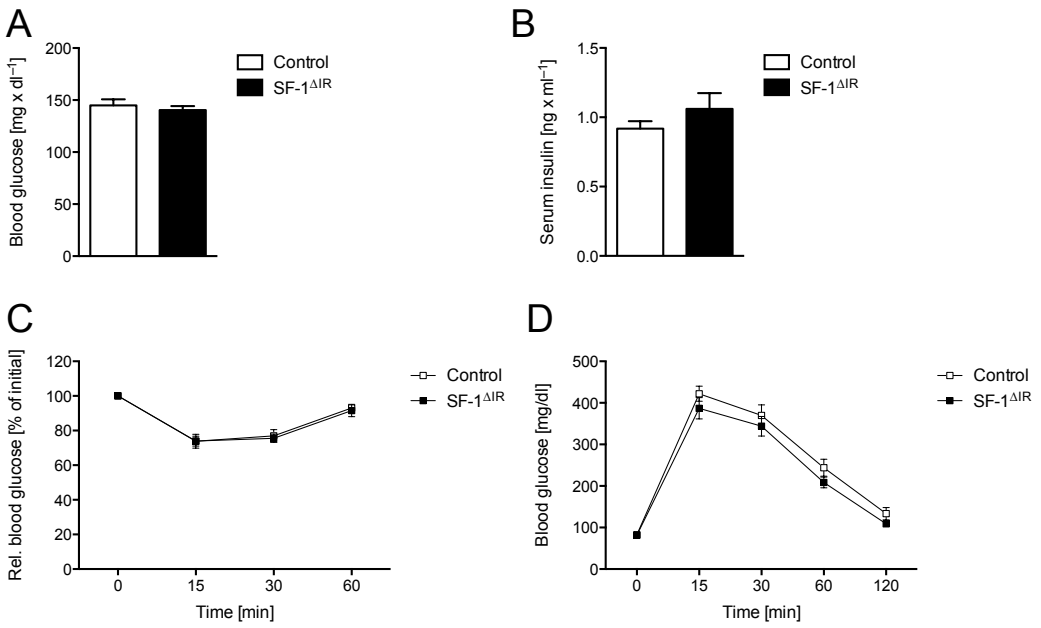

Figure 3.13: Control and SF-1$^{\Delta IR}$ did not show differences in glucose homeostasis when fed NCD. ***(A)*** Average blood glucose levels in 20 week old control and SF-1$^{\Delta IR}$ males on NCD (n > 15 per genotype). ***(B)*** Average serum insulin concentrations in 20 week old control and SF-1$^{\Delta IR}$ males on NCD (n > 15 per genotype). ***(C)*** Intraperitoneal insulin tolerance test performed in 15 week old control and SF-1$^{\Delta IR}$ males on NCD (n > 15 per genotype). ***(D)*** Intraperitoneal glucose tolerance test performed in 16 week old control and SF-1$^{\Delta IR}$ males on NCD (n > 15 per genotype). Displayed values are means ± S.E.M..

but insulin levels were significantly decreased in SF-1$^{\Delta IR}$ males, thereby indicating an increased insulin sensitivity under conditions of HFD-feeding. This was further confirmed by insulin and glucose tolerance tests. In both experiments, SF-1$^{\Delta IR}$ males showed an improved glucose clearance from the bloodstream, further indicating an improved insulin sensitivity in SF-1$^{\Delta IR}$ males under conditions of diet-induced obesity.

3.7 Increased PiP_3 formation in the VMH promotes weight gain

As shown before, abrogation of insulin receptor mediated signaling in SF-1 neurons in the VMH improves diet-induced obesity and glucose metabolism. To investigate whether insulin-dependent signaling might be overactivated in conditions of diet-induced obesity (DIO), PI_3K signaling was investigated in control (SF-1^{lacZ}) mice under conditions of obesity. To this end, control SF-1^{lacZ} and SF-1$^{lacZ:\Delta IR}$ fed HFD were fasted overnight, injected with saline into the *vena cava inferior* and subsequently stained for PiP_3. Under condi-

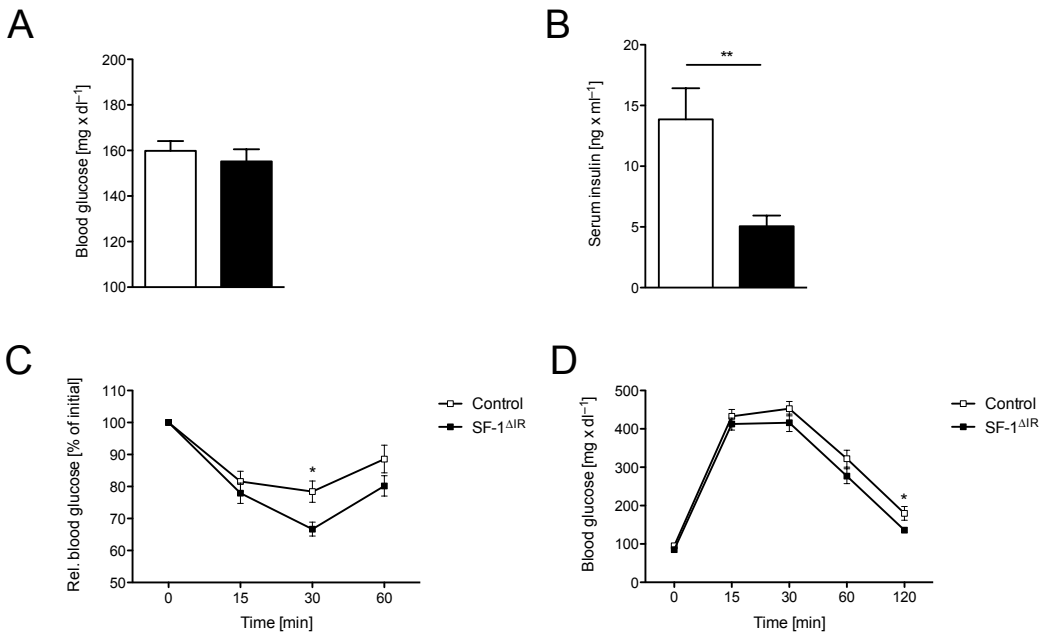

Figure 3.14: SF-1$^{\Delta IR}$ show an improved glucose homeostasis under condtions of HFD-feeding. ***(A)*** Average blood glucose levels in 20 week old control and SF-1$^{\Delta IR}$ males on HFD (n > 20 per genotype). ***(B)*** Average serum insulin concentrations in 20 week old control and SF-1$^{\Delta IR}$ males on HFD (n > 20 per genotype). ***(C)*** Intraperitoneal insulin tolerance test performed in 15 week old control and SF-1$^{\Delta IR}$ males on HFD (n > 18 per genotype). ***(D)*** Intraperitoneal glucose tolerance test performed in 16 week old control and SF-1$^{\Delta IR}$ males on HFD (n > 18 per genotype). Displayed values are means $\pm$ S.E.M.; *, $p \leq 0.05$.

tions of DIO, control mice display a higher PiP_3 aggregation when compared to controls under lean condition. When fed NCD, only 10 % of SF-1 neurons show high levels of PiP_3 accumulation (figure 3.6A). In HFD-fed controls, although they were fasted for 16 hours, the percentage of high immunoreactive SF-1 neurons increased to 40%. This effect was ameliorated in SF-1$^{lacZ:\Delta IR}$ mice (figure 3.15A). However, the percentage of SF-1 VMH neurons showing moderate PiP_3 immunoreactivity was higher in HFD-exposed SF-1$^{lacZ:\Delta IR}$1 mice than in HFD-fed controls (figure 3.15A), indicating some residual diet-induced activation of PI_3K signaling in SF-1 VMH neurons even in the absence of insulin receptor signaling. These experiments clearly indicate that HFD massively increases PI3K activity in SF-1 VMH neurons and that this activation to substantial proportion depends on insulin receptor signaling in these neurons.

To further functionally address the importance of diet-induced, insulin-dependent overactivation of PI3K signaling in the VMH, it was aimed to mimic this effect through genetic PI3K overactivation *in vivo*. Phosphatase and tensin homolog (PTEN) negatively

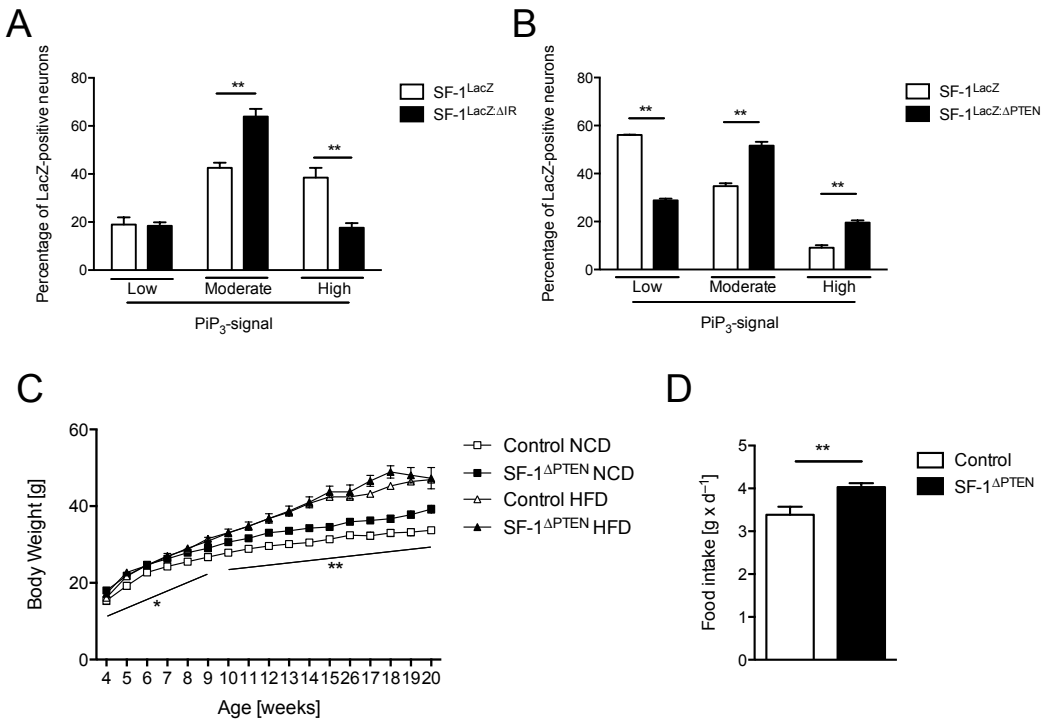

Figure 3.15: Enhanced PI_3K activation by HFD or PTEN deletion results in hyperphagia and increased body weight.
(A) PiP_3 levels after an overnight fast of control SF-1^{lacZ} and SF-$1^{lacZ:\Delta IR}$ males exposed to HFD for 10 weeks (n = 3 mice per genotype). ***(B)*** PiP_3 levels after an overnight fast of control SF-1^{lacZ} and SF-$1^{lacZ:\Delta PTEN}$ males exposed to HFD for 10 weeks (n = 3 mice per genotype). ***(C)*** Body weight curve of control ($PTEN^{fl/fl}$) and SF-$1^{\Delta PTEN}$ on either NCD or HFD for 17 weeks (n > 10 per genotype and diet). ***(D)*** Average daily food intake of 12 week old control and SF-$1^{\Delta PTEN}$ males on NCD.
Displayed values are means $\pm$ S.E.M.; *, $p \leq 0.05$; **, $p \leq 0.01$.

regulates PI_3K signaling by dephosphorylating PiP_3 to PiP_2. Thus, deletion of PTEN leads to accumulation of PiP_3 and subsequent hyperactivation of the PI_3K pathway (Maehama & Dixon, 1998; Plum *et al.* , 2006). Therefore, mice were crossed as described in Material and Methods. The ablation of PTEN yielded a greater number of SF-1 neurons with moderate to high levels of PiP_3 compared to that in control mice when the mice were fed NCD (figure 3.15B). Thus, SF-1 VMH neuron-restricted PTEN ablation mimics diet-induced overactivation of PI_3K signaling in these neurons and therefore provides an *in vivo* model of PI_3K hyperactivation. This model was used to investigate the effect of PI_3K hyperactivation in the VMH on body weight and caloric intake. As shown in figure 3.15C (rectangles), SF-$1^{\Delta PTEN}$ males displayed a significantly increased body weight when fed NCD, accompanied with an increased food intake (figure 3.15D). In contrast,

HFD exposure of these mice results in a disappearance of the phenotype (figure 3.15C triangles). Thus, hyperactivation of the PI_3K pathway results in modest obesity under NCD conditions, likely mimicking the effect of HFD-exposure at least partially.

To directly address the contribution of impaired PI_3K activation in SF-1 neurons of SF-$1^{\Delta IR}$ mice to the protection of these mice from the development of diet-induced obesity, we generated mice lacking both insulin receptor and PTEN in SF-1 neurons (SF-$1^{\Delta IR:\Delta PTEN}$ mice). Comparing body weight (figure 3.16A), total body fat content (figure 3.16B), epigonadal fat mass (figure 3.16C) and adipocyte size (figure 3.16D) in control (PTEN$^{fl/fl}$:IR$^{fl/fl}$) and SF-$1^{\Delta IR:\Delta PTEN}$ mice exposed to HFD revealed that protection from diet-induced weight gain and obesity in SF-$1^{\Delta IR}$ mice was abrogated by simultaneous ablation of PTEN in these neurons.

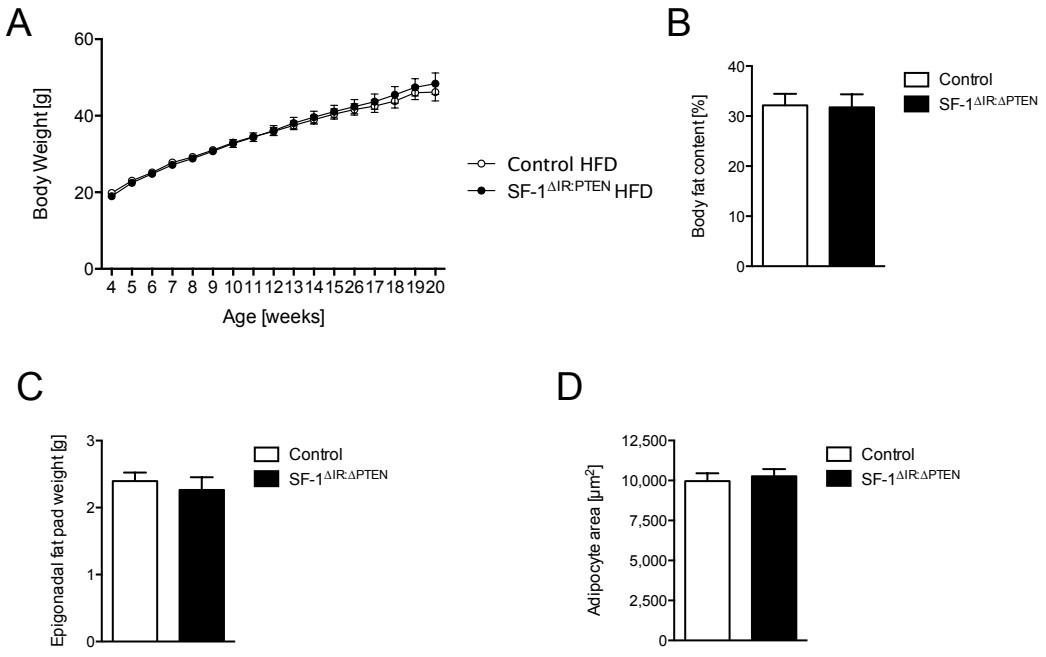

Figure 3.16: The additional deletion of PTEN in SF-$1^{\Delta IR}$ males normalizes body weight and adiposity under HFD conditions.
(A) Body weight curve of control (PTEN$^{fl/fl}$:IR$^{fl/fl}$) and SF-$1^{\Delta IR:\Delta PTEN}$ under HFD conditions (n > 15 per genotype). ***(B)*** Average total body fat content measured by NMR in 20 week old control and SF-$1^{\Delta IR:\Delta PTEN}$ males on HFD (n > 15 per genotype). ***(C)*** Average epigonadal fat pad weight of 20 week old control and SF-$1^{\Delta IR:\Delta PTEN}$ males on HFD (n > 15 per genotype). ***(D)*** Average size of adipocytes in the epigonadal white adipose tissue (WAT) of control and SF-$1^{\Delta IR:\Delta PTEN}$ males on HFD at the age of 20 weeks (n = 3 mice per genotype).
Displayed values are means ± S.E.M..

Collectively, these experiments indicate that insulin-stimulated overactivation of PI_3K signaling in SF-1 VMH neurons is important in the development of HFD-induced obesity.

3.8 Increased firing frequency of POMC neurons in SF-1$^{\Delta IR}$ males under HFD conditions

To further investigate the molecular mechanism underlying the altered body weight regulation in SF-1$^{\Delta IR}$ males, we analyzed the expression of hypothalamic neuropeptides of critical importance in the neuronal regulation of energy homeostasis (Asnicar *et al.* , 2001; Clark *et al.* , 1985; Fan *et al.* , 1997; Gropp *et al.* , 2005; Li *et al.* , 2003; McMinn *et al.* , 2000). Figure 3.17 indicates that the deficiency for the insulin receptor does not affect the expression of neuropeptides involved in the regulation of the melanocortin system (figure 3.17A). Furthermore, VMH specific neuropeptides, that are implicated in the regulation of energy homeostasis were also analyzed for their expression levels (Kernie *et al.* , 2000; Kim *et al.* , 2012; Liao *et al.* , 2012). Figure 3.17B indicates that the expression of both brain-derived neurotrophic factor (*BDNF*) and steroidogenic factor 1 (*SF-1*) was unaltered between the genotypes.

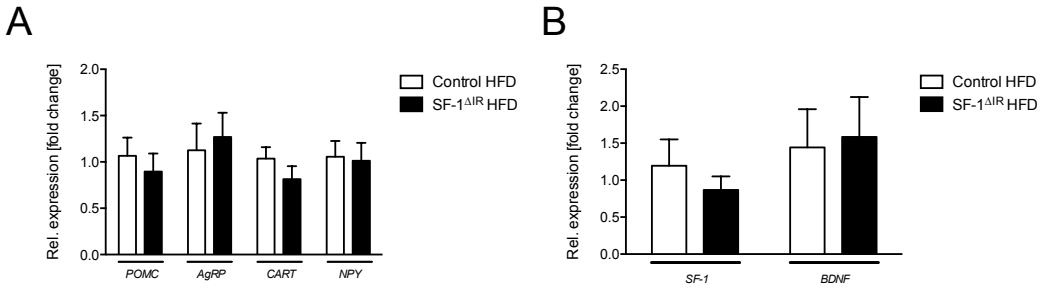

Figure 3.17: Quantitative real-time PCR on neuropeptides involved in the regulation of energy homeostasis.
(A) Relative expression of pro-opiomelanocortin (*POMC*), agouti-related peptide (*AgRP*), cocaine and amphetamine regulated transcript (*CART*) and neuropeptide Y (*NPY*) in 20 week old, HFD-fed control and SF-1$^{\Delta IR}$ males at the age of 20 weeks. ***(B)*** Relative expression of steroidogenic factor 1 (*SF-1*) and brain-derived neurotrophic factor (*BDNF*) in HFD-fed control and SF-1$^{\Delta IR}$ males at the age of 20 weeks.
Displayed values are means $\pm$ S.E.M..

Thus, changes in the expression of the investigated gene products do not explain the metabolic phenotype in mice lacking the insulin receptor in SF-1 neurons.

This raised the question how the leaner phenotype of SF-1$^{\Delta IR}$ mice was accomplished. Another possible mechanism was published by Sternson and colleagues, who could show that glutamatergic inputs from the VMH can alter the activity of POMC neurons

in the ARC (Sternson *et al.* , 2005). To this end, electrophysiological recordings were performed of POMC neurons, either in a control (POMC^{GFP}) or in a SF-1$^{\Delta IR}$ background (POMC^{GFP};SF-1$^{\Delta IR}$) under HFD conditions. As shown in figure 3.18, POMC neurons have an average firing rate of 1 Hz under conditions of HFD feeding. When POMC neurons were recorded in the SF-1$^{\Delta IR}$ background, basal firing was increased to 3 Hz (figure 3.18B). Additionally, the number of silent POMC neurons was decreased from 50 % in POMC^{GFP} to 30 % in POMC^{GFP};SF-1$^{\Delta IR}$ mice (figure 3.18C). Figure 3.18A shows representative recording traces of both genotypes.

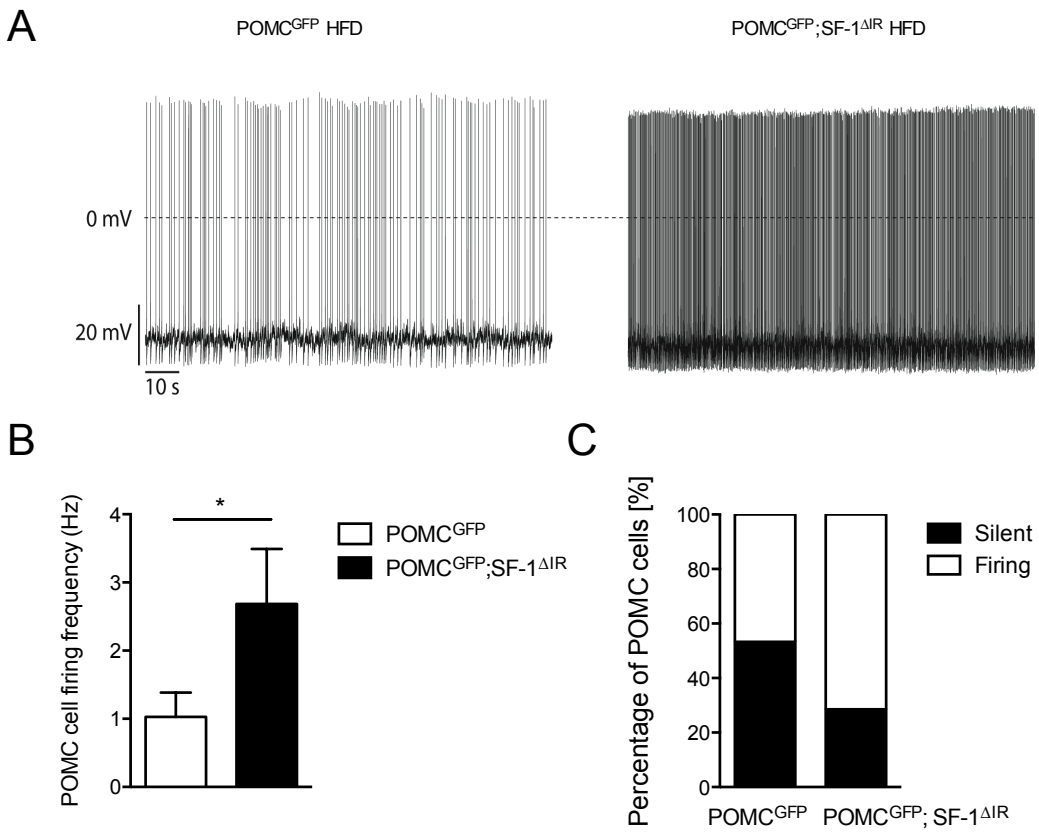

Figure 3.18: Electrophysiological recordings of POMC neurons of either control (POMC^{GFP};IR$^{fl/fl}$) or SF-1$^{\Delta IR}$ (POMC^{GFP};SF-1$^{\Delta IR}$) mice under HFD conditions.
(A) Representative recording traces of POMC neurons of control and SF-1$^{\Delta IR}$ mice under HFD conditions. ***(B)*** Average firing frequency of POMC neurons of control and SF-1$^{\Delta IR}$ mice under HFD conditions. ***(C)*** Percentage of silent and spontaneously firing SF-1 POMC neurons of control and POMC^{GFP};SF-1$^{\Delta IR}$ mice under HFD conditions.
Displayed values are means $\pm$ S.E.M.; *, $p \leq 0.05$.

Taken together, the lack of insulin receptors in the VMH does not influence the transcriptional profile of the melanocortin system or other VMH specific neuropeptides, but

rather influences the electrophysiological activity of the neighboring POMC neurons by either direct or indirect synaptic inputs.

To test this hypothesis, inhibitory (IPSC) and excitatory post synaptic currents (EPSC) were measured on POMC neurons in control (POMC^{GFP}) or in POMC^{GFP};SF-1$^{\Delta IR}$ under HFD conditions. As shown in figure 3.19, the frequency of IPSCs is significantly decreased in SF-1$^{\Delta IR}$ mice, whereas the EPSCs tend to be higher but do not reach significance. Additionally, the ratio of EPSC to IPSC was significantly increased in SF-1$^{\Delta IR}$ animals, further pointing towards a role of insulin signaling in the VMH in the electrophysiological regulation of POMC neuron activity. Thus, the increased firing activity of POMC neurons in SF-1$^{\Delta IR}$ might be caused by either altered activity of neuronal inputs on POMC neurons or by modifications in the synaptic organization in the ARC.

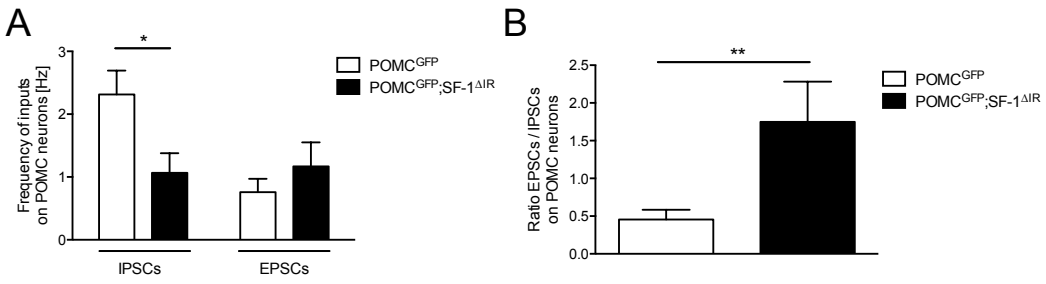

Figure 3.19: Measurement of post synaptic currents (PSC) in HFD-fed POMC^{GFP} and POMC^{GFP};SF-1$^{\Delta IR}$ males.
(A) Average frequency of inhibitory post synaptic currents (IPSC) and excitatory post synaptic currents (EPSC) on POMC neurons in HFD-fed POMC^{GFP} and POMC^{GFP};SF-1$^{\Delta IR}$ males. ***(B)*** Ratio of EPSC to IPSC on POMC neurons in HFD-fed POMC^{GFP} and POMC^{GFP};SF-1$^{\Delta IR}$ males. Displayed values are means $\pm$ S.E.M.; *, $p \leq 0.05$; **, $p \leq 0.01$.

To test this, synaptic inputs on POMC neurons of control and SF-1$^{\Delta IR}$ animals were examined by electron-microscopy as described by Pinto and colleagues (Pinto *et al.* , 2004). Inhibitory (GABAergic) and excitatory (glutamatergic) synapses differ in their morphology, when observed by electron microscopy. GABAergic synapses show a symmetric morphology, whereas glutamatergic synapses display a rather asymmetric morphology. To confirm this findings, synapses are additionally stained for GABA and glutamate. As shown in figure 3.20A and B, no alterations could be observed between control and SF-1$^{\Delta IR}$ animals under conditions of NCD-feeding. When those mice were fed HFD, the number of synapses changed dramatically. As shown before (Horvath *et al.* (2010)), the

number of inhibitory synapses on POMC neurons increased massively upon HFD feeding (figure 3.20A and C), whereas only slight changes were observable in the number of excitatory inputs. Accordingly, the ratio of excitatory to inhibitory inputs was significantly increased in SF-1$^{\Delta IR}$ males on HFD when compared to their littermate controls (figure 3.20D).

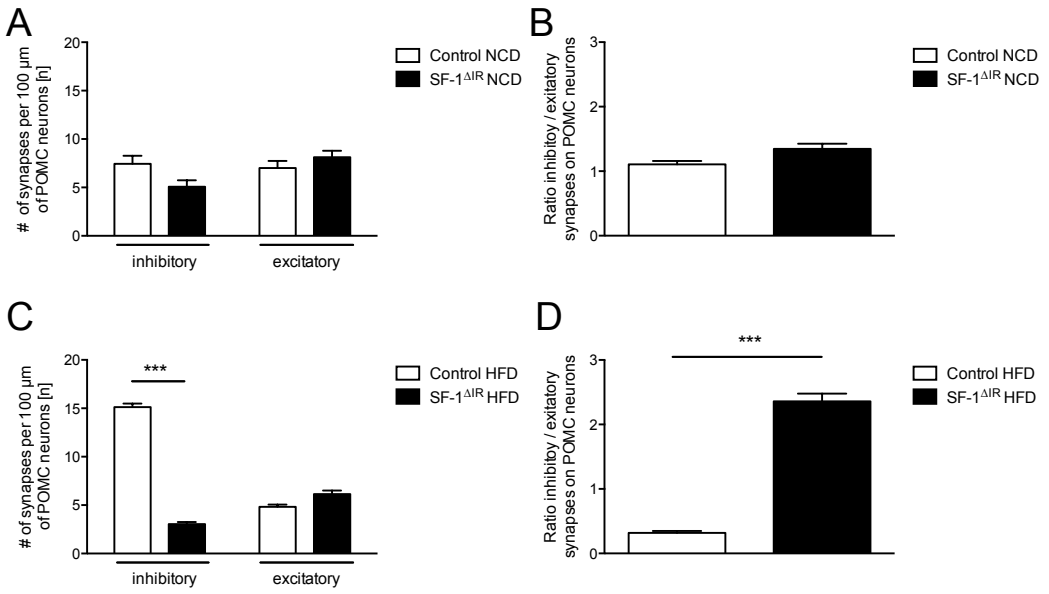

Figure 3.20: Number of inhibitory and excitatory synapses on POMC neurons per 100 μm perikarya of control and SF-1$^{\Delta IR}$ males under NCD and HFD conditions.
(A) Average number of inhibitory and excitatory synapses on POMC neurons per 100 μm perikarya in control and SF-1$^{\Delta IR}$ males on NCD. ***(B)*** Ratio of excitatory to inhibitory synapses on POMC neurons in control and SF-1$^{\Delta IR}$ males on NCD. ***(C)*** Average number of inhibitory and excitatory synapses on POMC neurons per 100 μm perikarya in HFD-fed control and SF-1$^{\Delta IR}$ males. ***(D)*** Ratio of excitatory to inhibitory synapses on POMC neurons in HFD-fed control and SF-1$^{\Delta IR}$ males.
Displayed values are means $\pm$ S.E.M.; ***, $p \leq 0.001$.

Taken together, POMC neurons are inhibited in their activity upon HFD-feeding, which is ameliorated in SF-1$^{\Delta IR}$ males (figure 3.18). As shown by post synaptic current measurements, this is likely caused by alterations in the type post-synaptic currents on POMC neurons (figure 3.19) and could be further confirmed by electron-microscopical examination of synaptic inputs (figure 3.20).

3.9 Counterregulatory response to hypoglycemia

To elucidate a role of insulin signaling in SF-1 neurons in the counter-regulatory response to hypoglycemia (CRR), control and SF-1$^{\Delta IR}$ females and males were operated as described in Material and Methods. After 7 days of recovery, mice were exposed to a hypoglycemic-hyperinsulinemic clamp (figure 3.21).

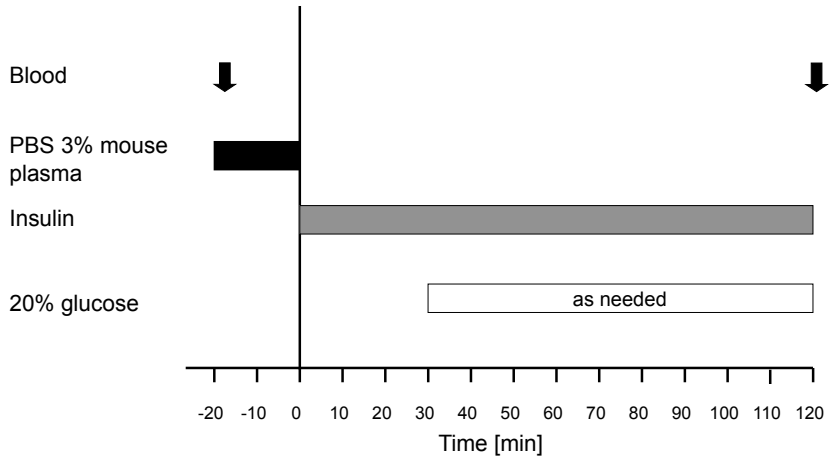

Figure 3.21: Protocol for the hypoglycemic-hyperinsulinemic clamp studies.
Mice were adjusted to a blood glucose level of ∼50 mg/dL by a constant infusion of insulin and an adapted infusion of 20% glucose solution. Blood samples were taken before insulin is infused (at -20) and in the steady state.

Hypoglycemic-hyperinsulinemic clamp studies were conducted on female (figure 3.22) and male (figure 3.23) control and SF-1$^{\Delta IR}$ mice at the age of 12 to 14 weeks. During the clamp, blood glucose levels were monitored every 10 minutes. When blood glucose values reached a threshold of 70 mg/dL, glucose infusion was started to prevent a hypoglycemic shock. The glucose infusion rate was adapted to reach a steady state at least 90 min after initiation of insulin infusion. As shown in figure 3.22A, both controls and SF-1$^{\Delta IR}$ females reached a steady-state at least after 90 min of insulin infusion. The glucose infusion rate (GIR), as depicted in figure 3.22B, was significantly higher in SF-1$^{\Delta IR}$

females when compared to controls, thus indicating in impaired counter-regulatory response to hypoglycemia (CRR). Thus, plasma samples that were taken during the clamp were analyzed for circulating epinephrine, norepinephrine, corticosterone and glucagon concentrations. Figure 3.22C and D indicate no differences between SF-1$^{\Delta IR}$ females and controls, neither in epinephrine, norepinephrine, corticosterone nor circulating glucagon levels. Although glucagon levels seem to be slightly decreased in SF-1$^{\Delta IR}$ females in the steady-state, it did not reach statistical significance.

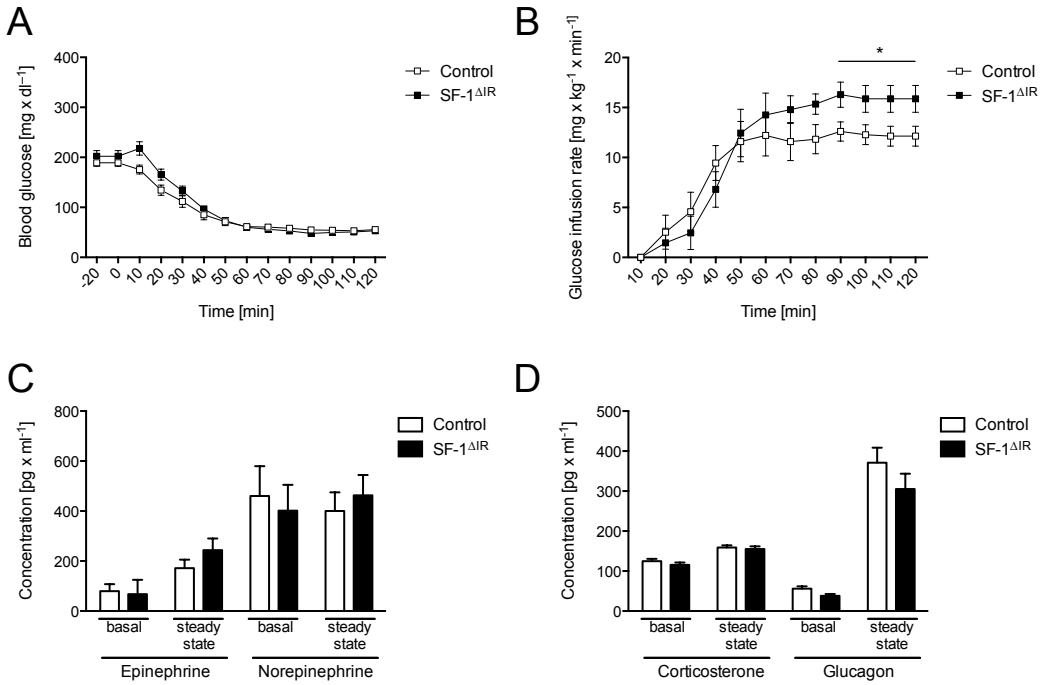

Figure 3.22: Hypoglycemic-hyperinsulinemic clamp studies of 12 to 14 week old female control and SF-1$^{\Delta IR}$ animals.
(A) Average blood glucose values during the clamp study of control and SF-1$^{\Delta IR}$ females. (n > 9) ***(B)*** Average glucose infusion rate of control and SF-1$^{\Delta IR}$ females. (n > 9) ***(C)*** Enzyme immunoassay of basal and steady state plasma samples from control and SF-1$^{\Delta IR}$ females for epinephrine and norepinephrine. (n > 9) ***(D)*** Enzyme immunoassay and radioimmuno assay of basal and steady state plasma samples from control and SF-1$^{\Delta IR}$ females for corticosterone and for glucagon. (n > 9).
Displayed values are means $\pm$ S.E.M.; *, $p \leq 0.05$.

Due to the fact that significant differences in body weight were only observed in male animals, hypoglycemic-hyperinsulinemic clamps were also conducted in male control and SF-1$^{\Delta IR}$ males on NCD. Also in males, a steady-state was reached by constant infusion of insulin and a variable infusion of glucose (figure 3.23A). Whereas female mice

showed an increased GIR during the steady-state of the clamp, male mice also tend to have an increased GIR, but did not reach significance (figure 3.23B).

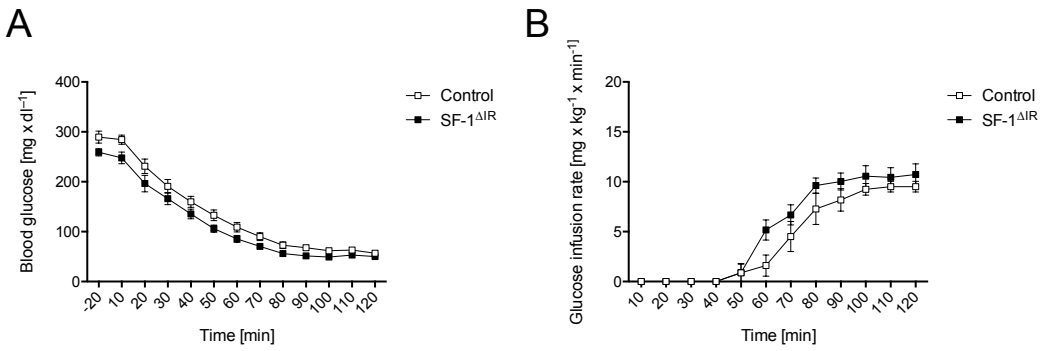

Figure 3.23: Hypoglycemic-hyperinsulinemic clamp studies of 12 to 14 week old male control and SF-1$^{\Delta IR}$ animals.
(A) Average blood glucose values during the clamp study of control and SF-1$^{\Delta IR}$ males. ***(B)*** Average glucose infusion rate of control and SF-1$^{\Delta IR}$ males.
Displayed values are means $\pm$ S.E.M..

Thus, SF-1$^{\Delta IR}$ females require an increased GIR to reach the steady state, but the reason for the increased GIR needs to be further elucidated. Male SF-1$^{\Delta IR}$ mice also have the tendency to need an increased GIR, but more animals have to be analyzed to verify these findings.

4 Discussion

Over the last decades, growing evidence suggested that obesity and insulin resistance, with T2DM as a consequence, are strongly associated and obesity is now considered as the pandemic of the 21^{st} century (Mokdad *et al.* , 2003; WHO, 2012). The increases in the incidence for obesity and insulin resistance worldwide create a mandatory necessity for the understanding of neuronal and peripheral mechanisms underlying the development of obesity and its co-morbidities. Furthermore, evidence from the last years suggest that especially maternal obesity is able to contribute massively to the further propagation of obesity in western countries by epigenetical imprinting (Heerwagen *et al.* , 2010).

Although an overwhelming amount of studies, dealing with obesity, have been published over the last decades, the underlying molecular mechanisms still remain to be elucidated. It is still not fully understood how the peripheral hormones leptin and insulin control the regulation of energy homeostasis in the brain and a lot of target brain areas of these hormones still have to be investigated. Whereas the hypothalamus has been identified as a pivotal brain region in the control of energy homeostasis more than 70 years ago (Hetherington & Ranson, 1940), the projection sites and further connections to higher brain regions have not yet been accurately defined. One of the best characterized circuits in the hypothalamus and definitely a major target for insulin's and leptin's action is the melanocortin system in the ARC, including the first order neuronal populations of POMC and AgRP expressing neurons. As shown by several knockout and ablation studies in rodents, the melanocortin system in the ARC is not the only circuit in the CNS controlling energy balance. For example, deletion of the IR in POMC neurons does not influence body weight, whereas either LepR deficiency or even the specific ablation of POMC neurons results in modest obesity (Cohen *et al.* , 2001; Cowley *et al.* , 2001; Gropp *et al.* , 2005; Könner *et al.* , 2007; Luquet *et al.* , 2005). Furthermore, LepRs and IRs are widely expressed in the brain, indicating a role for leptin and insulin signaling in the regulation of energy homeostasis in other brain areas as well (Havrankova *et al.* , 1978a;

Mercer *et al.* , 1996b; Oomura & Kita, 1981). Thus, the exact mechanisms downstream of the melanocortin system is still a subject of research.

Already before the discovery of the melanocortin circuits in the ARC, the neighboring VMH was considered to be the main satiety center in the brain (Gold, 1973; Marshall & Mayer, 1956). Initially identified by lesion experiments and electrical stimulations, the signals that control VMH neuron activity and output have been further defined by new methods and techniques, such as the cre-loxP system. By the abrogation of leptin signaling in SF-1 neurons, leptin has been identified as key mediator in the VMH in the control of energy homeostasis. Leptin is able to directly stimulate firing activity in VMH SF-1 neurons, and lack of LepRs results in modest obesity, suprisingly to a similar extent as POMC-specific LepR deficiency (Dhillon *et al.* , 2006). Furthermore, the deletion of LepRs in both POMC and SF-1 neurons has additive effects, resulting in severe obesity. Notably, upon HFD-exposure LepR deficiency in SF1 neurons aggravates the diet-induced weight gain, thus proposing a role for SF-1 neurons to compensate for the diet-induced leptin resistance in POMC neurons (Dhillon *et al.* , 2006; Munzberg *et al.* , 2004). In contrast, the lack of leptin's negative regulator, SOCS-3, improves glucose homeostasis and leptin signaling in the VMH, but has no effect on body weight or adiposity (Zhang *et al.* , 2008a).

Further evidence suggests that the VMH specific neurotrophin brain-derived neurotrophic factor (BDNF) is involved in the control of energy homeostasis. BDNF is expressed in the hindbrain and some hypothalamic nuclei, but most abundantly in the VMH (Conner *et al.* , 1997; Wang *et al.* , 2010). When BDNF is infused into the brain of rats, it reduces the food intake and accordingly, BDNF mRNA levels are reduced upon fasting (Lapchak & Hefti, 1992; Tran *et al.* , 2006; Xu *et al.* , 2003). Furthermore, the deletion of BDNF in the VMH and DMH results in hyperphagia and consequently obesity (Unger *et al.* , 2007). However, how the anorectic effects of BDNF are transmitted is unclear.

The effect of insulin in the CNS is still under investigation, although its role in the periphery and certain brain areas has been intensively studied. Initially identified by Woods and colleagues as an adiposity signal from the periphery (Woods *et al.* , 1979), insulin's role in the CNS mediated control of energy homeostasis has been further clarified over the last years. The neuron-specific insulin receptor knockout (NIRKO) mouse

develops modest obesity, clearly indicating an important role for insulin in the CNS in the control of energy homeostasis (Brüning *et al.* , 2000). Further studies revealed that central insulin is also implicated in the control of lipid metabolism and hepatic gluconeogenesis. When insulin signaling is abolished in the brain, mice exhibit unrestrained lipolysis in the adipose tissue and consequently increased levels of fatty acids in the circulation (Koch *et al.* , 2008; Scherer *et al.* , 2011). As shown by Könner and colleagues, insulin regulates hepatic glucose production via AgRP neurons (Könner *et al.* , 2007). In POMC neurons, insulin activates, together with leptin, the transcription of POMC in a PDK1 dependent manner (Belgardt *et al.* , 2008). Furthermore, over-activation of insulin signaling in POMC neurons by the deletion of PTEN likewise results in modest obesity (Plum *et al.* , 2006).

Although the VMH has been investigated for many years, the VMH derived signals are not yet fully understood. In addition to leptin's role as a stimulator of SF-1 VMH neuron firing activity and BDNF as a satiety signal within the VMH, glutamatergic projections from the VMH are necessary to maintain a normal body weight. When glutamate is prevented to be transported into secretory vesicles, disturbances in energy balance are observed (Tong *et al.* , 2007a). Moreover, glutamatergic inputs from the VMH to POMC neurons could be observed in uncaging experiments, further supporting the importance of glutamate release from the VMH in the maintenance of body weight (Sternson *et al.* , 2005). However, the exact mechanisms that regulate SF-1 VMH neuron activity and transcriptional profile have to be elucidated.

Although both insulin signaling and SF-1 neurons are implicated in the CNS-mediated control of energy homeostasis and insulin receptors are highly expressed in the VMH (Oomura & Kita, 1981), insulin's role in SF-1 expressing neurons in the VMH has not been studied so far.

4.1 Successful generation of SF-1 cell specific insulin receptor knockout mice

To get insights into insulin's role in VMH SF-1 neurons, Cre mediated recombination was used to delete specifically exon 4 of the *insulin receptor* gene in SF-1 expressing cells. Even

though *SF-1* is reported to be expressed in the pituitary gland, adrenal gland, spleen, testis and ovaries, no alterations in the protein level of the IR were observed. To exclude any defects in the hypothalmus-pituitary-gonadal (HPG) axis by either IR deficiency in the hypothalamus, pituitary gland or the gonads, breeding efficiency was analyzed. No alterations could be observed in average litter frequency or average litter size. Furthermore, the expression of hormones, regulating the HPG axis in the pituitary gland, was unchanged and free triiodthyronin (T_3) levels in the serum of control and SF-$1^{\Delta IR}$ males were unaltered. Thus, the integrity of the HPG axis and proper gonadal function was assured. Whereas the deletion of the *SF-1* gene results in developmental defects in the VMH and subsequently in a complete lack of this hypothalamic nuclei, no structural or morphological abnormalities were visible. Moreover, *in situ* hybridization against exon 4 of the *insulin receptor* mRNA showed a reduction of 50 %, whereas no significant reduction was seen in the neighboring DMH. This reduction was congruent with the observed expression pattern of the SF-1 Cre, as only about 50 % of the neurons in the VMH were Cre positive (personal observation). As shown by other researchers, SF-1 is not expressed in every neuron in the VMH, thus in line with the observed reduction in *insulin receptor* mRNA (Dhillon *et al.* , 2006; Kim *et al.* , 2009).

To confirm the functionality of the IR deletion, VMH sections of saline injected and insulin stimulated control and SF-$1^{\Delta IR}$ animals were analyzed for PiP_3 formation. By the quantification of insulin stimulated PiP_3 accumulation, the efficient Cre-mediated recombination of the *insulin receptor* gene was verified. In control reporter animals, an increase in PiP_3 formation upon insulin stimulation could be observed, indicating a cell-autonomous activation of SF-1 neurons in the VMH by insulin. This effect was completely absent in SF-$1^{\Delta IR}$ reporter animals, as no increase in PiP_3 formation could be observed. Notably, a subset of $\sim$20 % of SF-1 neurons revealed low PiP_3 formation despite a 20 min stimulation with insulin, possibly representing SF-1 neurons that do not express the IR. Furthermore, differences in the ability of insulin to stimulate PiP_3 formation were observed. SF-1 neurons in the medio-basal part of the VMH showed higher PiP_3 levels than SF-1 neurons in the ventro-lateral area, both after 10 and 20 min of insulin stimulation. This can be caused either by a different responsiveness to insulin through

higher insulin receptor expression or by a different accessibility of insulin to the brain regions. Insulin is transported across the blood-brain barrier (BBB) by a saturable transport mechanism (Banks *et al.* , 1997), but the further distribution in the brain via diffusion or ventricular cerebro-spinal fluid has not been studied so far.

Taken together, the majority of SF-1 neurons in the VMH are insulin responsive and insulin receptors in these neurons were efficiently deleted, although a subpopulation of VMH SF-1 neurons is not responsive to insulin. Thus, the mechanisms of insulin's distribution and the expression pattern of insulin receptors has to be further studied.

4.2 Insulin electrically inhibits SF-1 neurons via K_{ATP} channels

To examine the effect of insulin on electrophysiological properties of SF-1 neurons, patch-clamp recordings of identified SF-1 neurons were performed. In control SF-1^{GFP} neurons, insulin was able to hyperpolarize SF-1 neurons and thereby reduce their firing rate. This inhibition of firing activity was reversible when tolbutamide, a selective ATP-dependent potassium (K_{ATP}) channel blocker, was added to the bath, thus indicating that the hyperpolarization is mediated by K_{ATP} channels. Importantly, only 40 % of the recorded SF-1 neurons were responsive to insulin, and most of them were clustered in the medio-basal part of the VMH, recapitulating the observations acquired by insulin stimulated PiP_3 formation experiments. Of note, insulin stimulated depolarization could be observed in only 1 out of 14 control SF-1 neuron.

When SF-1$^{GFP:\Delta IR}$ neurons were recorded, no effect of insulin could be observed. Insulin application did not result in obvious effects on membrane potential or firing rate, thus confirming the efficient Cre-mediated deletion of the IR. Furthermore, basal properties of SF-1^{GFP} and SF-1$^{GFP:\Delta IR}$, such as whole-cell capacitance and input resistance, were indistinguishable between both genotypes, thus indicating no functional defect in SF-1 neurons upon IR deficiency. Moreover, 2 out of 12 neurons from SF-1$^{GFP:\Delta IR}$ animals depolarized after insulin application, thus indicating an unspecific effect, also in the one depolarized control SF-1 neuron.

To investigate the interplay of leptin and insulin in SF-1 neurons, either single or sequential application during electrophysiological recordings were performed. The single

application revealed that a subpopulation of SF-1 neurons are both leptin and insulin sensitive, but the majority of the recorded neurons did not respond to either of the applications (22 out of 70 responded to leptin and 5 out of 18 to insulin). When leptin and insulin were sequentially applied, none of the examined neurons (n = 39) responded to both leptin and insulin.

Thus, insulin is able to silence a subpopulation of SF-1 neurons in the VMH, mainly in the medio-basal part, via K_{ATP} channels. Furthermore, SF-1 neurons obviously represent a heterogenic population of VMH neurons, that likely segregate into leptin and insulin responsive neurons, which has to be further investigated. To this end, mice will be analyzed that lack the IR and/or the LepR in VMH SF-1 neurons to unravel if the lack of IRs can partially compensate the obesity-promoting effect of LepR deficiency (Dhillon *et al.* , 2006).

4.3 Attenuation of obesity upon SF-1 specific IR deficiency

Earlier studies, e.g. by Woods and Porte, indicated a role for insulin in the brain as a adiposity and satiety signal (Woods *et al.* , 1979). In line with these observations, mice lacking the insulin receptor in the whole brain are moderately obese (Brüning *et al.* , 2000). But as mentioned earlier, the exact neuronal population of insulin's anorectic action remains unclear.

As shown by Könner and colleagues, insulin receptor deficiency in POMC and AgRP neurons does not alter body weight or adiposity (Könner *et al.* , 2007). Thus the VMH represents a possible target for the anorectic effect of insulin. But under NCD conditions, no alterations in body weight, glucose homeostasis or adiposity could be observed. In contrast, when control and SF-$1^{\Delta IR}$ mice were fed a HFD, SF-$1^{\Delta IR}$ males were significantly lighter and until 14 weeks of age completely protected against the diet-induced weight gain. Females had the same tendency towards reduced body weight and adiposity, but this never reached significance due to high deviations within the genotypes (personal observation). The decreased body weight was caused by a decreased fat mass, as the reduction in body weight reflects the reduction in fat mass. On average both genotypes

had a lean mass of ∼24 g, but control animals had ∼21 g fat mass in contrast to ∼17 g fat mass in SF-1$^{\Delta IR}$ males.

The decreased adiposity was also reflected by the serum leptin levels. Whereas no differences could be observed under NCD conditions, SF-1$^{\Delta IR}$ males had significantly lower circulating leptin levels when exposed to HFD, both at 8 and 20 weeks of age, and reduced mean adipocyte size, which has been shown to influence leptin secretion (Skurk *et al.* , 2007). Thus, leptin sensitivity seems to be increased in SF-1$^{\Delta IR}$ males on HFD, as it is reported in lean vs. obese subjects (Heymsfield *et al.* , 1999).

In order to obtain further insights into the underlying mechanism of the reduced adiposity upon HFD-feeding in SF-1$^{\Delta IR}$ males, food intake and energy expenditure were measured in 6 to 7 and 12 to 13 week old males. In younger control and SF-1$^{\Delta IR}$ males, that did not differ in body weight, both food intake and energy expenditure were not significantly changed. Also in older (12 to 13 week old) animals, energy expenditure was unchanged, whereas the absolute food intake was significantly decreased in SF-1$^{\Delta IR}$ males. However, when normalized to body weight, no changes could be observed between both genotypes. This indicates that the reduction in food intake might also be a secondary effect of the reduced adiposity in SF-1$^{\Delta IR}$ animals.

To test if young SF-1$^{\Delta IR}$ males already show differences in leptin's ability to reduce food intake, 8 week old mice were injected icv with leptin and food intake was monitored. This revealed a significantly improved leptin sensitivity in young SF-1$^{\Delta IR}$ males, although the body weight did not differ from controls at this age.

Taken together, insulin receptor deficiency in VMH SF-1 neurons partially protects against diet-induced weight gain by improving leptin's ability to decrease food intake before obvious effects on body weight could be monitored. This effect did only reach statistical significance in male animals, not in females. A possible reason for this effect is the effect of estrogen. As shown by Gao and colleagues, estrogen is able to reduce food intake by changing the synaptic input of the ARC melanocortin system, independent of leptin (Gao *et al.* , 2007). Thus, the differences observed in male animals in leptin's ability to reduce food intake might be overruled by different levels of circulating estrogen during the cycle and thus leading to the observed high deviations within the genotypes.

4.4 Improved glucose metabolism in SF-1$^{\Delta IR}$ males on HFD

Under NCD conditions, control and SF-1$^{\Delta IR}$ animals did not show any alterations in the examined metabolic parameters. The same holds true for glucose tolerance and insulin sensitivity, assessed by glucose and insulin tolerance tests. Though, SF-1$^{\Delta IR}$ males on HFD showed increased glucose tolerance and improved insulin sensitivity. As these experiments were performed at 15 and 16 weeks of age, both genotypes displayed already significant differences in body weight and presumably also adiposity (not measured at that age). As there is no direct connection between VMH neurons and peripheral glucose metabolism known so far, the improved glucose clearance in both experiments is most likely a secondary effect of the reduced adiposity. This finding is supported by the fact that obesity and insulin resistance are intimately linked conditions.

4.5 PiP$_3$ formation in SF-1 VMH neurons promotes obesity

As VMH SF-1 neurons are insulin responsive under NCD conditions, shown by PiP$_3$ formation upon insulin stimulation, the effect of HFD-feeding on insulin responsiveness in VMH SF-1 neurons was investigated. By the analysis of PiP$_3$ levels in HFD fed control (SF-1^{lacZ}) and knockout reporter (SF-1$^{lacZ:\Delta IR}$) animals, we could show that HFD-feeding induces PiP$_3$ accumulation in the VMH even after 16 hours of fasting. Although it is known that HFD-feeding leads to hyperinsulinemia in the periphery, it was so far unclear if the brain and, in particular, the VMH are affected by increased circulating insulin. Whereas neurons in the ARC, such as POMC and AgRP neurons, are considered to become insulin resistant upon HFD feeding (Clegg *et al.* , 2011; Ernst *et al.* , 2009; Mayer & Belsham, 2010), we could show that neurons in the VMH remain insulin sensitive. Furthermore, this enhanced insulin signaling in SF-1 neurons, compared to ARC neurons, probably contributes to the diet-induced weight gain, as insulin receptor deficiency in SF-1 neurons partially protects against diet-induced obesity and PiP$_3$ formation is significantly reduced in SF-1$^{\Delta IR}$ males on HFD.

To further test this hypothesis, mice were generated lacking the negative regulator of PI$_3$K signaling, PTEN (SF-1$^{\Delta PTEN}$). The efficient ablation of PTEN in VMH SF-1 neu-

rons could be shown by increased PiP_3 formation under unstimulated, saline injected NCD conditions after a 16 h fasting period. SF-$1^{\Delta PTEN}$ mice showed an increased body weight upon NCD feeding, whereas no alterations could be observed between control (PTEN$^{fl/fl}$) and SF-$1^{\Delta PTEN}$ males when fed a HFD. The elevated body weight on NCD was caused by an increase in food intake.

Importantly, the beneficial effects of insulin receptor deficiency in SF-1 neurons upon HFD feeding was completely normalized when PTEN was additionally deleted. This is likely caused by other stimuli of the PI_3K pathway, such as leptin or insulin like growth factor 1 (IGF1) receptor signaling. Both have been shown to either activate the PI_3K pathway, either by leptin-stimulated phosphorylation of insulin receptor substrates by JAK or by direct binding of insulin to the insulin-like growth factor 1 receptor (IGF1-R) (Cohen *et al.* , 1996; Hill *et al.* , 2008; Latres *et al.* , 2005; Pomerance *et al.* , 1995). When PTEN is absent in SF-1 neurons, both stimuli can slightly activate PI_3K, despite IR deficiency, which leads to an accumulation of PiP_3, as it cannot be de-phosphorylated to PiP_2.

These experiments further support the findings that PiP_3 formation in VMH SF-1 neurons promotes weight gain, shown by both diet-induced but also genetically induced obesity. As SF-$1^{\Delta PTEN}$ mice on HFD do not display any differences in body weight, we hypothesize that the deficiency for PTEN mimics the effect of HFD feeding in VMH SF-1 neurons.

Another noteworthy finding of this study is the fact that VMH SF-1 neurons remain insulin sensitive, in contrast to other neuronal populations. This phenomenon of selective insulin resistance is already known from peripheral organs. In the liver of obese mice, insulin fails to inhibit hepatic glucose production via the PI_3K pathway and FOXO1, but continues to promote lipid synthesis via the SREBP-1c pathway (Biddinger *et al.* , 2008). Interestingly, selective insulin resistance for different pathways develops in the liver, although hepatocytes represent a quite homogenous population of cells. In contrast to the liver, the brain consists of thousands of specialized neuronal subpopulations, each with specialized gene expression profiles and connections. Hence, selective insulin resistance for different pathways is also known for the CNS. Insulin is still able to activate the

MAPK pathway, but fails to induce signaling via the PI_3K pathway in obese Zucker rats (Carvalheira *et al.* , 2003).

In this study it was shown for the first time that selective insulin resistance also affects the same signaling pathway in distinct neuronal populations. Exposure to HFD leads to the development of insulin resistance in POMC neurons, associated with a decreased POMC expression and the inability of insulin to decrease food intake (Clegg *et al.* , 2011; Mayer & Belsham, 2010). In contrast to ARC neurons, VMH SF-1 neurons remain insulin sensitive, at least up to 5 weeks of HFD-feeding. It is possible that the prolonged exposure to HFD leads to a complete neuronal and peripheral insulin resistance, which would explain the loss of protection against diet-induced weight gain after 12 weeks of HFD feeding. From this age on, control and SF-$1^{\Delta IR}$ males show a similar weight gain, although SF-$1^{\Delta IR}$ males are still significantly lighter. One important factor for the development of insulin and leptin resistance are elevated levels of circulating saturated free fatty acids (sFFA), like palmitate, as they are able to induce inhibitory signaling via the c-Jun n-terminal kinase (JNK) pathway and ER stress (Cintra *et al.* , 2012; Kleinridders *et al.* , 2009; Mayer & Belsham, 2010). POMC and AgRP neurons in the ARC are directly exposed to metabolites from the blood circulation due to their proximity to the blood-brain barrier (BBB). As VMH SF-1 neurons are located in a greater distance from the BBB, they might be exposed to lower levels of circulating insulin, FFA and inflammatory cytokines from the periphery and thus retain their insulin sensitivity.

Taken together, insulin signaling in SF-1 VMH neurons promotes obesity in a PI_3K dependent manner. Furthermore, VMH SF-1 neurons retain their insulin responsiveness under HFD conditions longer than ARC neurons and thus further promote the development of obesity, but the phenomenon of selective insulin resistance and the underlying molecular mechanisms have to be further investigated.

4.6 Unaltered expression of hypothalamic neuropeptides, but increased activity of POMC neurons

Leptin exerts several effects in the hypothalamus to reduce food intake and increase energy expenditure. Besides a lot of yet unidentified targets, leptin has been shown to

increase the expression of POMC and to inhibit the expression of its antagonist, AgRP (Mizuno *et al.* , 1998; Schwartz *et al.* , 1997). Additionally, NPY and CART are also regulated by leptin (Kristensen *et al.* , 1998; Schwartz *et al.* , 1998). Thus, the expression of neuropeptides was analyzed by quantitative real-time PCR. None of the examined neuropeptides showed alterations in mRNA levels, nor did BDNF, which is strongly associated with the control of energy homeostasis in the VMH (Caruso *et al.* , 2012; Jo, 2012; Kernie *et al.* , 2000; Liao *et al.* , 2012; Unger *et al.* , 2007; Wang *et al.* , 2010). Thus, changes in the expression level of neuropeptides are not the reason for the reduced adiposity. Recent publications also indicate a role for FOXO1 in VMH SF-1 neurons in the regulation of energy homeostasis by modulating energy expenditure via the sympathetic nervous system and that FOXO1 regulates the expression of SF-1 (Kim *et al.* , 2012). However, expression of SF-1 mRNA remained unaltered. Furthermore, when the PiP_3 dependent downstream kinase (PDK1) is deleted, no effect is observed neither on NCD nor on HFD (personal communication with Bengt F. Belgardt). Due to the fact that PDK1 phosphorylates and thereby activates AKT, that mediates insulin effects on the transcriptional level, alterations in gene expression can be excluded as a reason for the observed phenotype.

As we have previously demonstrated, leptin's ability to reduce food intake is improved in SF-$1^{\Delta IR}$ males on HFD. Therefore we analyzed further targets of leptin's action in the hypothalamus. Leptin is able to modulate POMC neurons activity by non-specific cation channels and thereby regulates the release of POMC cleavage product, α-MSH, into the target areas of POMC neurons. We could show that POMC neurons in SF-$1^{\Delta IR}$ animals have an increased spontaneous firing activity as compared to POMC neurons in control ($IR^{fl/fl}$) animals under HFD conditions. Furthermore, the number of silent POMC neurons is largely reduced in HFD-fed SF-$1^{\Delta IR}$ animals compared to their control littermates.

Thus, the decreased body weight in SF-$1^{\Delta IR}$ males upon HFD-feeding is likely to be caused by an enhanced basal firing rate of POMC neurons and thereby an increased release of α-MSH into the target areas, leading to a reduced food intake.

However, it is still unclear how SF-1 neurons contribute to this effect, and especially how insulin signaling in these neurons contributes to the firing rate of POMC neurons.

We could show in patch-clamp recordings of control SF-1 neurons that insulin significantly hyperpolarizes SF-1 neurons and thereby reduces their firing rate. Most of the neurons that display the hyperpolarization-response to insulin are located in the medio-basal part of the VMH, thus in the direct proximity of the ARC, where POMC and AgRP neurons are located. Thus, we hypothesize that SF-1 neurons send excitatory synapses from the medio-basal VMH to POMC neurons in the ARC. This hypothesis is supported by two publications: (I) Tong and colleagues were able to show that glutamate release from SF-1 neurons is necessary for the regulation of body weight under HFD conditions (Tong *et al.* , 2007a). When glutamate packaging into synaptic vesicles was prevented by the deletion of the glutamate transporter Vglut2 in SF-1 neurons, mice became even more obese when fed a HFD. Notably, this increased body weight also resulted from an increase in fat mass, whereas lean mass was unaltered. Thus, glutamate release from SF-1 neurons is important for body weight and fat mass regulation, especially under HFD conditions. (II) Further support arises from the publication of Sternson and colleagues. They topographically mapped connections between the ARC and the VMH by laser scanning photostimulation, where glutamate is uncaged at several distinct locations by simultaneously recording possible target neurons. By these experiments they were able to create heat-maps of GABAergic and glutamatergic projections to POMC, NPY and unidentified neurons in the ARC (Sternson *et al.* , 2005).

Inhibitory inputs on POMC neurons mainly arise from projections within the ARC, presumably NPY/AgRP neurons (Sternson *et al.* , 2005). This implicates that the changes in the inhibitory input, observed in post-synaptic current measurements and also in the electron-microscopy, are rather a secondary effect of the reduced adiposity. As Pinto and colleagues could show, leptin is able to re-organize the synaptic input of POMC neurons (Pinto *et al.* , 2004). In states of leptin resistance, either genetically or diet-induced, the number and frequency of inhibitory inputs is massively increased on POMC neurons. Due to the fact that both post-synaptic current measurements as well as electron-microscopy were performed in mice that already differed in body weight and adiposity, leptin resistance was more pronounced in control than SF-1$^{\Delta IR}$ animals, thus explain-

ing the observed differences in IPSC frequency and number of GABAergic synapses on POMC neurons.

On the other hand, excitatory glutamatergic input on POMC neurons mainly arises from an area in the "medial VMH" (or medio-basal VMH, mVMH) (Sternson *et al.* , 2005), the area where most of the PiP_3 formation was observed and the area with the highest density of insulin-responsive SF-1 neurons. This indicates that the glutamatergic neurons in the mVMH are inhibited in their ability to elicit action potentials by the HFD-induced hyperinsulinemia and thus in their ability to release glutamate on POMC neurons. This results in decreased α-MSH release from POMC-nerve terminals onto MC4R expressing second-order neurons and consequently in increased food intake. This insulin-induced hyperpolarization is absent SF-$1^{\Delta IR}$ animals, resulting in an increased excitatory tone on POMC neurons. This further enables the occurrence of action potentials in POMC neurons (either leptin induced, but also in states of leptin resistance), resulting in an elevated release of α-MSH and finally reduced food intake via MC4R signaling. Although the differences in excitatory input are not as obvious as the changes in inhibitory input, this might be again influenced by the age of the analyzed mice. Both, electron-microscopy and post-synaptic current measurements were performed in animals with significant differences in body weight and adiposity, indicating a different degree of leptin resistance between the genotypes and thus a more prominent change in the inhibitory input reorganization. And although the changes in excitatory inputs did not reach statistical significance in both experiments, mean values of the excitatory input were higher in SF-$1^{\Delta IR}$ animals on HFD compared to controls. Further analysis of synaptic input organization on POMC neurons in younger animals is needed to confirm this hypothesis.

Finally, the excitatory projections from the mVMH are reduced when mice were fasted and this reduction is not reversed by additional treatment with leptin (Sternson *et al.* , 2005). This indicates that glutamatergic neurons in the mVMH are likely to be glucose-excited neurons, that induce satiety upon elevated glucose concentrations. As shown by Cotero and colleagues, insulin is able to reduce the sensitivity to glucose in glucose-excited VMH neurons via K_{ATP} channels, which is completely in line with our observa-

tions (Cotero & Routh, 2009). The fact that leptin is not able to reverse the effect of fasting indicates that leptin and insulin responsive neurons are indeed segregating populations.

Taken together, results from this study indicate that VMH SF-1 neurons send glutamatergic projections to POMC neurons to trigger α-MSH release in the PVN. Under HFD conditions, hyperinsulinemia impairs the release of glutamate to POMC neurons, which further decreases activity of POMC neurons and leads to increased weight gain (figure 4.1). Although this model is supported by two other publications, further studies about the synaptic connections of VMH SF-1 neurons will be performed by using iZ/WAP mice to unravel projection targets of SF-1 neurons (Louis *et al.* , 2010).

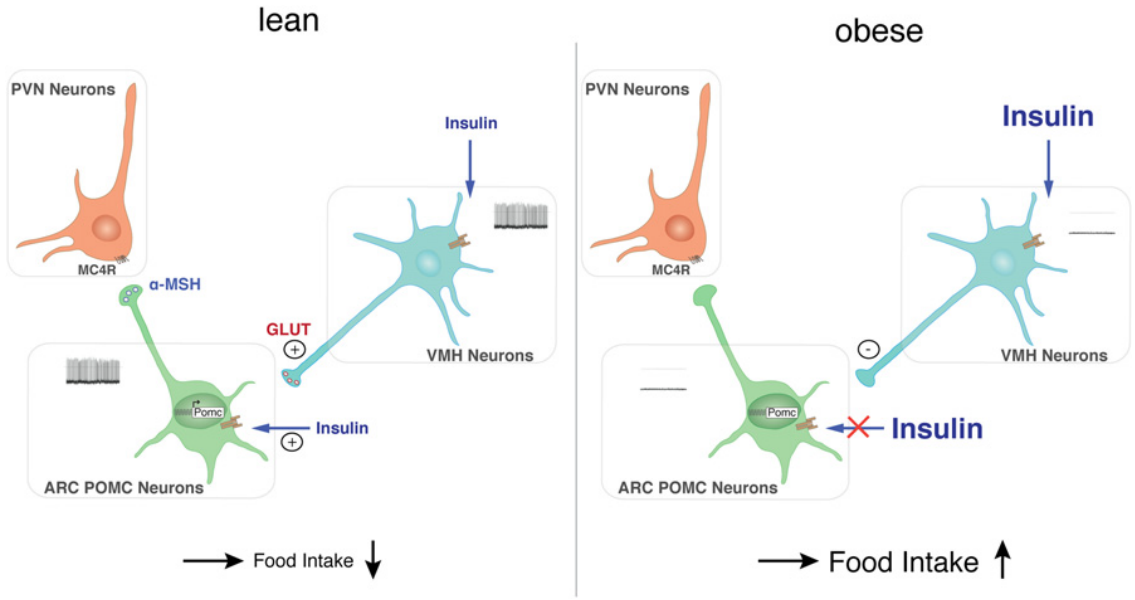

Figure 4.1: Model of insulin's effect in VMH SF-1 neurons. Image taken from Könner & Bruning (2012).
In lean animals, VMH SF-1 neurons provide glutamatergic synapses on POMC neurons to trigger the release of α-MSH from POMC neurons in the ARC. Obesity associated hyperinsulinemia impairs the activity of VMH SF-1 neurons, further decreasing the activity of POMC neurons. Furthermore, insulin resistance in POMC neurons upon HFD feeding impairs the transcription of *POMC*, whereas VMH SF-1 neurons remain insulin sensitive.

4.7 Impaired counter-regulatory response to hypoglycemia in SF-1$^{\Delta IR}$ animals

The aforementioned results raise the question if insulin signaling in VMH SF-1 neurons also contributes any beneficial effects. As shown by Fisher and colleagues, insulin in

the CNS is mandatory to induce the counter-regulatory response to hypoglycemia (CRR) (Fisher *et al.* , 2005). Furthermore, Tong and colleagues could show that glutamate in SF-1 neurons plays a pivotal role in the induction of CRR by innervation of the adrenal gland and the pancreas via the vagus nerve (Tong *et al.* , 2007a). Recent results by Diggs-Andrews and colleagues could show that insulin signaling in the VMH is necessary to drive the expression of the insulin-dependent glucose transporter GLUT4 in these neurons, and that GLUT4 is mandatory for the glucose sensing properties of VMH neurons (Diggs-Andrews *et al.* , 2010).

Thus we hypothesized that the lack of insulin signaling in VMH SF-1 neurons may be responsible for the defective CRR observed in NIRKO mice. To this end, hypoglycemic-hyperinsulinemic clamp studies were performed in control and SF-1$^{\Delta IR}$ males and females.

On the level of the glucose infusion rate, we were able to identify SF-1 neurons as the responsible neuronal population in the VMH for the induction of the CRR in females, as female SF-1$^{\Delta IR}$ animals needed significantly more glucose to maintain blood glucose levels of $\sim$50 mg/dL in the steady state. Unfortunately, this could not be verified by the analysis of plasma epinephrine, norepinephrine, corticosterone and glucagon levels. All of these hormones are involved in the CRR by promoting hepatic gluconeogenesis, but no differences could be observed in their plasma levels. Male SF-1$^{\Delta IR}$ animals showed the same tendency towards an increased glucose infusion rate upon insulin-induced hypoglycemia but this did not reach statistical significance.

As already mentioned, the SF-1 Cre is expressed in approximately 50 % of the neurons in the VMH. Thus, there might be other neurons in the VMH, that do not express the SF-1 Cre, but are responsible for the induction of the CRR. Besides insulin mediated GLUT4 expression, other factors are also involved in the CRR. A study by Fioramonti and colleagues indicates an important role for nitric oxide synthases in glucose-inhibited VMH neurons for the CRR (Fioramonti *et al.* , 2010). Thus, other neurons in the VMH and other glucose-sensing mechanisms might compensate for the loss of insulin signaling in SF-1 neurons and thereby still enable a sufficient induction of the counter-regulatory response to hypoglycemia.

Thus, the SF-1 Cre might not be the ideal tool to investigate the role of the VMH in the CRR, but SF-1 neurons are obviously involved, as the increased GIR in female SF-1$^{\Delta IR}$ animals indicates. Therefore it is necessary to find other marker genes for the VMH that enables the expression of the Cre in every neuron in the VMH.

4.8 Perspectives

By the deletion of the insulin receptor in SF-1 neurons we identified insulin signaling in the VMH as a critical component in the development of obesity. In contrast to previous findings, where the acute role of insulin signaling in the regulation of energy homeostasis was revealed, we could show that prolonged and sustained insulin signaling in VMH SF-1 neurons contributes to the initial phase of obesity propagation. Although insulin serves as a satiety signal in the CNS and especially in the ARC, diet-induced hyperinsulinemia seems to inhibit VMH SF-1 neurons in their ability to maintain body weight. This could be shown by two different mouse models, either partially protecting from diet-induced weight gain (SF-1$^{\Delta IR}$) or promoting obesity under NCD conditions (SF-1$^{\Delta PTEN}$). However, further studies are mandatory to reveal the exact mechanism underlying the phenotype. Due to the fact that only a part of SF-1 neurons are responsive to insulin, further subpopulations have to be identified. Accordingly, it is still unknown how the activity of VMH SF-1 neurons is regulated. As VMH neurons consist of glucose excited and glucose inhibited neurons, most likely the glucose excited neurons serve as a possible candidate subpopulation that mediate the satiety promoting effects of SF-1 neurons by glucose-stimulated glutamate-release to POMC neurons and the subsequent release of α-MSH onto second-order neurons. Moreover, also the projection sites of SF-1 neurons have to be identified, as a subset of SF-1 neurons is reported to express MC4R (Xu *et al.* , 2003). Thus it is possible that SF-1 and POMC neurons are connected vice versa. Furthermore, recent results indicate a role for BDNF in the inhibitory input organization within the VMH (Jo, 2012), a mechanism where insulin could also play a role.

Taken together, this study about insulin signaling in SF-1 neurons provides further insights into the complex regulatory mechanism of CNS mediated control of energy home-

ostasis and a better understanding of this regulatory network is mandatory to fight the obesity pandemic of the 21^{st} century.

List of Figures

1.1 Schematic overview of hypothalamic nuclei 5

1.2 Hypothalamic melanocortin system 8

1.3 Leptin Signaling pathway 12

1.4 Insulin Signaling pathway 18

1.5 Counter-regulatory response to hypoglycemia 23

3.1 Scheme of SF-1 Cre mediated recombination of the insulin receptor allele . 42

3.2 GFP expression in SF-1^{GFP} mice in the brain and peripheral organs 43

3.3 Western Blot analysis of brain regions and peripheral tissues from control (IR$^{fl/fl}$) and SF-1$^{\Delta IR}$ mice 44

3.4 Unaltered fertility and hypothalamic-pituitary-gonadal axis of control and SF-1$^{lacZ:\Delta IR}$ animals 46

3.5 *In situ* hybridization against *insulin receptor* mRNA in control (SF-1^{lacZ}) and SF-1$^{lacZ:\Delta IR}$ animals 46

3.6 Insulin stimulated accumulation of PiP_3 in control (SF-1^{lacZ}) and SF-1$^{lacZ:\Delta IR}$ animals 48

3.7 Effects of insulin on electrical activity of SF-1-positive VMH neurons . . . 50

3.8 Body weight and body composition of control and SF-1$^{\Delta IR}$ males on NCD and HFD 53

3.9 Leptin levels and average adipocyte size of control and SF-1$^{\Delta IR}$ males on NCD and HFD 54

3.10 Unaltered energy expenditure and food intake of 6 to 7 week old control and SF-1$^{\Delta IR}$ males on HFD 55

3.11 Unaltered energy expenditure food intake of 12 to 13 week old control and SF-1$^{\Delta IR}$ males on HFD 56

3.12 Increased leptin sensitivity in 8 week old SF-1$^{\Delta IR}$ males on HFD 57

3.13 Unaltered glucose homeostasis in control and SF-1$^{\Delta IR}$ males on NCD . . . 58

3.14 Improved glucose homeostasis in SF-1$^{\Delta IR}$ males on HFD 59
3.15 PI_3K activation promotes hyperphagia and weight gain 60
3.16 Deletion of IR and PTEN in SF-1 neurons normalized body weight and adiposity upon HFD exposure 61
3.17 Expression of hypothalamic neuropeptides 62
3.18 Spontaneous firing activity of POMC neurons 63
3.19 Measurement of post synaptic currents on POMC neurons 64
3.20 Number of inhibitory and excitatory synapses on POMC neurons 65
3.21 Hypoglycemic-hyperinsulinemic Clamp protocoll 66
3.22 Hypoglycemic clamps of female control and SF-1$^{\Delta IR}$ animals 67
3.23 Hypoglycemic clamps of ‚ale control and SF-1$^{\Delta IR}$ animals 68

4.1 Model of insulin's effect on VMH SF-1 neurons 82

List of Tables

2.1 PCR primers 30

2.2 Real-time PCR probes 31

2.3 Primary western blot antibodies 38

2.4 Chemicals 1 39

2.5 Chemicals 2 40

2.6 Chemicals 3 41

3.1 Electrophysiological parameters of SF-1 neurons in SF-1^{GFP} and SF-1$^{GFP:\Delta IR}$ mice. 49

3.2 Responses of SF-1 neurons to leptin and insulin. 51

3.3 Responses of SF-1 neurons to sequential leptin and insulin double application. 51

3.4 Responses of SF-1 neurons to sequential insulin and leptin double application. 52

Bibliography

AGUIRRE, V, UCHIDA, T, YENUSH, L, DAVIS, R, & WHITE, M F. 2000. The c-Jun NH(2)-terminal kinase promotes insulin resistance during association with insulin receptor substrate-1 and phosphorylation of Ser(307). *Journal of biological chemistry*, **275**(12), 9047–9054.

AGUIRRE, VINCENT, WERNER, ERIC D, GIRAUD, JODEL, LEE, YONG HEE, SHOELSON, STEVE E, & WHITE, MORRIS F. 2002. Phosphorylation of Ser307 in insulin receptor substrate-1 blocks interactions with the insulin receptor and inhibits insulin action. *Journal of biological chemistry*, **277**(2), 1531–1537.

ALESSI, D R, DEAK, M, CASAMAYOR, A, CAUDWELL, F B, MORRICE, N, NORMAN, D G, GAFFNEY, P, REESE, C B, MACDOUGALL, C N, HARBISON, D, ASHWORTH, A, & BOWNES, M. 1997a. 3-Phosphoinositide-dependent protein kinase-1 (PDK1): structural and functional homology with the Drosophila DSTPK61 kinase. *Curr biol*, **7**(10), 776–789.

ALESSI, D R, JAMES, S R, DOWNES, C P, HOLMES, A B, GAFFNEY, P R, REESE, C B, & COHEN, P. 1997b. Characterization of a 3-phosphoinositide-dependent protein kinase which phosphorylates and activates protein kinase Balpha. *Curr biol*, **7**(4), 261–269.

ANAND, B K, & BROBECK, J R. 1951. Localization of a "feeding center" in the hypothalamus of the rat. *Proceedings of the society for experimental biology and medicine society for experimental biology and medicine (new york, ny)*, **77**(2), 323–324.

ANDERSON, K E, COADWELL, J, STEPHENS, L R, & HAWKINS, P T. 1998. Translocation of PDK-1 to the plasma membrane is important in allowing PDK-1 to activate protein kinase B. *Curr biol*, **8**(12), 684–691.

APONTE, YEXICA, ATASOY, DENIZ, & STERNSON, SCOTT M. 2011. AGRP neurons are sufficient to orchestrate feeding behavior rapidly and without training. *Nature neuroscience*, **14**(3), 351–355.

ARAVICH, P F, & SCLAFANI, A. 1983. Paraventricular hypothalamic lesions and medial hypothalamic knife cuts produce similar hyperphagia syndromes. *Behav neurosci*, **97**(6), 970–983.

ARRUDA, ANA PAULA, MILANSKI, MARCIANE, COOPE, ANDRESSA, TORSONI, ADRIANA S, ROPELLE, EDUARDO, CARVALHO, DENISE P, CARVALHEIRA, JOSÉ B, & VELLOSO, LICIO A. 2011. Low-grade hypothalamic inflammation leads to defective thermogenesis, insulin resistance, and impaired insulin secretion. *Endocrinology*, **152**(4), 1314–1326.

ASHCROFT, F M. 2006. K(ATP) channels and insulin secretion: a key role in health and disease. *Biochemical society transactions*, **34**(Pt 2), 243–246.

ASHCROFT, FRANCES M. 2005. ATP-sensitive potassium channelopathies: focus on insulin secretion. *Journal of clinical investigation*, **115**(8), 2047–2058.

ASNICAR, M A, SMITH, D P, YANG, D D, HEIMAN, M L, FOX, N, CHEN, Y F, HSIUNG, H M, & KÖSTER, A. 2001. Absence of cocaine- and amphetamine-regulated transcript results in obesity in mice fed a high caloric diet. *Endocrinology*, **142**(10), 4394–4400.

ATASOY, DENIZ, BETLEY, J NICHOLAS, SU, HELEN H, & STERNSON, SCOTT M. 2012. Deconstruction of a neural circuit for hunger. *Nature*, **488**(7410), 172–177.

BADO, A, LEVASSEUR, S, ATTOUB, S, KERMORGANT, S, LAIGNEAU, J P, BORTOLUZZI, M N, MOIZO, L, LEHY, T, GUERRE-MILLO, M, LE MARCHAND-BRUSTEL, Y, & LEWIN, M J. 1998. The stomach is a source of leptin. *Nature*, **394**(6695), 790–793.

BAILLY-MAITRE, BÉATRICE, BELGARDT, BENGT F, JORDAN, SABINE D, COORNAERT, BEATRICE, VON FREYEND, MIRIAM JOHN, KLEINRIDDERS, ANDRÉ, MAUER, JAN, CUDDY, MICHAEL, KRESS, CHRISTINA L, WILLMES, DIANA, ESSIG, MANUELA, HAMPEL, BRIGITTE, PROTZER, ULRIKE, REED, JOHN C, & BRUNING, JENS C. 2010. Hepatic Bax inhibitor-1 inhibits IRE1alpha and protects from obesity-associated insulin resistance and glucose intolerance. *The journal of biological chemistry*, **285**(9), 6198–6207.

BALTHASAR, NINA, COPPARI, ROBERTO, MCMINN, JULIE, LIU, SHUN M, LEE, CHARLOTTE E, TANG, VINSEE, KENNY, CHRISTOPHER D, MCGOVERN, ROBERT A, CHUA, STREAMSON C, ELMQUIST, JOEL K, & LOWELL, BRADFORD B. 2004. Leptin receptor signaling in POMC neurons is required for normal body weight homeostasis. *Neuron*, **42**(6), 983–991.

BANDYOPADHYAY, G K, YU, J G, OFRECIO, J, & OLEFSKY, J M. 2005. Increased p85/55/50 expression and decreased phosphotidylinositol 3-kinase activity in insulin-resistant human skeletal muscle. *Diabetes*, **54**(8), 2351–2359.

BANKS, A S, DAVIS, S M, BATES, S H, & MYERS, M G. 2000. Activation of downstream signals by the long form of the leptin receptor. *Journal of biological chemistry*, **275**(19), 14563–14572.

BANKS, W A, JASPAN, J B, & KASTIN, A J. 1997. Selective, physiological transport of insulin across the blood-brain barrier: novel demonstration by species-specific radioimmunoassays. *Peptides*, **18**(8), 1257–1262.

BANNO, RYOICHI, ZIMMER, DEREK, DE JONGHE, BART C, ATIENZA, MARYBLESS, RAK, KIMBERLY, YANG, WENTIAN, & BENCE, KENDRA K. 2010. PTP1B and SHP2 in POMC neurons reciprocally regulate energy balance in mice. *Journal of clinical investigation*, **120**(3), 720–734.

BANTING, FREDERIK GRANT, BEST, CHRS HOLGER, COLLIP, JOHN BEN, CAMPBELL, WILLIAM ROBERT, & FLETCHER, ANDREW ALLEN. 1922. Pancreatic extracts in the treatment of diabetes mellitus. Preliminary report. *Cmaj*, Sept., 141–146.

BASKIN, D G, SIPOLS, A J, SCHWARTZ, M W, & WHITE, M F. 1993. Immunocytochemical detection of insulin receptor substrate-1 (IRS-1) in rat brain: colocalization with phosphotyrosine. *Regulatory peptides*, **48**(1-2), 257–266.

BATAILLE, D, GESPACH, C, TATEMOTO, K, MARIE, J C, COUDRAY, A M, ROSSELIN, G, & MUTT, V. 1981. Bioactive enteroglucagon (oxyntomodulin): present knowledge on its chemical structure and its biological activities. *Peptides*, **2 Suppl 2**, 41–44.

BELGARDT, BENGT F, HUSCH, ANDREAS, ROTHER, EVA, ERNST, MARIANNE B, WUNDERLICH, F THOMAS, HAMPEL, BRIGITTE, KLÖCKENER, TIM, ALESSI, DARIO, KLOPPENBURG, PETER, & BRUNING, JENS C. 2008. PDK1 deficiency in POMC-expressing cells reveals FOXO1-dependent and -independent pathways in control of energy homeostasis and stress response. *Cell metabolism*, **7**(4), 291–301.

BELGARDT, BENGT F, MAUER, JAN, WUNDERLICH, F THOMAS, ERNST, MARIANNE B, PAL, MARTIN, SPOHN, GABRIELE, BRÖNNEKE, HELLA S, BRODESSER, SUSANNE, HAMPEL, BRIGITTE, SCHAUSS, ASTRID C, & BRÜNING, JENS C. 2010. Hypothalamic and pituitary c-Jun N-terminal kinase 1 signaling coordinately regulates glucose metabolism. *Proceedings of the national academy of sciences of the united states of america*, **107**(13), 6028–6033.

BENCE, KK, DELIBEGOVIC, M, XUE, B, GORGUN, CZ, HOTAMISLIGIL, GS, NEEL, BG, & KAHN, BB. 2006. Neuronal PTP1B regulates body weight, adiposity and leptin action. *Nature medicine*, **12**(8), 917–924.

BENECKE, H, FLIER, J S, & MOLLER, D E. 1992. Alternatively spliced variants of the insulin receptor protein. Expression in normal and diabetic human tissues. *Journal of clinical investigation*, **89**(6), 2066–2070.

BENOIT, STEPHEN C, KEMP, CHRISTOPHER J, ELIAS, CAROL F, ABPLANALP, WILLIAM, HERMAN, JAMES P, MIGRENNE, STEPHANIE, LEFEVRE, ANNE-LAURE, CRUCIANI-GUGLIELMACCI, CÉLINE, MAGNAN, CHRISTOPHE, YU, FANG, NISWENDER, KEVIN, IRANI, BOMAN G, HOLLAND, WILLIAM L, & CLEGG, DEBORAH J. 2009. Palmitic acid mediates hypothalamic insulin resistance by altering PKC-theta subcellular localization in rodents. *Journal of clinical investigation*, **119**(9), 2577–2589.

BERGHÖFER, ANNE, PISCHON, TOBIAS, REINHOLD, THOMAS, APOVIAN, CAROLINE M, SHARMA, ARYA M, & WILLICH, STEFAN N. 2008. Obesity prevalence from a European perspective: a systematic review. *Bmc public health*, **8**, 200.

BERNALES, SEBASTIÁN, PAPA, FEROZ R, & WALTER, PETER. 2006. Intracellular signaling by the unfolded protein response. *Annual review of cell and developmental biology*, **22**, 487–508.

BIDDINGER, SUDHA B, HERNANDEZ-ONO, ANTONIO, RASK-MADSEN, CHRISTIAN, HAAS, JOEL T, ALEMÁN, JOSÉ O, SUZUKI, RYO, SCAPA, EREZ F, AGARWAL, CHHAVI, CAREY, MARTIN C, STEPHANOPOULOS, GREGORY, COHEN, DAVID E, KING,

GEORGE L, GINSBERG, HENRY N, & KAHN, C RONALD. 2008. Hepatic insulin resistance is sufficient to produce dyslipidemia and susceptibility to atherosclerosis. *Cell metabolism*, **7**(2), 125–134.

BINGHAM, NC, ANDERSON, KK, REUTER, AL, STALLINGS, NR, & PARKER, KL. 2008. Selective loss of leptin receptors in the ventromedial hypothalamic nucleus results in increased adiposity and a metabolic syndrome. *Endocrinology*, **149**(5), 2138.

BITTENCOURT, J C, PRESSE, F, ARIAS, C, PETO, C, VAUGHAN, J, NAHON, J L, VALE, W, & SAWCHENKO, P E. 1992. The melanin-concentrating hormone system of the rat brain: An immuno- and hybridization histochemical characterization. *The journal of comparative neurology*, **319**(2), 218–245.

BJORBAEK, C, ELMQUIST, J K, FRANTZ, J D, SHOELSON, S E, & FLIER, J S. 1998. Identification of SOCS-3 as a potential mediator of central leptin resistance. *Molecular cell*, **1**(4), 619–625.

BJÖRNHOLM, MARIE, MÜNZBERG, HEIKE, LESHAN, REBECCA L, VILLANUEVA, ENEIDA C, BATES, SARAH H, LOUIS, GWENDOLYN W, JONES, JUSTIN C, ISHIDA-TAKAHASHI, RYOKO, BJØRBAEK, CHRISTIAN, & MYERS, MARTIN G. 2007. Mice lacking inhibitory leptin receptor signals are lean with normal endocrine function. *Journal of clinical investigation*, **117**(5), 1354–1360.

BLOND-ELGUINDI, S, CWIRLA, S E, DOWER, W J, LIPSHUTZ, R J, SPRANG, S R, SAMBROOK, J F, & GETHING, M J. 1993. Affinity panning of a library of peptides displayed on bacteriophages reveals the binding specificity of BiP. *Cell*, **75**(4), 717–728.

BLÜHER, MATTHIAS, MICHAEL, M DODSON, PERONI, ODILE D, UEKI, KOHJIRO, CARTER, NATHAN, KAHN, BARBARA B, & KAHN, C RONALD. 2002. Adipose tissue selective insulin receptor knockout protects against obesity and obesity-related glucose intolerance. *Developmental cell*, **3**(1), 25–38.

BORG, M A, SHERWIN, R S, BORG, W P, TAMBORLANE, W V, & SHULMAN, G I. 1997. Local ventromedial hypothalamus glucose perfusion blocks counterregulation during systemic hypoglycemia in awake rats. *Journal of clinical investigation*, **99**(2), 361–365.

BORG, M A, BORG, W P, TAMBORLANE, W V, BRINES, M L, SHULMAN, G I, & SHERWIN, R S. 1999. Chronic hypoglycemia and diabetes impair counterregulation induced by localized 2-deoxy-glucose perfusion of the ventromedial hypothalamus in rats. *Diabetes*, **48**(3), 584–587.

BORG, W P, DURING, M J, SHERWIN, R S, BORG, M A, BRINES, M L, & SHULMAN, G I. 1994. Ventromedial hypothalamic lesions in rats suppress counterregulatory responses to hypoglycemia. *Journal of clinical investigation*, **93**(4), 1677–1682.

BORG, W P, SHERWIN, R S, DURING, M J, BORG, M A, & SHULMAN, G I. 1995. Local ventromedial hypothalamus glucopenia triggers counterregulatory hormone release. *Diabetes*, **44**(2), 180–184.

BOULTON, T G, ZHONG, Z, WEN, Z, DARNELL, J E, STAHL, N, & YANCOPOULOS, G D. 1995. STAT3 activation by cytokines utilizing gp130 and related transducers involves a secondary modification requiring an H7-sensitive kinase. *Proceedings of the national academy of sciences of the united states of america*, **92**(15), 6915–6919.

BOYLE, P. C., & KEESEY, R E. 1975. Chronically reduced body weight in rats sustaining lesions of the lateral hypothalamus and maintained on palatable diets and drinking solutions. *J comp physiol psychol*, **88**(1), 218–223.

BROADWELL, R D, & BRIGHTMAN, M W. 1976. Entry of peroxidase into neurons of the central and peripheral nervous systems from extracerebral and cerebral blood. *The journal of comparative neurology*, **166**(3), 257–283.

BROBECK, J R. 1946. Mechanism of the development of obesity in animals with hypothalamic lesions. *Physiol rev*, **26**(4), 541–559.

BROWN, LM, CLEGG, DJ, BENOIT, SC, & WOODS, SC. 2006. Intraventricular insulin and leptin reduce food intake and body weight in C57BL/6J mice. *Physiology & behavior*, **89**(5), 687–691.

BRÜNING, J C, WINNAY, J, BONNER-WEIR, S, TAYLOR, S I, ACCILI, D, & KAHN, C R. 1997. Development of a novel polygenic model of NIDDM in mice heterozygous for IR and IRS-1 null alleles. *Cell*, **88**(4), 561–572.

BRÜNING, J C, MICHAEL, M D, WINNAY, J N, HAYASHI, T, HÖRSCH, D, ACCILI, D, GOODYEAR, L J, & KAHN, C R. 1998. A muscle-specific insulin receptor knockout exhibits features of the metabolic syndrome of NIDDM without altering glucose tolerance. *Molecular cell*, **2**(5), 559–569.

BRÜNING, J C, GAUTAM, D, BURKS, D J, GILLETTE, J, SCHUBERT, M, ORBAN, P C, KLEIN, R, KRONE, W, MÜLLER-WIELAND, D, & KAHN, C R. 2000. Role of brain insulin receptor in control of body weight and reproduction. *Science (new york, ny)*, **289**(5487), 2122–2125.

BURKS, D J, PONS, S, TOWERY, H, SMITH-HALL, J, MYERS, M G, YENUSH, L, & WHITE, M F. 1997. Heterologous pleckstrin homology domains do not couple IRS-1 to the insulin receptor. *Journal of biological chemistry*, **272**(44), 27716–27721.

BURKS, D J, WANG, J, TOWERY, H, ISHIBASHI, O, LOWE, D, RIEDEL, H, & WHITE, M F. 1998. IRS pleckstrin homology domains bind to acidic motifs in proteins. *Journal of biological chemistry*, **273**(47), 31061–31067.

BUTLER, ANDREW A. 2006. The melanocortin system and energy balance. *Peptides*, **27**(2), 281–290.

CAI, DONGSHENG, YUAN, MINSHENG, FRANTZ, DANIEL F, MELENDEZ, PETER A, HANSEN, LONE, LEE, JONGSOON, & SHOELSON, STEVEN E. 2005. Local and systemic insulin resistance resulting from hepatic activation of IKK-beta and NF-kappaB. *Nature medicine*, **11**(2), 183–190.

CAMPFIELD, L A, SMITH, F J, & BURN, P. 1996. The OB protein (leptin) pathway–a link between adipose tissue mass and central neural networks. *Hormone and metabolic research = hormon- und stoffwechselforschung = hormones et métabolisme*, **28**(12), 619–632.

CANABAL, DEBRA D, SONG, ZHENTAO, POTIAN, JOSEPH G, BEUVE, ANNIE, MCARDLE, JOSEPH J, & ROUTH, VANESSA H. 2007. Glucose, insulin, and leptin signaling pathways modulate nitric oxide synthesis in glucose-inhibited neurons in the ventromedial hypothalamus. *American journal of physiology- regulatory, integrative and comparative physiology*, **292**(4), R1418–28.

CARUSO, CARLA, CARNIGLIA, LILA, DURAND, DANIELA, GONZALEZ, PATRICIA V, SCIMONELLI, TERESA N, & LASAGA, MERCEDES. 2012. Melanocortin 4 receptor activation induces brain-derived neurotrophic factor expression in rat astrocytes through cyclic AMP-protein kinase A pathway. *Molecular and cellular endocrinology*, **348**(1), 47–54.

CARVALHEIRA, J B C, RIBEIRO, E B, ARAUJO, E P, GUIMARÃES, R B, TELLES, M M, TORSONI, M, GONTIJO, J A R, VELLOSO, L A, & SAAD, M J A. 2003. Selective impairment of insulin signalling in the hypothalamus of obese Zucker rats. *Diabetologia*, **46**(12), 1629–1640.

CASAMAYOR, A, MORRICE, N A, & ALESSI, D R. 1999. Phosphorylation of Ser-241 is essential for the activity of 3-phosphoinositide-dependent protein kinase-1: identification of five sites of phosphorylation in vivo. *Biochemical journal*, **342 (Pt 2)**(Sept.), 287–292.

CHAVEZ, JOSE A, & SUMMERS, SCOTT A. 2012. A Ceramide-Centric View of Insulin Resistance. *Cell metabolism*, **15**(5), 585–594.

CHEN, H, CHARLAT, O, TARTAGLIA, L A, WOOLF, E A, WENG, X, ELLIS, S J, LAKEY, N D, CULPEPPER, J, MOORE, K J, BREITBART, R E, DUYK, G M, TEPPER, R I, & MORGENSTERN, J P. 1996. Evidence that the diabetes gene encodes the leptin receptor: identification of a mutation in the leptin receptor gene in db/db mice. *Cell*, **84**(3), 491–495.

CHEN, XI, SHEN, JINGSHI, & PRYWES, RON. 2002. The luminal domain of ATF6 senses endoplasmic reticulum (ER) stress and causes translocation of ATF6 from the ER to the Golgi. *Journal of biological chemistry*, **277**(15), 13045–13052.

CHUA, S C, KOUTRAS, I K, HAN, L, LIU, S M, KAY, J, YOUNG, S J, CHUNG, W K, & LEIBEL, R L. 1997. Fine structure of the murine leptin receptor gene: splice site suppression is required to form two alternatively spliced transcripts. *Genomics*, **45**(2), 264–270.

CINTRA, DENNYS E, ROPELLE, EDUARDO R, MORAES, JULIANA C, PAULI, JOSÉ R, MORARI, JOSEANE, SOUZA, CLAUDIO T DE, GRIMALDI, RENATO, STAHL, MARCELA, CARVALHEIRA, JOSÉ B, SAAD, MARIO J, & VELLOSO, LICIO A. 2012. Unsaturated

fatty acids revert diet-induced hypothalamic inflammation in obesity. *Plos one*, **7**(1), e30571.

CLARK, J T, KALRA, P S, & KALRA, S P. 1985. Neuropeptide Y stimulates feeding but inhibits sexual behavior in rats. *Endocrinology*, **117**(6), 2435–2442.

CLAYCOMBE, K J, JONES, B H, STANDRIDGE, M K, GUO, Y, CHUN, J T, TAYLOR, J W, & MOUSTAÏD-MOUSSA, N. 1998. Insulin increases fatty acid synthase gene transcription in human adipocytes. *The american journal of physiology*, **274**(5 Pt 2), R1253–9.

CLEGG, DEBORAH J, GOTOH, KORO, KEMP, CHRISTOPHER, WORTMAN, MATTHEW D, BENOIT, STEPHEN C, BROWN, LYNDA M, D'ALESSIO, DAVID, TSO, PATRICK, SEELEY, RANDY J, & WOODS, STEPHEN C. 2011. Consumption of a high-fat diet induces central insulin resistance independent of adiposity. *Physiology & behavior*, **103**(1), 10–16.

COHEN, B, NOVICK, D, & RUBINSTEIN, M. 1996. Modulation of insulin activities by leptin. *Science (new york, ny)*, **274**(5290), 1185–1188.

COHEN, P, ZHAO, C, CAI, X, MONTEZ, J M, ROHANI, S C, FEINSTEIN, P, MOMBAERTS, P, & FRIEDMAN, J M. 2001. Selective deletion of leptin receptor in neurons leads to obesity. *Journal of clinical investigation*, **108**(8), 1113–1121.

COLEMAN, D L. 1973. Effects of parabiosis of obese with diabetes and normal mice. *Diabetologia*, **9**(4), 294–298.

COLEMAN, D L, & HUMMEL, K P. 1969. Effects of parabiosis of normal with genetically diabetic mice. *The american journal of physiology*, **217**(5), 1298–1304.

COLL, ANTHONY P, FAROOQI, I SADAF, CHALLIS, BENJAMIN G, YEO, GILES S H, & O'RAHILLY, STEPHEN. 2004. Proopiomelanocortin and energy balance: insights from human and murine genetics. *Journal of clinical endocrinology & metabolism*, **89**(6), 2557–2562.

CONNER, J M, LAUTERBORN, J C, YAN, Q, GALL, C M, & VARON, S. 1997. Distribution of brain-derived neurotrophic factor (BDNF) protein and mRNA in the normal adult rat CNS: evidence for anterograde axonal transport. *The journal of neuroscience : the official journal of the society for neuroscience*, **17**(7), 2295–2313.

CONSIDINE, R V, SINHA, M K, HEIMAN, M L, KRIAUCIUNAS, A, STEPHENS, T W, NYCE, M R, OHANNESIAN, J P, MARCO, C C, MCKEE, L J, & BAUER, T L. 1996. Serum immunoreactive-leptin concentrations in normal-weight and obese humans. *The new england journal of medicine*, **334**(5), 292–295.

COTERO, VICTORIA E, & ROUTH, VANESSA H. 2009. Insulin blunts the response of glucose-excited neurons in the ventrolateral-ventromedial hypothalamic nucleus to decreased glucose. *American journal of physiology- endocrinology and metabolism*, **296**(5), E1101–9.

COWLEY, M A, SMART, J L, RUBINSTEIN, M, CERDÁN, M G, DIANO, S, HORVATH, T L, CONE, R D, & LOW, M J. 2001. Leptin activates anorexigenic POMC neurons through a neural network in the arcuate nucleus. *Nature*, **411**(6836), 480–484.

COWLEY, MA, CONE, RD, ENRIORI, P, LOUISELLE, I, WILLIAMS, SM, & EVANS, AE. 2003. Electrophysiological actions of peripheral hormones on melanocortin neurons. *Annals of the new york academy of sciences*, **994**(THE MELANOCORTIN SYSTEM), 175–186.

CROSS, D A, ALESSI, D R, COHEN, P, ANDJELKOVICH, M, & HEMMINGS, B A. 1995. Inhibition of glycogen synthase kinase-3 by insulin mediated by protein kinase B. *Nature*, **378**(6559), 785–789.

CRYER, PHILIP E. 2008. The barrier of hypoglycemia in diabetes. *Diabetes*, **57**(12), 3169–3176.

CRYER, PHILIP E, DAVIS, STEPHEN N, & SHAMOON, HARRY. 2003. Hypoglycemia in diabetes. *Diabetes care*, **26**(6), 1902–1912.

CURRIE, R A, WALKER, K S, GRAY, A, DEAK, M, CASAMAYOR, A, DOWNES, C P, COHEN, P, ALESSI, D R, & LUCOCQ, J. 1999. Role of phosphatidylinositol 3,4,5-trisphosphate in regulating the activity and localization of 3-phosphoinositide-dependent protein kinase-1. *Biochemical journal*, **337 (Pt 3)**(Feb.), 575–583.

DAGOGO-JACK, S E, CRAFT, S, & CRYER, P E. 1993. Hypoglycemia-associated autonomic failure in insulin-dependent diabetes mellitus. Recent antecedent hypoglycemia reduces autonomic responses to, symptoms of, and defense against subsequent hypoglycemia. *Journal of clinical investigation*, **91**(3), 819–828.

DAVIDSON, H W, RHODES, C J, & HUTTON, J C. 1988. Intraorganellar calcium and pH control proinsulin cleavage in the pancreatic beta cell via two distinct site-specific endopeptidases. *Nature*, **333**(6168), 93–96.

DAVIS, J E, GABLER, N K, WALKER-DANIELS, J, & SPURLOCK, M E. 2009. The c-Jun N-terminal kinase mediates the induction of oxidative stress and insulin resistance by palmitate and toll-like receptor 2 and 4 ligands in 3T3-L1 adipocytes. *Hormone and metabolic research = hormon- und stoffwechselforschung = hormones et métabolisme*, **41**(7), 523–530.

DE LECEA, L, KILDUFF, T S, PEYRON, C, GAO, X, FOYE, P E, DANIELSON, P E, FUKUHARA, C, BATTENBERG, E L, GAUTVIK, V T, BARTLETT, F S, FRANKEL, W N, VAN DEN POL, A N, BLOOM, F E, GAUTVIK, K M, & SUTCLIFFE, J G. 1998. The hypocretins: hypothalamus-specific peptides with neuroexcitatory activity. *Proceedings of the national academy of sciences of the united states of america*, **95**(1), 322–327.

DE LUCA, CARL, KOWALSKI, TIMOTHY J, ZHANG, YIYING, ELMQUIST, JOEL K, LEE, CHARLOTTE, KILIMANN, MANFRED W, LUDWIG, THOMAS, LIU, SHUN-MEI, &

CHUA, STREAMSON C. 2005. Complete rescue of obesity, diabetes, and infertility in db/db mice by neuron-specific LEPR-B transgenes. *Journal of clinical investigation*, **115**(12), 3484–3493.

DE TAEYE, B M, NOVITSKAYA, T, MCGUINNESS, O P, GLEAVES, L, MEDDA, M, COVINGTON, J W, & VAUGHAN, D E. 2007. Macrophage TNF- contributes to insulin resistance and hepatic steatosis in diet-induced obesity. *American journal of physiology-endocrinology and metabolism*, **293**(3), E713–E725.

DEBONS, A F, SILVER, L, CRONKITE, E P, JOHNSON, H A, BRECHER, G, TENZER, D, & SCHWARTZ, I L. 1962. Localization of gold in mouse brain in relation to gold thioglucose obesity. *The american journal of physiology*, **202**(Apr.), 743–750.

DENIS, R G, ARRUDA, A P, ROMANATTO, T, MILANSKI, M, COOPE, A, SOLON, C, RAZOLLI, D S, & VELLOSO, L A. 2010. TNF-α transiently induces endoplasmic reticulum stress and an incomplete unfolded protein response in the hypothalamus. *Neuroscience*, **170**(4), 1035–1044.

DHILLON, H, ZIGMAN, JM, YE, C, LEE, CE, MCGOVERN, RA, TANG, V, KENNY, CD, CHRISTIANSEN, LM, WHITE, RD, & EDELSTEIN, EA. 2006. Leptin directly activates SF1 neurons in the VMH, and this action by leptin is required for normal body-weight homeostasis. *Neuron*, **49**(2), 191–203.

DIETRICH, MARCELO O, BOBER, JEREMY, FERREIRA, JOZÉLIA G, TELLEZ, LUIS A, MINEUR, YANN S, SOUZA, DIOGO O, GAO, XIAO-BING, PICCIOTTO, MARINA R, ARAÚJO, IVAN, LIU, ZHONG-WU, & HORVATH, TAMAS L. 2012. AgRP neurons regulate development of dopamine neuronal plasticity and nonfood-associated behaviors. *Nature neuroscience*, **15**(8), 1108–1110.

DIGGS-ANDREWS, KELLY A, ZHANG, XUEZHAO, SONG, ZHENTAO, DAPHNA-IKEN, DORIT, ROUTH, VANESSA H, & FISHER, SIMON J. 2010. Brain insulin action regulates hypothalamic glucose sensing and the counterregulatory response to hypoglycemia. *Diabetes*, **59**(9), 2271–2280.

DIXON, JOHN B. 2010. The effect of obesity on health outcomes. *Molecular and cellular endocrinology*, **316**(2), 104–108.

DOCHERTY, K, & HUTTON, J C. 1983. Carboxypeptidase activity in the insulin secretory granule. *Febs letters*, **162**(1), 137–141.

DOMINGOS, ANA I, VAYNSHTEYN, JAKE, VOSS, HENNING U, REN, XUEYING, GRADINARU, VIVIANA, ZANG, FENG, DEISSEROTH, KARL, DE ARAUJO, IVAN E, & FRIEDMAN, JEFFREY. 2011. Leptin regulates the reward value of nutrient. *Nature neuroscience*, **14**(12), 1562–1568.

ECK, M J, DHE-PAGANON, S, TRÜB, T, NOLTE, R T, & SHOELSON, S E. 1996. Structure of the IRS-1 PTB domain bound to the juxtamembrane region of the insulin receptor. *Cell*, **85**(5), 695–705.

EL-HASCHIMI, KARIM, PIERROZ, DOMINIQUE D, HILEMAN, STANLEY M, BJØRBAEK, CHRISTIAN, & FLIER, JEFFREY S. 2000. Two defects contribute to hypothalamic leptin resistance in mice with diet-induced obesity. *Journal of clinical investigation*, **105**(12), 1827–1832.

ELCHEBLY, M, PAYETTE, P, MICHALISZYN, E, CROMLISH, W, COLLINS, S, LOY, A L, NORMANDIN, D, CHENG, A, HIMMS-HAGEN, J, CHAN, C C, RAMACHANDRAN, C, GRESSER, M J, TREMBLAY, M L, & KENNEDY, B P. 1999. Increased insulin sensitivity and obesity resistance in mice lacking the protein tyrosine phosphatase-1B gene. *Science (new york, ny)*, **283**(5407), 1544–1548.

ELMQUIST, J K, AHIMA, R S, MARATOS-FLIER, E, FLIER, J S, & SAPER, C B. 1997. Leptin activates neurons in ventrobasal hypothalamus and brainstem. *Endocrinology*, **138**(2), 839–842.

ELMQUIST, J K, BJORBAEK, C, AHIMA, R S, FLIER, J S, & SAPER, C B. 1998a. Distributions of leptin receptor mRNA isoforms in the rat brain. *The journal of comparative neurology*, **395**(4), 535–547.

ELMQUIST, J K, AHIMA, R S, ELIAS, C F, FLIER, J S, & SAPER, C B. 1998b. Leptin activates distinct projections from the dorsomedial and ventromedial hypothalamic nuclei. *Proceedings of the national academy of sciences of the united states of america*, **95**(2), 741–746.

ENDO, T A, MASUHARA, M, YOKOUCHI, M, SUZUKI, R, SAKAMOTO, H, MITSUI, K, MATSUMOTO, A, TANIMURA, S, OHTSUBO, M, MISAWA, H, MIYAZAKI, T, LEONOR, N, TANIGUCHI, T, FUJITA, T, KANAKURA, Y, KOMIYA, S, & YOSHIMURA, A. 1997. A new protein containing an SH2 domain that inhibits JAK kinases. *Nature*, **387**(6636), 921–924.

ENRIORI, PABLO J, EVANS, ANNE E, SINNAYAH, PUSPHA, JOBST, ERIN E, TONELLI-LEMOS, LUCIANA, BILLES, SONJA K, GLAVAS, MARIA M, GRAYSON, BERNADETTE E, PERELLO, MARIO, NILLNI, EDUARDO A, GROVE, KEVIN L, & COWLEY, MICHAEL A. 2007. Diet-induced obesity causes severe but reversible leptin resistance in arcuate melanocortin neurons. *Cell metabolism*, **5**(3), 181–194.

ERNST, MARIANNE B, WUNDERLICH, CLAUDIA M, HESS, SIMON, PAEHLER, MORITZ, MESAROS, ANDREA, KORALOV, SERGEI B, KLEINRIDDERS, ANDRÉ, HUSCH, ANDREAS, MÜNZBERG, HEIKE, HAMPEL, BRIGITTE, ALBER, JENS, KLOPPENBURG, PETER, BRUNING, JENS C, & WUNDERLICH, F THOMAS. 2009. Enhanced Stat3 activation in POMC neurons provokes negative feedback inhibition of leptin and insulin signaling in obesity. *Journal of neuroscience*, **29**(37), 11582–11593.

ESPOSITO, KATHERINE, PONTILLO, ALESSANDRO, GIUGLIANO, FRANCESCO, GIUGLIANO, GIOVANNI, MARFELLA, RAFFAELE, NICOLETTI, GIANFRANCO, & GIUGLIANO, DARIO. 2003. Association of low interleukin-10 levels with the metabolic

syndrome in obese women. *Journal of clinical endocrinology & metabolism*, **88**(3), 1055–1058.

FAN, W, BOSTON, B A, KESTERSON, R A, HRUBY, V J, & CONE, R D. 1997. Role of melanocortinergic neurons in feeding and the agouti obesity syndrome. *Nature*, **385**(6612), 165–168.

FAROOQI, I S, & O'RAHILLY, S. 2004. Monogenic human obesity syndromes. *Recent progress in hormone research*, **59**, 409–424.

FAROOQI, I S, YEO, G S, KEOGH, J M, AMINIAN, S, JEBB, S A, BUTLER, G, CHEETHAM, T, & O'RAHILLY, S. 2000. Dominant and recessive inheritance of morbid obesity associated with melanocortin 4 receptor deficiency. *Journal of clinical investigation*, **106**(2), 271–279.

FIORAMONTI, XAVIER, MARSOLLIER, NICOLAS, SONG, ZHENTAO, FAKIRA, KURT A, PATEL, REEMA M, BROWN, STACEY, DUPARC, THIBAUT, PICA-MENDEZ, ARNALDO, SANDERS, NICOLE M, KNAUF, CLAUDE, VALET, PHILIPPE, MCCRIMMON, RORY J, BEUVE, ANNIE, MAGNAN, CHRISTOPHE, & ROUTH, VANESSA H. 2010. Ventromedial hypothalamic nitric oxide production is necessary for hypoglycemia detection and counterregulation. *Diabetes*, **59**(2), 519–528.

FISHER, SJ, BRÜNING, JC, LANNON, S, & KAHN, CR. 2005. Insulin signaling in the central nervous system is critical for the normal sympathoadrenal response to hypoglycemia. *Diabetes*, **54**(5), 1447.

FREDERICH, R C, HAMANN, A, ANDERSON, S, LÖLLMANN, B, LOWELL, B B, & FLIER, J S. 1995. Leptin levels reflect body lipid content in mice: evidence for diet-induced resistance to leptin action. *Nature medicine*, **1**(12), 1311–1314.

FRIEDMAN, J M. 1998. Leptin, leptin receptors, and the control of body weight. *Nutrition reviews*, **56**(2 Pt 2), s38–46; discussion s54–75.

FRÖHLICH, A. 1901. Ein fall von tumor der hypophysis cerebri ohne akromegalie. *Wien klin. rundsch.*, 883–886.

FU, LI-YING, & VAN DEN POL, ANTHONY N. 2008. Agouti-related peptide and MC3/4 receptor agonists both inhibit excitatory hypothalamic ventromedial nucleus neurons. *Journal of neuroscience*, **28**(21), 5433–5449.

GALBO, THOMAS, OLSEN, GRITH SKYTTE, QUISTORFF, BJØRN, & NISHIMURA, ERICA. 2011. Free fatty acid-induced PP2A hyperactivity selectively impairs hepatic insulin action on glucose metabolism. *Plos one*, **6**(11), e27424.

GAO, QIAN, WOLFGANG, MICHAEL J, NESCHEN, SUSANNE, MORINO, KATSUTARO, HORVATH, TAMAS L, SHULMAN, GERALD I, & FU, XIN-YUAN. 2004. Disruption of neural signal transducer and activator of transcription 3 causes obesity, diabetes, infertility, and thermal dysregulation. *Proceedings of the national academy of sciences of the united states of america*, **101**(13), 4661–4666.

GAO, QIAN, MEZEI, GABOR, NIE, YONGZHAN, RAO, YAN, CHOI, CHEOL SOO, BECHMANN, INGO, LERANTH, CSABA, TORAN-ALLERAND, DOMINIQUE, PRIEST, CATHERINE A, ROBERTS, JAMES L, GAO, XIAO-BING, MOBBS, CHARLES, SHULMAN, GERALD I, DIANO, SABRINA, & HORVATH, TAMAS L. 2007. Anorectic estrogen mimics leptin's effect on the rewiring of melanocortin cells and Stat3 signaling in obese animals. *Nature medicine*, **13**(1), 89–94.

GASTALDELLI, A, BALDI, S, PETTITI, M, TOSCHI, E, CAMASTRA, S, NATALI, A, LANDAU, B R, & FERRANNINI, E. 2000. Influence of obesity and type 2 diabetes on gluconeogenesis and glucose output in humans: a quantitative study. *Diabetes*, **49**(8), 1367–1373.

GIRAUDO, S Q, BILLINGTON, C J, & LEVINE, A S. 1998. Feeding effects of hypothalamic injection of melanocortin 4 receptor ligands. *Brain research*, **809**(2), 302–306.

GOLD, R M. 1973. Hypothalamic obesity: the myth of the ventromedial nucleus. *Science (new york, ny)*, **182**(4111), 488–490.

GROPP, E, SHANABROUGH, M, BOROK, E, XU, AW, JANOSCHEK, R, BUCH, T, PLUM, L, BALTHASAR, N, HAMPEL, B, & WAISMAN, A. 2005. Agouti-related peptide–expressing neurons are mandatory for feeding. *Nature neuroscience*, **8**(10), 1289–1291.

GROSSMAN, S P, DACEY, D, HALARIS, A E, COLLIER, T, & ROUTTENBERG, A. 1978. Aphagia and adipsia after preferential destruction of nerve cell bodies in hypothalamus. *Science (new york, ny)*, **202**(4367), 537–539.

HAJ, FAWAZ G, VERVEER, PETER J, SQUIRE, ANTHONY, NEEL, BENJAMIN G, & BASTIAENS, PHILIPPE I H. 2002. Imaging sites of receptor dephosphorylation by PTP1B on the surface of the endoplasmic reticulum. *Science (new york, ny)*, **295**(5560), 1708–1711.

HALLSCHMID, MANFRED, BENEDICT, CHRISTIAN, SCHULTES, BERND, FEHM, HORSTLORENZ, BORN, JAN, & KERN, WERNER. 2004. Intranasal insulin reduces body fat in men but not in women. *Diabetes*, **53**(11), 3024–3029.

HARRIS, R B S. 1999. Parabiosis between db/db and ob/ob or db/+ mice. *Endocrinology*, **140**(1), 138–145.

HAVRANKOVA, J, SCHMECHEL, D, ROTH, J, & BROWNSTEIN, M. 1978a. Identification of insulin in rat brain. *Proceedings of the national academy of sciences of the united states of america*, **75**(11), 5737–5741.

HAVRANKOVA, J, ROTH, J, & BROWNSTEIN, M. 1978b. Insulin receptors are widely distributed in the central nervous system of the rat. *Nature*, **272**(5656), 827–829.

HAVRANKOVA, J, ROTH, J, & BROWNSTEIN, M J. 1979. Concentrations of insulin and insulin receptors in the brain are independent of peripheral insulin levels. Studies of obese and streptozotocin-treated rodents. *Journal of clinical investigation*, **64**(2), 636–642.

HEERWAGEN, MARGARET J R, MILLER, MELISSA R, BARBOUR, LINDA A, & FRIEDMAN, JACOB E. 2010. Maternal obesity and fetal metabolic programming: a fertile epigenetic soil. *Ajp: Regulatory, integrative and comparative physiology*, **299**(3), R711–22.

HELLER, S R, & CRYER, P E. 1991. Reduced neuroendocrine and symptomatic responses to subsequent hypoglycemia after 1 episode of hypoglycemia in nondiabetic humans. *Diabetes*, **40**(2), 223–226.

HETHERINGTON, A W, & RANSON, S W. 1940. Hypothalamic lesions and adiposity in the rat. *Anat. rec.*

HEYMSFIELD, S B, GREENBERG, A S, FUJIOKA, K, DIXON, R M, KUSHNER, R, HUNT, T, LUBINA, J A, PATANE, J, SELF, B, HUNT, P, & MCCAMISH, M. 1999. Recombinant leptin for weight loss in obese and lean adults: a randomized, controlled, dose-escalation trial. *Jama : the journal of the american medical association*, **282**(16), 1568–1575.

HILEMAN, STANLEY M, PIERROZ, DOMINIQUE D, MASUZAKI, HIROAKI, BJØRBAEK, CHRISTIAN, EL-HASCHIMI, KARIM, BANKS, WILLIAM A, & FLIER, JEFFREY S. 2002. Characterizaton of short isoforms of the leptin receptor in rat cerebral microvessels and of brain uptake of leptin in mouse models of obesity. *Endocrinology*, **143**(3), 775–783.

HILL, JENNIFER W, WILLIAMS, KEVIN W, YE, CHIANPING, LUO, JI, BALTHASAR, NINA, COPPARI, ROBERTO, COWLEY, MICHAEL A, CANTLEY, LEWIS C, LOWELL, BRADFORD B, & ELMQUIST, JOEL K. 2008. Acute effects of leptin require PI3K signaling in hypothalamic proopiomelanocortin neurons in mice. *Journal of clinical investigation*, **118**(5), 1796–1805.

HILL, JENNIFER W, XU, YONG, PREITNER, FREDERIC, FUKUDA, MAKOTA, CHO, YOU-REE, LUO, JI, BALTHASAR, NINA, COPPARI, ROBERTO, CANTLEY, LEWIS C, KAHN, BARBARA B, ZHAO, JEAN J, & ELMQUIST, JOEL K. 2009. Phosphatidyl inositol 3-kinase signaling in hypothalamic proopiomelanocortin neurons contributes to the regulation of glucose homeostasis. *Endocrinology*, **150**(11), 4874–4882.

HILL, JENNIFER W, ELIAS, CAROL F, FUKUDA, MAKOTO, WILLIAMS, KEVIN W, BERGLUND, ERIC D, HOLLAND, WILLIAM L, CHO, YOU-REE, CHUANG, JEN-CHIEH, XU, YONG, CHOI, MICHELLE, LAUZON, DANIELLE, LEE, CHARLOTTE E, COPPARI, ROBERTO, RICHARDSON, JAMES A, ZIGMAN, JEFFREY M, CHUA, STREAMSON, SCHERER, PHILIPP E, LOWELL, BRADFORD B, BRUNING, JENS C, & ELMQUIST, JOEL K. 2010. Direct Insulin and Leptin Action on Pro-opiomelanocortin Neurons Is Required for Normal Glucose Homeostasis and Fertility. *Cell metabolism*, **11**(4), 286–297.

HIROSUMI, JIRO, TUNCMAN, GÜROL, CHANG, LUFEN, GORGUN, CEM Z, UYSAL, K TEOMAN, MAEDA, KAZUHISA, KARIN, MICHAEL, & HOTAMISLIGIL, GOKHAN S. 2002. A central role for JNK in obesity and insulin resistance. *Nature*, **420**(6913), 333–336.

HODAN, F, & BUZBY, J. 2005. The ERS Food Comsumption Data. *Usda*.

HORVATH, TAMAS L, SARMAN, BEATRIX, GARCÍA-CÁCERES, CRISTINA, ENRIORI, PABLO J, SOTONYI, PETER, SHANABROUGH, MARYA, BOROK, ERZSEBET, ARGENTE, JESÚS, CHOWEN, JULIE A, PEREZ-TILVE, DIEGO, PFLUGER, PAUL T, BRÖNNEKE, HELLA S, LEVIN, BARRY E, DIANO, SABRINA, COWLEY, MICHAEL A, & TSCHÖP, MATTHIAS H. 2010. Synaptic input organization of the melanocortin system predicts diet-induced hypothalamic reactive gliosis and obesity. *Proceedings of the national academy of sciences*, **107**(33), 14875–14880.

HOTAMISLIGIL, G S, SHARGILL, N S, & SPIEGELMAN, B M. 1993. Adipose expression of tumor necrosis factor-alpha: direct role in obesity-linked insulin resistance. *Science (new york, ny)*, **259**(5091), 87–91.

HOTAMISLIGIL, G S, PERALDI, P, BUDAVARI, A, ELLIS, R, WHITE, M F, & SPIEGELMAN, B M. 1996. IRS-1-mediated inhibition of insulin receptor tyrosine kinase activity in TNF-alpha- and obesity-induced insulin resistance. *Science (new york, ny)*, **271**(5249), 665–668.

HOWARD, JANE K, CAVE, BELINDA J, OKSANEN, LAURA J, TZAMELI, IPHIGENIA, BJØRBAEK, CHRISTIAN, & FLIER, JEFFREY S. 2004. Enhanced leptin sensitivity and attenuation of diet-induced obesity in mice with haploinsufficiency of Socs3. *Nature medicine*, **10**(7), 734–738.

HUANG, HAOJIE, & TINDALL, DONALD J. 2007. Dynamic FoxO transcription factors. *Journal of cell science*, **120**(Pt 15), 2479–2487.

HUSZAR, D, LYNCH, C A, FAIRCHILD-HUNTRESS, V, DUNMORE, J H, FANG, Q, BERKEMEIER, L R, GU, W, KESTERSON, R A, BOSTON, B A, CONE, R D, SMITH, F J, CAMPFIELD, L A, BURN, P, & LEE, F. 1997. Targeted disruption of the melanocortin-4 receptor results in obesity in mice. *Cell*, **88**(1), 131–141.

IKEDA, Y, SHEN, WH, INGRAHAM, HA, & PARKER, KL. 1994. Developmental expression of mouse steroidogenic factor-1, an essential regulator of the steroid hydroxylases. *Molecular endocrinology*, **8**(5), 654.

INGALLS, A M, DICKIE, M M, & SNELL, G D. 1950. Obese, a new mutation in the house mouse. *The journal of heredity*, **41**(12), 317–318.

INOUE, S, & BRAY, G A. 1977. The effects of subdiaphragmatic vagotomy in rats with ventromedial hypothalamic obesity. *Endocrinology*, **100**(1), 108–114.

JACOBS, A R, LEROITH, D, & TAYLOR, S I. 2001. Insulin receptor substrate-1 pleckstrin homology and phosphotyrosine-binding domains are both involved in plasma membrane targeting. *Journal of biological chemistry*, **276**(44), 40795–40802.

JAWORSKI, K, SARKADI-NAGY, E, DUNCAN, R E, AHMADIAN, M, & SUL, H S. 2007. Regulation of Triglyceride Metabolism. * IV. Hormonal regulation of lipolysis in adipose tissue. *Ajp: Gastrointestinal and liver physiology*, **293**(1), G1–G4.

JO, YOUNG-HWAN. 2012. Endogenous BDNF regulates inhibitory synaptic transmission in the ventromedial nucleus of the hypothalamus. *Journal of neurophysiology*, **107**(1), 42–49.

KAHN, C R. 1994a. Banting Lecture. Insulin action, diabetogenes, and the cause of type II diabetes. *Diabetes*, **43**(8), 1066–1084.

KAHN, C R. 1994b. Banting Lecture. Insulin action, diabetogenes, and the cause of type II diabetes. *Diabetes*.

KAHN, C R, BAIRD, K L, JARRETT, D B, & FLIER, J S. 1978. Direct demonstration that receptor crosslinking or aggregation is important in insulin action. *Proceedings of the national academy of sciences of the united states of america*, **75**(9), 4209–4213.

KANG, L, DUNN-MEYNELL, AA, ROUTH, VH, GASPERS, LD, NAGATA, Y, NISHIMURA, T, EIKI, J, ZHANG, BB, & LEVIN, BE. 2006. Glucokinase is a critical regulator of ventromedial hypothalamic neuronal glucosensing. *Diabetes*, **55**(2), 412.

KASUGA, M, HEDO, J A, YAMADA, K M, & KAHN, C R. 1982. The structure of insulin receptor and its subunits. Evidence for multiple nonreduced forms and a 210,000 possible proreceptor. *Journal of biological chemistry*, **257**(17), 10392–10399.

KERN, P A, RANGANATHAN, S, LI, C, WOOD, L, & RANGANATHAN, G. 2001. Adipose tissue tumor necrosis factor and interleukin-6 expression in human obesity and insulin resistance. *American journal of physiology- endocrinology and metabolism*, **280**(5), E745–51.

KERNIE, S G, LIEBL, D J, & PARADA, L F. 2000. BDNF regulates eating behavior and locomotor activity in mice. *The embo journal*, **19**(6), 1290–1300.

KERSHAW, ERIN E, HAMM, JONATHAN K, VERHAGEN, LINDA A W, PERONI, ODILE, KATIC, MASA, & FLIER, JEFFREY S. 2006. Adipose triglyceride lipase: function, regulation by insulin, and comparison with adiponutrin. *Diabetes*, **55**(1), 148–157.

KIEVIT, PAUL, HOWARD, JANE K, BADMAN, MICHAEL K, BALTHASAR, NINA, COPPARI, ROBERTO, MORI, HIROYUKI, LEE, CHARLOTTE E, ELMQUIST, JOEL K, YOSHIMURA, AKIHIKO, & FLIER, JEFFREY S. 2006. Enhanced leptin sensitivity and improved glucose homeostasis in mice lacking suppressor of cytokine signaling-3 in POMC-expressing cells. *Cell metabolism*, **4**(2), 123–132.

KIM, E M, O'HARE, E, GRACE, M K, WELCH, C C, BILLINGTON, C J, & LEVINE, A S. 2000a. ARC POMC mRNA and PVN alpha-MSH are lower in obese relative to lean zucker rats. *Brain research*, **862**(1-2), 11–16.

KIM, KI WOO, DONATO, JOSE, BERGLUND, ERIC D, CHOI, YUN-HEE, KOHNO, DAISUKE, ELIAS, CAROL F, DEPINHO, RONALD A, & ELMQUIST, JOEL K. 2012. FOXO1 in the ventromedial hypothalamus regulates energy balance. *Journal of clinical investigation*, **122**(7), 2578–2589.

KIM, KW, ZHAO, L, & PARKER, KL. 2009. Central nervous system-specific knockout of steroidogenic factor 1. *Molecular and cellular endocrinology*, **300**(1-2), 132–136.

KIM, M S, ROSSI, M, ABUSNANA, S, SUNTER, D, MORGAN, D G, SMALL, C J, EDWARDS, C M, HEATH, M M, STANLEY, S A, SEAL, L J, BHATTI, J R, SMITH, D M, GHATEI, M A, & BLOOM, S R. 2000b. Hypothalamic localization of the feeding effect of agouti-related peptide and alpha-melanocyte-stimulating hormone. *Diabetes*, **49**(2), 177–182.

KIM, M S, SMALL, C J, STANLEY, S A, MORGAN, D G, SEAL, L J, KONG, W M, EDWARDS, C M, ABUSNANA, S, SUNTER, D, GHATEI, M A, & BLOOM, S R. 2000c. The central melanocortin system affects the hypothalamo-pituitary thyroid axis and may mediate the effect of leptin. *Journal of clinical investigation*, **105**(7), 1005–1011.

KITAMURA, T, FENG, Y, KITAMURA, Y I, CHUA, S C JR, XU, A W, BARSH, G S, ROSSETTI, L, & ACCILI, D. 2006. Forkhead protein FoxO1 mediates Agrp-dependent effects of leptin on food intake. *Nat med*, **12**(5), 534–540.

KLEINRIDDERS, ANDRÉ, SCHENTEN, DOMINIK, KÖNNER, A CHRISTINE, BELGARDT, BENGT F, MAUER, JAN, OKAMURA, TOMOO, WUNDERLICH, F THOMAS, MEDZHITOV, RUSLAN, & BRÜNING, JENS C. 2009. MyD88 signaling in the CNS is required for development of fatty acid-induced leptin resistance and diet-induced obesity. *Cell metabolism*, **10**(4), 249–259.

KLÖCKENER, TIM, HESS, SIMON, BELGARDT, BENGT F, PAEGER, LARS, VERHAGEN, LINDA A W, HUSCH, ANDREAS, SOHN, JONG-WOO, HAMPEL, BRIGITTE, DHILLON, HARVEEN, ZIGMAN, JEFFREY M, LOWELL, BRADFORD B, WILLIAMS, KEVIN W, ELMQUIST, JOEL K, HORVATH, TAMAS L, KLOPPENBURG, PETER, & BRUNING, JENS C. 2011. High-fat feeding promotes obesity via insulin receptor/PI3K-dependent inhibition of SF-1 VMH neurons. *Nature neuroscience*, **14**(7), 911–918.

KOCH, CHRISTIANE, AUGUSTINE, RACHAEL A, STEGER, JULIANE, GANJAM, GOUTHAM K, BENZLER, JONAS, PRACHT, CORINNA, LOWE, CHRISHANTHI, SCHWARTZ, MICHAEL W, SHEPHERD, PETER R, ANDERSON, GREG M, GRATTAN, DAVID R, & TUPS, ALEXANDER. 2010. Leptin rapidly improves glucose homeostasis in obese mice by increasing hypothalamic insulin sensitivity. *Journal of neuroscience*, **30**(48), 16180–16187.

KOCH, L, WUNDERLICH, FT, SEIBLER, J, KÖNNER, AC, HAMPEL, B, IRLENBUSCH, S, BRABANT, G, KAHN, CR, SCHWENK, F, & BRÜNING, JC. 2008. Central insulin action regulates peripheral glucose and fat metabolism in mice. *Journal of clinical investigation*, **118**(6), 2132.

KOJIMA, M, HOSODA, H, DATE, Y, NAKAZATO, M, MATSUO, H, & KANGAWA, K. 1999. Ghrelin is a growth-hormone-releasing acylated peptide from stomach. *Nature*, **402**(6762), 656–660.

KÖNNER, A CHRISTINE, & BRUNING, JENS C. 2012. Selective Insulin and Leptin Resistance in Metabolic Disorders. *Cell metabolism*, **16**(2), 144–152.

KÖNNER, A CHRISTINE, JANOSCHEK, RUTH, PLUM, LEONA, JORDAN, SABINE D, ROTHER, EVA, MA, XIAOSONG, XU, CHUN, ENRIORI, PABLO, HAMPEL, BRIGITTE, BARSH, GREGORY S, KAHN, C RONALD, COWLEY, MICHAEL A, ASHCROFT, FRANCES M, & BRUNING, JENS C. 2007. Insulin action in AgRP-expressing neurons is required for suppression of hepatic glucose production. *Cell metabolism*, **5**(6), 438–449.

KOWALSKI, T J, LIU, S M, LEIBEL, R L, & CHUA, S C. 2001. Transgenic complementation of leptin-receptor deficiency. I. Rescue of the obesity/diabetes phenotype of LEPR-null mice expressing a LEPR-B transgene. *Diabetes*, **50**(2), 425–435.

KRISTENSEN, P, JUDGE, M E, THIM, L, RIBEL, U, CHRISTJANSEN, K N, WULFF, B S, CLAUSEN, J T, JENSEN, P B, MADSEN, O D, VRANG, N, LARSEN, P J, & HASTRUP, S. 1998. Hypothalamic CART is a new anorectic peptide regulated by leptin. *Nature*, **393**(6680), 72–76.

KUBLAOUI, BASSIL M, HOLDER, J LLOYD, GEMELLI, TERRY, & ZINN, ANDREW R. 2006. Sim1 haploinsufficiency impairs melanocortin-mediated anorexia and activation of paraventricular nucleus neurons. *Molecular endocrinology (baltimore, md.)*, **20**(10), 2483–2492.

LACQUANITI, ANTONIO, DONATO, VALENTINA, CHIRICO, VALERIA, BUEMI, ANTOINE, & BUEMI, MICHELE. 2011. Obestatin: an interesting but controversial gut hormone. *Annals of nutrition & metabolism*, **59**(2-4), 193–199.

LAPCHAK, P A, & HEFTI, F. 1992. BDNF and NGF treatment in lesioned rats: effects on cholinergic function and weight gain. *Neuroreport*, **3**(5), 405–408.

LATRES, ESTHER, AMINI, AMI R, AMINI, ASHLEY A, GRIFFITHS, JENNIFER, MARTIN, FRANCIS J, WEI, YI, LIN, HSIN CHIEH, YANCOPOULOS, GEORGE D, & GLASS, DAVID J. 2005. Insulin-like growth factor-1 (IGF-1) inversely regulates atrophy-induced genes via the phosphatidylinositol 3-kinase/Akt/mammalian target of rapamycin (PI3K/Akt/mTOR) pathway. *Journal of biological chemistry*, **280**(4), 2737–2744.

LAVAN, B E, & LIENHARD, G E. 1993. The insulin-elicited 60-kDa phosphotyrosine protein in rat adipocytes is associated with phosphatidylinositol 3-kinase. *Journal of biological chemistry*, **268**(8), 5921–5928.

LAVAN, B E, KUHNÉ, M R, GARNER, C W, ANDERSON, D, REEDIJK, M, PAWSON, T, & LIENHARD, G E. 1992. The association of insulin-elicited phosphotyrosine proteins with src homology 2 domains. *Journal of biological chemistry*, **267**(16), 11631–11636.

LAVAN, B E, FANTIN, V R, CHANG, E T, LANE, W S, KELLER, S R, & LIENHARD, G E. 1997a. A novel 160-kDa phosphotyrosine protein in insulin-treated embryonic kidney cells is a new member of the insulin receptor substrate family. *Journal of biological chemistry*, **272**(34), 21403–21407.

LAVAN, B E, LANE, W S, & LIENHARD, G E. 1997b. The 60-kDa phosphotyrosine protein in insulin-treated adipocytes is a new member of the insulin receptor substrate family. *Journal of biological chemistry*, **272**(17), 11439–11443.

LEIBOWITZ, S F, HAMMER, N J, & CHANG, K. 1981. Hypothalamic paraventricular nucleus lesions produce overeating and obesity in the rat. *Physiol behav*, **27**(6), 1031–1040.

LEINNINGER, GINA M, OPLAND, DARREN M, JO, YOUNG-HWAN, FAOUZI, MIRO, CHRISTENSEN, LYNDSAY, CAPPELLUCCI, LAURA A, RHODES, CHRISTOPHER J, GNEGY, MARGARET E, BECKER, JILL B, POTHOS, EMMANUEL N, SEASHOLTZ, AUDREY F, THOMPSON, ROBERT C, & MYERS, MARTIN G. 2011. Leptin action via neurotensin neurons controls orexin, the mesolimbic dopamine system and energy balance. *Cell metabolism*, **14**(3), 313–323.

LEVIN, BARRY E, ROUTH, VANESSA H, KANG, LING, SANDERS, NICOLE M, & DUNN-MEYNELL, AMBROSE A. 2004. Neuronal glucosensing: what do we know after 50 years? *Diabetes*, **53**(10), 2521–2528.

LI, GANG, MOBBS, CHARLES V, & SCARPACE, PHILIP J. 2003. Central pro-opiomelanocortin gene delivery results in hypophagia, reduced visceral adiposity, and improved insulin sensitivity in genetically obese Zucker rats. *Diabetes*, **52**(8), 1951–1957.

LIAO, GUEY-YING, AN, JUAN JI, GHARAMI, KUSUMIKA, WATERHOUSE, EMILY G, VANEVSKI, FILIP, JONES, KEVIN R, & XU, BAOJI. 2012. Dendritically targeted Bdnf mRNA is essential for energy balance and response to leptin. *Nature medicine*, **18**(4), 564–571.

LIN, K, DORMAN, J B, RODAN, A, & KENYON, C. 1997. daf-16: An HNF-3/forkhead family member that can function to double the life-span of Caenorhabditis elegans. *Science (new york, ny)*, **278**(5341), 1319–1322.

LIU, Z-J, BIAN, J, ZHAO, Y-L, ZHANG, X, ZOU, N, & LI, D. 2011. Lentiviral vector-mediated knockdown of SOCS3 in the hypothalamus protects against the development of diet-induced obesity in rats. *Diabetes, obesity and metabolism*, **13**(10), 885–892.

LOUIS, GWENDOLYN W, LEINNINGER, GINA M, RHODES, CHRISTOPHER J, & MYERS, MARTIN G. 2010. Direct innervation and modulation of orexin neurons by lateral hypothalamic LepRb neurons. *Journal of neuroscience*, **30**(34), 11278–11287.

LU, XIN-YUN, BARSH, GREGORY S, AKIL, HUDA, & WATSON, STANLEY J. 2003. Interaction between alpha-melanocyte-stimulating hormone and corticotropin-releasing hormone in the regulation of feeding and hypothalamo-pituitary-adrenal responses. *Journal of neuroscience*, **23**(21), 7863–7872.

LUQUET, S, PEREZ, F A, HNASKO, T S, & PALMITER, R D. 2005. NPY/AgRP neurons are essential for feeding in adult mice but can be ablated in neonates. *Science (new york, ny)*, **310**(5748), 683–685.

LÜTTICKEN, C, WEGENKA, U M, YUAN, J, BUSCHMANN, J, SCHINDLER, C, ZIEMIECKI, A, HARPUR, A G, WILKS, A F, YASUKAWA, K, & TAGA, T. 1994. Association of transcription factor APRF and protein kinase Jak1 with the interleukin-6 signal transducer gp130. *Science (new york, ny)*, **263**(5143), 89–92.

MAEHAMA, T, & DIXON, J E. 1998. The tumor suppressor, PTEN/MMAC1, dephosphorylates the lipid second messenger, phosphatidylinositol 3,4,5-trisphosphate. *J biol chem*, **273**(22), 13375–13378.

MAFFEI, M, HALAAS, J, RAVUSSIN, E, PRATLEY, R E, LEE, G H, ZHANG, Y, FEI, H, KIM, S, LALLONE, R, & RANGANATHAN, S. 1995. Leptin levels in human and rodent: measurement of plasma leptin and ob RNA in obese and weight-reduced subjects. *Nature medicine*, **1**(11), 1155–1161.

MAJDIC, G, YOUNG, M, GOMEZ-SANCHEZ, E, ANDERSON, P, SZCZEPANIAK, LS, DOBBINS, RL, MCGARRY, JD, & PARKER, KL. 2002. Knockout mice lacking steroidogenic factor 1 are a novel genetic model of hypothalamic obesity. *Endocrinology*, **143**(2), 607.

MARGETIC, S, GAZZOLA, C, PEGG, G G, & HILL, R A. 2002. Leptin: a review of its peripheral actions and interactions. *International journal of obesity and related metabolic disorders : journal of the international association for the study of obesity*, **26**(11), 1407–1433.

MARSHALL, N B, & MAYER, J. 1956. Specificity of gold thioglucose for ventromedial hypothalamic lesions and hyperphagia. *Nature*, **178**(4547), 1399–1400.

MARTIN, B C, WARRAM, J H, KROLEWSKI, A S, BERGMAN, R N, SOELDNER, J S, & KAHN, C R. 1992. Role of glucose and insulin resistance in development of type 2 diabetes mellitus: results of a 25-year follow-up study. *Lancet*, **340**(8825), 925–929.

MASSAGLIA, A, PENNISI, F, ROSA, U, RONCA-TESTONI, S, & ROSSI, C A. 1968. The effect of chemical modifications induced in insulin on the reactivity of the interchain disulphide bonds towards sodium sulphite. *Biochemical journal*, **108**(2), 247–255.

MASUZAKI, H, OGAWA, Y, SAGAWA, N, HOSODA, K, MATSUMOTO, T, MISE, H, NISHIMURA, H, YOSHIMASA, Y, TANAKA, I, MORI, T, & NAKAO, K. 1997. Nonadipose tissue production of leptin: leptin as a novel placenta-derived hormone in humans. *Nature medicine*, **3**(9), 1029–1033.

MAYER, CHRISTOPHER M, & BELSHAM, DENISE D. 2010. Palmitate attenuates insulin signaling and induces endoplasmic reticulum stress and apoptosis in hypothalamic neurons: rescue of resistance and apoptosis through adenosine 5′ monophosphate-activated protein kinase activation. *Endocrinology*, **151**(2), 576–585.

MCCRIMMON, RORY J, FAN, XIAONING, CHENG, HAIYING, MCNAY, EWAN, CHAN, OWEN, SHAW, MARGARET, DING, YUYAN, ZHU, WANLING, & SHERWIN, ROBERT S. 2006. Activation of AMP-activated protein kinase within the ventromedial hypothalamus amplifies counterregulatory hormone responses in rats with defective counterregulation. *Diabetes*, **55**(6), 1755–1760.

MCMINN, J E, WILKINSON, C W, HAVEL, P J, WOODS, S C, & SCHWARTZ, M W. 2000. Effect of intracerebroventricular alpha-MSH on food intake, adiposity, c-Fos induction, and neuropeptide expression. *American journal of physiology- regulatory, integrative and comparative physiology*, **279**(2), R695–703.

MERCER, J G, HOGGARD, N, WILLIAMS, L M, LAWRENCE, C B, HANNAH, L T, MORGAN, P J, & TRAYHURN, P. 1996a. Coexpression of leptin receptor and preproneuropeptide Y mRNA in arcuate nucleus of mouse hypothalamus. *Journal of neuroendocrinology*, **8**(10), 733–735.

MERCER, J G, HOGGARD, N, WILLIAMS, L M, LAWRENCE, C B, HANNAH, L T, & TRAYHURN, P. 1996b. Localization of leptin receptor mRNA and the long form splice variant (Ob-Rb) in mouse hypothalamus and adjacent brain regions by in situ hybridization. *Febs letters*, **387**(2-3), 113–116.

MESAROS, A, KORALOV, SB, ROTHER, E, WUNDERLICH, FT, ERNST, MB, BARSH, GS, RAJEWSKY, K, & BRÜNING, JC. 2008. Activation of Stat3 signaling in AgRP neurons promotes locomotor activity. *Cell metabolism*, **7**(3), 236–248.

METLAKUNTA, ANANTHA S, SAHU, MAITRAYEE, YASUKAWA, HIDEO, DHILLON, SANDEEP S, BELSHAM, DENISE D, YOSHIMURA, AKIHIKO, & SAHU, ABHIRAM. 2011. Neuronal suppressor of cytokine signaling-3 deficiency enhances hypothalamic leptin-dependent phosphatidylinositol 3-kinase signaling. *Ajp: Regulatory, integrative and comparative physiology*, **300**(5), R1185–93.

MICHAEL, M D, KULKARNI, R N, POSTIC, C, PREVIS, S F, SHULMAN, G I, MAGNUSON, M A, & KAHN, C R. 2000. Loss of insulin signaling in hepatocytes leads to severe insulin resistance and progressive hepatic dysfunction. *Molecular cell*, **6**(1), 87–97.

MIKI, T, LISS, B, MINAMI, K, SHIUCHI, T, SARAYA, A, KASHIMA, Y, HORIUCHI, M, ASHCROFT, F, MINOKOSHI, Y, ROEPER, J, & SEINO, S. 2001. ATP-sensitive K+ channels in the hypothalamus are essential for the maintenance of glucose homeostasis. *Nature neuroscience*, **4**(5), 507–512.

MILLINGTON, G W M. 2006. Proopiomelanocortin (POMC): the cutaneous roles of its melanocortin products and receptors. *Clinical and experimental dermatology*, **31**(3), 407–412.

MIRALPEIX, M, SUN, X J, BACKER, J M, MYERS, M G, ARAKI, E, & WHITE, M F. 1992. Insulin stimulates tyrosine phosphorylation of multiple high molecular weight substrates in Fao hepatoma cells. *Biochemistry*, **31**(37), 9031–9039.

MIZUNO, T M, & MOBBS, C V. 1999. Hypothalamic agouti-related protein messenger ribonucleic acid is inhibited by leptin and stimulated by fasting. *Endocrinology*, **140**(2), 814–817.

MIZUNO, T M, KLEOPOULOS, S P, BERGEN, H T, ROBERTS, J L, PRIEST, C A, & MOBBS, C V. 1998. Hypothalamic pro-opiomelanocortin mRNA is reduced by fasting and [corrected] in ob/ob and db/db mice, but is stimulated by leptin. *Diabetes*, **47**(2), 294–297.

MOKDAD, ALI H, FORD, EARL S, BOWMAN, BARBARA A, DIETZ, WILLIAM H, VINICOR, FRANK, BALES, VIRGINIA S, & MARKS, JAMES S. 2003. Prevalence of obesity, diabetes, and obesity-related health risk factors, 2001. *Jama : the journal of the american medical association*, **289**(1), 76–79.

MOLLER, D E, YOKOTA, A, CARO, J F, & FLIER, J S. 1989. Tissue-specific expression of two alternatively spliced insulin receptor mRNAs in man. *Molecular endocrinology (baltimore, md.)*, **3**(8), 1263–1269.

MORI, HIROYUKI, HANADA, REIKO, HANADA, TOSHIKATSU, AKI, DAISUKE, MASHIMA, RYUICHI, NISHINAKAMURA, HITOMI, TORISU, TAKEHIRO, CHIEN, KENNETH R, YASUKAWA, HIDEO, & YOSHIMURA, AKIHIKO. 2004. Socs3 deficiency in the brain elevates leptin sensitivity and confers resistance to diet-induced obesity. *Nature medicine*, **10**(7), 739–743.

MOUNIEN, LOURDES, MARTY, NELL, TARUSSIO, DAVID, METREF, SALIMA, GENOUX, DAVID, PREITNER, FREDERIC, FORETZ, MARC, & THORENS, BERNARD. 2010. Glut2-dependent glucose-sensing controls thermoregulation by enhancing the leptin sensitivity of NPY and POMC neurons. *Faseb journal : official publication of the federation of american societies for experimental biology*, **24**(6), 1747–1758.

MUNZBERG, H, FLIER, JS, & BJORBAEK, C. 2004. Region-specific leptin resistance within the hypothalamus of diet-induced obese mice. *Endocrinology*, **145**(11), 4880.

MURPHY, BETH ANN, FAKIRA, KURT A, SONG, ZHENTAO, BEUVE, ANNIE, & ROUTH, VANESSA H. 2009. AMP-activated protein kinase and nitric oxide regulate the glucose sensitivity of ventromedial hypothalamic glucose-inhibited neurons. *American journal of physiology. cell physiology*, **297**(3), C750–8.

MYERS, M G, BACKER, J M, SUN, X J, SHOELSON, S, HU, P, SCHLESSINGER, J, YOAKIM, M, SCHAFFHAUSEN, B, & WHITE, M F. 1992. IRS-1 activates phosphatidylinositol 3'-kinase by associating with src homology 2 domains of p85. *Proceedings of the national academy of sciences of the united states of america*, **89**(21), 10350–10354.

MYERS, M G, SUN, X J, CHEATHAM, B, JACHNA, B R, GLASHEEN, E M, BACKER, J M, & WHITE, M F. 1993. IRS-1 is a common element in insulin and insulin-like growth factor-I signaling to the phosphatidylinositol 3'-kinase. *Endocrinology*, **132**(4), 1421–1430.

MYERS, M G, GRAMMER, T C, WANG, L M, SUN, X J, PIERCE, J H, BLENIS, J, & WHITE, M F. 1994a. Insulin receptor substrate-1 mediates phosphatidylinositol 3'-kinase and p70S6k signaling during insulin, insulin-like growth factor-1, and interleukin-4 stimulation. *Journal of biological chemistry*, **269**(46), 28783–28789.

MYERS, M G, WANG, L M, SUN, X J, ZHANG, Y, YENUSH, L, SCHLESSINGER, J, PIERCE, J H, & WHITE, M F. 1994b. Role of IRS-1-GRB-2 complexes in insulin signaling. *Mol cell biol*, **14**(6), 3577–3587.

NAKA, T, NARAZAKI, M, HIRATA, M, MATSUMOTO, T, MINAMOTO, S, AONO, A, NISHIMOTO, N, KAJITA, T, TAGA, T, YOSHIZAKI, K, AKIRA, S, & KISHIMOTO, T. 1997. Structure and function of a new STAT-induced STAT inhibitor. *Nature*, **387**(6636), 924–929.

NAKAZATO, M, MURAKAMI, N, DATE, Y, KOJIMA, M, MATSUO, H, KANGAWA, K, & MATSUKURA, S. 2001. A role for ghrelin in the central regulation of feeding. *Nature*, **409**(6817), 194–198.

NOVAK, A, GUO, C, YANG, W, NAGY, A, & LOBE, CG. 2000. Z/EG, a double reporter mouse line that expresses enhanced green fluorescent protein upon Cre-mediated excision. *Genesis (new york, ny : 2000)*, **28**(3-4), 147–155.

OBICI, S, ZHANG, B B, KARKANIAS, G, & ROSSETTI, L. 2002a. Hypothalamic insulin signaling is required for inhibition of glucose production. *Nat med*, **8**(12), 1376–1382.

OBICI, SILVANA, FENG, ZHAOHUI, KARKANIAS, GEORGE, BASKIN, DENIS G, & ROSSETTI, LUCIANO. 2002b. Decreasing hypothalamic insulin receptors causes hyperphagia and insulin resistance in rats. *Nature neuroscience*, **5**(6), 566–572.

OGG, S, PARADIS, S, GOTTLIEB, S, PATTERSON, G I, LEE, L, TISSENBAUM, H A, & RUVKUN, G. 1997. The Fork head transcription factor DAF-16 transduces insulin-like metabolic and longevity signals in C. elegans. *Nature*, **389**(6654), 994–999.

OGIMOTO, KAYOKO, HARRIS, MARVIN K, & WISSE, BRENT E. 2006. MyD88 is a key mediator of anorexia, but not weight loss, induced by lipopolysaccharide and interleukin-1 beta. *Endocrinology*, **147**(9), 4445–4453.

OLLMANN, M M. 1997. Antagonism of Central Melanocortin Receptors in Vitro and in Vivo by Agouti-Related Protein. *Science (new york, ny)*, **278**(5335), 135–138.

OLNEY, J W, & SHARPE, L G. 1969. Brain lesions in an infant rhesus monkey treated with monsodium glutamate. *Science (new york, ny)*, **166**(3903), 386–388.

OOMURA, Y, & KITA, H. 1981. Insulin acting as a modulator of feeding through the hypothalamus. *Diabetologia*, **20 Suppl**(Mar.), 290–298.

OPSAHL, C A, & POWLEY, T L. 1974. Failure of vagotomy to reverse obesity in the genetically obese Zucker rat. *The american journal of physiology*, **226**(1), 34–38.

ORSKOV, C, RABENHØJ, L, WETTERGREN, A, KOFOD, H, & HOLST, J J. 1994. Tissue and plasma concentrations of amidated and glycine-extended glucagon-like peptide I in humans. *Diabetes*, **43**(4), 535–539.

OZCAN, LALE, ERGIN, AYSE SEDA, LU, ALLEN, CHUNG, JASON, SARKAR, SUMIT, NIE, DUYU, MYERS, MARTIN G, & OZCAN, UMUT. 2009. Endoplasmic reticulum stress plays a central role in development of leptin resistance. *Cell metabolism*, **9**(1), 35–51.

OZCAN, U, CAO, Q, YILMAZ, E, LEE, AH, IWAKOSHI, NN, OZDELEN, E, TUNCMAN, G, GORGUN, C, GLIMCHER, LH, & HOTAMISLIGIL, GS. 2004. Endoplasmic reticulum stress links obesity, insulin action, and type 2 diabetes. *Science's stke*, **306**(5695), 457.

PARKER, KL, RICE, DA, LALA, DS, IKEDA, Y, LUO, X, WONG, M, BAKKE, M, ZHAO, L, FRIGERI, C, & HANLEY, NA. 2002. Steroidogenic factor 1: an essential mediator of endocrine development. *Recent progress in hormone research*, **57**(1), 19.

PARSONS, J A, BRELJE, T C, & SORENSON, R L. 1992. Adaptation of islets of Langerhans to pregnancy: increased islet cell proliferation and insulin secretion correlates with the onset of placental lactogen secretion. *Endocrinology*, **130**(3), 1459–1466.

PAZ, K, HEMI, R, LEROITH, D, KARASIK, A, ELHANANY, E, KANETY, H, & ZICK, Y. 1997. A molecular basis for insulin resistance. Elevated serine/threonine phosphorylation of IRS-1 and IRS-2 inhibits their binding to the juxtamembrane region of the insulin receptor and impairs their ability to undergo insulin-induced tyrosine phosphorylation. *Journal of biological chemistry*, **272**(47), 29911–29918.

PINTO, SHIRLY, ROSEBERRY, AARON G, LIU, HONGYAN, DIANO, SABRINA, SHANABROUGH, MARYA, CAI, XIAOLI, FRIEDMAN, JEFFREY M, & HORVATH, TAMAS L. 2004. Rapid rewiring of arcuate nucleus feeding circuits by leptin. *Science (new york, ny)*, **304**(5667), 110–115.

PIPELEERS, D G. 1992. Heterogeneity in pancreatic beta-cell population. *Diabetes*, **41**(7), 777–781.

PLUM, LEONA, MA, XIAOSONG, HAMPEL, BRIGITTE, BALTHASAR, NINA, COPPARI, ROBERTO, MÜNZBERG, HEIKE, SHANABROUGH, MARYA, BURDAKOV, DENIS, ROTHER, EVA, JANOSCHEK, RUTH, ALBER, JENS, BELGARDT, BENGT F, KOCH, LINDA, SEIBLER, JOST, SCHWENK, FRIEDER, FEKETE, CSABA, SUZUKI, AKIRA, MAK, TAK W, KRONE, WILHELM, HORVATH, TAMAS L, ASHCROFT, FRANCES M, & BRÜNING, JENS C. 2006. Enhanced PIP3 signaling in POMC neurons causes KATP channel activation and leads to diet-sensitive obesity. *Journal of clinical investigation*, **116**(7), 1886–1901.

POCAI, A, LAM, T K, GUTIERREZ-JUAREZ, R, OBICI, S, SCHWARTZ, G J, BRYAN, J, AGUILAR-BRYAN, L, & ROSSETTI, L. 2005. Hypothalamic K(ATP) channels control hepatic glucose production. *Nature*, **434**(7036), 1026–1031.

POMERANCE, M, GAVARET, J M, BRETON, M, & PIERRE, M. 1995. Effects of growth factors on phosphatidylinositol-3 kinase in astroglial cells. *Journal of neuroscience research*, **40**(6), 737–746.

PORTE, D, & WOODS, S C. 1981. Regulation of food intake and body weight in insulin. *Diabetologia*, **20 Suppl**(Mar.), 274–280.

PUIGSERVER, P, RHEE, J, DONOVAN, J, WALKEY, C J, YOON, J C, ORIENTE, F, KITAMURA, Y, ALTOMONTE, J, DONG, H, ACCILI, D, & SPIEGELMAN, B M. 2003. Insulin-regulated hepatic gluconeogenesis through FOXO1-PGC-1alpha interaction. *Nature*, **423**(6939), 550–555.

PULLEN, N, DENNIS, P B, ANDJELKOVIC, M, DUFNER, A, KOZMA, S C, HEMMINGS, B A, & THOMAS, G. 1998. Phosphorylation and activation of p70s6k by PDK1. *Science (new york, ny)*, **279**(5351), 707–710.

QU, D, LUDWIG, D S, GAMMELTOFT, S, PIPER, M, PELLEYMOUNTER, M A, CULLEN, M J, MATHES, W F, PRZYPEK, R, KANAREK, R, & MARATOS-FLIER, E. 1996. A role for melanin-concentrating hormone in the central regulation of feeding behaviour. *Nature*, **380**(6571), 243–247.

RADIN, M S, SINHA, S, BHATT, B A, DEDOUSIS, N, & O'DOHERTY, R M. 2008. Inhibition or deletion of the lipopolysaccharide receptor Toll-like receptor-4 confers partial protection against lipid-induced insulin resistance in rodent skeletal muscle. *Diabetologia*, **51**(2), 336–346.

REAVEN, G M. 1995. Pathophysiology of insulin resistance in human disease. *Physiol rev*, **75**(3), 473–486.

REYNA, SARA M, GHOSH, SANGEETA, TANTIWONG, PUNTIP, MEKA, C S REDDY, EAGAN, PHYLLIS, JENKINSON, CHRISTOPHER P, CERSOSIMO, EUGENIO, DEFRONZO, RALPH A, COLETTA, DAWN K, SRIWIJITKAMOL, APIRADEE, & MUSI, NICOLAS. 2008. Elevated toll-like receptor 4 expression and signaling in muscle from insulin-resistant subjects. *Diabetes*, **57**(10), 2595–2602.

ROTH, JONATHAN D, ROLAND, BARBARA L, COLE, REBECCA L, TREVASKIS, JAMES L, WEYER, CHRISTIAN, KODA, JOY E, ANDERSON, CHRISTEN M, PARKES, DAVID G, & BARON, ALAIN D. 2008. Leptin responsiveness restored by amylin agonism in diet-induced obesity: evidence from nonclinical and clinical studies. *Proceedings of the national academy of sciences*, **105**(20), 7257–7262.

SABIO, GUADALUPE, DAS, MADHUMITA, MORA, ALFONSO, ZHANG, ZHIYOU, JUN, JOHN Y, KO, HWI JIN, BARRETT, TAMERA, KIM, JASON K, & DAVIS, ROGER J. 2008. A stress signaling pathway in adipose tissue regulates hepatic insulin resistance. *Science (new york, ny)*, **322**(5907), 1539–1543.

SABIO, GUADALUPE, CAVANAGH-KYROS, JULIE, KO, HWI JIN, JUNG, DAE YOUNG, GRAY, SUSAN, JUN, JOHN Y, BARRETT, TAMERA, MORA, ALFONSO, KIM, JASON K, & DAVIS, ROGER J. 2009. Prevention of steatosis by hepatic JNK1. *Cell metabolism*, **10**(6), 491–498.

SABIO, GUADALUPE, KENNEDY, NORMAN J, CAVANAGH-KYROS, JULIE, JUNG, DAE YOUNG, KO, HWI JIN, ONG, HELENA, BARRETT, TAMERA, KIM, JASON K, & DAVIS, ROGER J. 2010. Role of muscle c-Jun NH2-terminal kinase 1 in obesity-induced insulin resistance. *Molecular and cellular biology*, **30**(1), 106–115.

SADOVSKY, Y, CRAWFORD, PA, WOODSON, KG, POLISH, JA, CLEMENTS, MA, TOURTELLOTTE, LM, SIMBURGER, K, & MILBRANDT, J. 1995. Mice deficient in the orphan receptor steroidogenic factor 1 lack adrenal glands and gonads but express P450 side-chain-cleavage enzyme in the placenta and have normal embryonic serum levels of corticosteroids. *Proceedings of the national academy of sciences*, **92**(24), 10939.

SAHU, A, KALRA, S P, CROWLEY, W R, & KALRA, P S. 1988. Evidence That Npy-Containing Neurons in the Brain-Stem Project Into Selected Hypothalamic Nuclei - Implication in Feeding-Behavior. *Brain research*, **457**(2), 376–378.

SAKURAI, T, AMEMIYA, A, ISHII, M, MATSUZAKI, I, CHEMELLI, R M, TANAKA, H, WILLIAMS, S C, RICHARDSON, J A, KOZLOWSKI, G P, WILSON, S, ARCH, J R, BUCKINGHAM, R E, HAYNES, A C, CARR, S A, ANNAN, R S, MCNULTY, D E, LIU, W S, TERRETT, J A, ELSHOURBAGY, N A, BERGSMA, D J, & YANAGISAWA, M. 1998. Orexins and orexin receptors: a family of hypothalamic neuropeptides and G protein-coupled receptors that regulate feeding behavior. *Cell*, **92**(4), 573–585.

SAMBROOK, JOSEPH, & RUSSELL, DAVID WILLIAM. 2001. *Molecular Cloning*. A Laboratory Manual. CSHL Press.

SARKAR, SUMIT, LÉGRÁDI, GÁBOR, & LECHAN, RONALD M. 2002. Intracerebroventricular administration of alpha-melanocyte stimulating hormone increases phosphorylation of CREB in TRH- and CRH-producing neurons of the hypothalamic paraventricular nucleus. *Brain research*, **945**(1), 50–59.

SCHERER, THOMAS, O'HARE, JAMES, DIGGS-ANDREWS, KELLY, SCHWEIGER, MARTINA, CHENG, BOB, LINDTNER, CLAUDIA, ZIELINSKI, ELIZABETH, VEMPATI, PRASHANT, SU, KAI, DIGHE, SHVETA, MILSOM, THOMAS, PUCHOWICZ, MICHELLE, SCHEJA, LUDGER, ZECHNER, RUDOLF, FISHER, SIMON J, PREVIS, STEPHEN F, & BUETTNER, CHRISTOPH. 2011. Brain Insulin Controls Adipose Tissue Lipolysis and Lipogenesis. *Cell metabolism*, **13**(2), 183–194.

SCHWARTZ, M W, SEELEY, R J, WOODS, S C, WEIGLE, D S, CAMPFIELD, L A, BURN, P, & BASKIN, D G. 1997. Leptin increases hypothalamic pro-opiomelanocortin mRNA expression in the rostral arcuate nucleus. *Diabetes*, **46**(12), 2119–2123.

SCHWARTZ, M W, ERICKSON, J C, BASKIN, D G, & PALMITER, R D. 1998. Effect of fasting and leptin deficiency on hypothalamic neuropeptide Y gene transcription in vivo revealed by expression of a lacZ reporter gene. *Endocrinology*, **139**(5), 2629–2635.

SEIBLER, JOST, ZEVNIK, BRANKO, KÜTER-LUKS, BIRGIT, ANDREAS, SUSANNE, KERN, HEIDRUN, HENNEK, THOMAS, RODE, ANJA, HEIMANN, CORNELIA, FAUST, NICOLE,

KAUSELMANN, GUNTHER, SCHOOR, MICHAEL, JAENISCH, RUDOLF, RAJEWSKY, KLAUS, KÜHN, RALF, & SCHWENK, FRIEDER. 2003. Rapid generation of inducible mouse mutants. *Nucleic acids research*, **31**(4), e12.

SEINO, S, & BELL, G I. 1989. Alternative splicing of human insulin receptor messenger RNA. *Biochem biophys res commun*, **159**(1), 312–316.

SEMENKOVICH, C F. 2006. Insulin resistance and atherosclerosis. *J clin invest*, **116**(7), 1813–1822.

SEMENKOVICH, C F, WIMS, M, NOE, L, ETIENNE, J, & CHAN, L. 1989. Insulin regulation of lipoprotein lipase activity in 3T3-L1 adipocytes is mediated at posttranscriptional and posttranslational levels. *Journal of biological chemistry*, **264**(15), 9030–9038.

SEMPLE, ROBERT K, SAVAGE, DAVID B, COCHRAN, ELAINE K, GORDEN, PHILLIP, & O'RAHILLY, STEPHEN. 2011. Genetic syndromes of severe insulin resistance. *Endocrine reviews*, **32**(4), 498–514.

SHEPHERD, P R, & KAHN, B B. 1999. Glucose transporters and insulin action–implications for insulin resistance and diabetes mellitus. *The new england journal of medicine*, **341**(4), 248–257.

SHI, HANG, KOKOEVA, MAIA V, INOUYE, KAREN, TZAMELI, IPHIGENIA, YIN, HUALI, & FLIER, JEFFREY S. 2006. TLR4 links innate immunity and fatty acid-induced insulin resistance. *Journal of clinical investigation*, **116**(11), 3015–3025.

SHOELSON, S E, LEE, J, & YUAN, M. 2003. Inflammation and the IKK beta/I kappa B/NF-kappa B axis in obesity- and diet-induced insulin resistance. *International journal of obesity and related metabolic disorders : journal of the international association for the study of obesity*, **27 Suppl 3**(Dec.), S49–52.

SILVER, LEE M. 1995. *Mouse Genetics*. Concepts and Applications. Oxford University Press, USA.

SKOLNIK, E Y, MARGOLIS, B, MOHAMMADI, M, LOWENSTEIN, E, FISCHER, R, DREPPS, A, ULLRICH, A, & SCHLESSINGER, J. 1991. Cloning of PI3 kinase-associated p85 utilizing a novel method for expression/cloning of target proteins for receptor tyrosine kinases. *Cell*, **65**(1), 83–90.

SKOLNIK, E Y, BATZER, A, LI, N, LEE, C H, LOWENSTEIN, E, MOHAMMADI, M, MARGOLIS, B, & SCHLESSINGER, J. 1993. The function of GRB2 in linking the insulin receptor to Ras signaling pathways. *Science (new york, ny)*, **260**(5116), 1953–1955.

SKURK, THOMAS, ALBERTI-HUBER, CATHERINE, HERDER, CHRISTIAN, & HAUNER, HANS. 2007. Relationship between adipocyte size and adipokine expression and secretion. *Journal of clinical endocrinology & metabolism*, **92**(3), 1023–1033.

SONG, Z, LEVIN, B E, MCARDLE, J J, BAKHOS, N, & ROUTH, V H. 2001. Convergence of pre- and postsynaptic influences on glucosensing neurons in the ventromedial hypothalamic nucleus. *Diabetes*, **50**(12), 2673–2681.

STAHL, N, & YANCOPOULOS, G D. 1994. The tripartite CNTF receptor complex: activation and signaling involves components shared with other cytokines. *Journal of neurobiology*, **25**(11), 1454–1466.

STANLEY, B G, KYRKOULI, S E, LAMPERT, S, & LEIBOWITZ, S F. 1986. Neuropeptide-Y Chronically Injected Into the Hypothalamus - a Powerful Neurochemical Inducer of Hyperphagia and Obesity. *Peptides*, **7**(6), 1189–1192.

STEINER, D F, CUNNINGHAM, D, SPIGELMAN, L, & ATEN, B. 1967. Insulin biosynthesis: evidence for a precursor. *Science (new york, ny)*, **157**(3789), 697–700.

STERNSON, SM, SHEPHERD, GMG, & FRIEDMAN, JM. 2005. Topographic mapping of VMH,Üí arcuate nucleus microcircuits and their reorganization by fasting. *Nature neuroscience*, **8**(10), 1356–1363.

STEVENSON, J A F, WELT, L G, & ORLOFF, J. 1950. Abnormalities of water and electrolyte metabolism in rats with hypothalamic lesions. *The american journal of physiology*, **161**(1), 35–39.

STRICKER, E M, SWERDLOFF, A F, & ZIGMOND, M J. 1978. Intrahypothalamic injections of kainic acid produce feeding and drinking deficits in rats. *Brain research*, **158**(2), 470–473.

SUN, X J, ROTHENBERG, P, KAHN, C R, BACKER, J M, ARAKI, E, WILDEN, P A, CAHILL, D A, GOLDSTEIN, B J, & WHITE, M F. 1991. Structure of the insulin receptor substrate IRS-1 defines a unique signal transduction protein. *Nature*, **352**(6330), 73–77.

SUN, X J, WANG, L M, ZHANG, Y, YENUSH, L, MYERS, M G, GLASHEEN, E, LANE, W S, PIERCE, J H, & WHITE, M F. 1995. Role of IRS-2 in insulin and cytokine signalling. *Nature*, **377**(6545), 173–177.

SUZUKI, A, YAMAGUCHI, M T, OHTEKI, T, SASAKI, T, KAISHO, T, KIMURA, Y, YOSHIDA, R, WAKEHAM, A, HIGUCHI, T, FUKUMOTO, M, TSUBATA, T, OHASHI, P S, KOYASU, S, PENNINGER, J M, NAKANO, T, & MAK, T W. 2001. T cell-specific loss of Pten leads to defects in central and peripheral tolerance. *Immunity*, **14**(5), 523–534.

TANG-CHRISTENSEN, MADS, VRANG, NIELS, ORTMANN, SYLVIA, BIDLINGMAIER, MARTIN, HORVATH, TAMAS L, & TSCHÖP, MATTHIAS. 2004. Central administration of ghrelin and agouti-related protein (83-132) increases food intake and decreases spontaneous locomotor activity in rats. *Endocrinology*, **145**(10), 4645–4652.

TARTAGLIA, L A. 1997. The leptin receptor. *Journal of biological chemistry*, **272**(10), 6093–6096.

TARTAGLIA, L A, DEMBSKI, M, WENG, X, DENG, N, CULPEPPER, J, DEVOS, R, RICHARDS, G J, CAMPFIELD, L A, CLARK, F T, DEEDS, J, MUIR, C, SANKER, S, MORIARTY, A, MOORE, K J, SMUTKO, J S, MAYS, G G, WOOL, E A, MONROE, C A, & TEPPER, R I. 1995. Identification and expression cloning of a leptin receptor, OB-R. *Cell*, **83**(7), 1263–1271.

TATEMOTO, K, & MUTT, V. 1980. Isolation of two novel candidate hormones using a chemical method for finding naturally occurring polypeptides. *nature.com*.

TONG, Q, YE, CP, MCCRIMMON, RJ, DHILLON, H, CHOI, B, KRAMER, MD, YU, J, YANG, Z, CHRISTIANSEN, LM, & LEE, CE. 2007a. Synaptic glutamate release by ventromedial hypothalamic neurons is part of the neurocircuitry that prevents hypoglycemia. *Cell metabolism*, **5**(5), 383–393.

TONG, QINGCHUN, YE, CHIANPING, MCCRIMMON, RORY J, DHILLON, HARVEEN, CHOI, BRIAN, KRAMER, MELISSA D, YU, JIA, YANG, ZONGFANG, CHRISTIANSEN, LAURYN M, LEE, CHARLOTTE E, CHOI, CHEOL SOO, ZIGMAN, JEFFREY M, SHULMAN, GERALD I, SHERWIN, ROBERT S, ELMQUIST, JOEL K, & LOWELL, BRADFORD B. 2007b. Synaptic glutamate release by ventromedial hypothalamic neurons is part of the neurocircuitry that prevents hypoglycemia. *Cell metabolism*, **5**(5), 383–393.

TRAN, PHU V, AKANA, SUSAN F, MALKOVSKA, IRENA, DALLMAN, MARY F, PARADA, LUIS F, & INGRAHAM, HOLLY A. 2006. Diminished hypothalamicbdnfexpression and impaired VMH function are associated with reduced SF-1 gene dosage. *The journal of comparative neurology*, **498**(5), 637–648.

TSUKUMO, DANIELA M L, CARVALHO-FILHO, MARCO A, CARVALHEIRA, JOSÉ B C, PRADA, PATRICIA O, HIRABARA, SANDRO M, SCHENKA, ANDRÉ A, ARAUJO, ELIANA P, VASSALLO, JOSÉ, CURI, RUI, VELLOSO, LICIO A, & SAAD, MARIO J A. 2007. Loss-of-function mutation in Toll-like receptor 4 prevents diet-induced obesity and insulin resistance. *Diabetes*, **56**(8), 1986–1998.

ULLRICH, A, BELL, J R, CHEN, E Y, HERRERA, R, PETRUZZELLI, L M, DULL, T J, GRAY, A, COUSSENS, L, LIAO, Y C, & TSUBOKAWA, M. 1985. Human insulin receptor and its relationship to the tyrosine kinase family of oncogenes. *Nature*, **313**(6005), 756–761.

UNGER, THADDEUS J, CALDERON, GERMAN A, BRADLEY, LEILA C, SENA-ESTEVES, MIGUEL, & RIOS, MARIBEL. 2007. Selective deletion of Bdnf in the ventromedial and dorsomedial hypothalamus of adult mice results in hyperphagic behavior and obesity. *Journal of neuroscience*, **27**(52), 14265–14274.

UOTANI, S, BJORBAEK, C, TORNØE, J, & FLIER, J S. 1999. Functional properties of leptin receptor isoforms: internalization and degradation of leptin and ligand-induced receptor downregulation. *Diabetes*, **48**(2), 279–286.

VAISSE, C, CLEMENT, K, GUY-GRAND, B, & FROGUEL, P. 1998. A frameshift mutation in human MC4R is associated with a dominant form of obesity. *Nature genetics*, **20**(2), 113–114.

VAN DE WALL, E, LESHAN, R, XU, AW, BALTHASAR, N, COPPARI, R, LIU, SM, JO, YH, MACKENZIE, RG, ALLISON, DB, & DUN, NJ. 2008. Collective and individual functions of leptin receptor modulated neurons controlling metabolism and ingestion. *Endocrinology*, **149**(4), 1773.

VAN DE WALL, ESTHER, LESHAN, REBECCA, XU, ALLISON W, BALTHASAR, NINA, COPPARI, ROBERTO, LIU, SHUN MEI, JO, YOUNG HWAN, MACKENZIE, ROBERT G, ALLISON, DAVID B, DUN, NAE J, ELMQUIST, JOEL, LOWELL, BRADFORD B, BARSH, GREGORY S, DE LUCA, CARL, MYERS, MARTIN G, SCHWARTZ, GARY J, & CHUA, STREAMSON C. 2008. Collective and individual functions of leptin receptor modulated neurons controlling metabolism and ingestion. *Endocrinology*, **149**(4), 1773–1785.

VAN DIJK, G, THIELE, T E, DONAHEY, J C, CAMPFIELD, L A, SMITH, F J, BURN, P, BERNSTEIN, I L, WOODS, S C, & SEELEY, R J. 1996. Central infusions of leptin and GLP-1-(7-36) amide differentially stimulate c-FLI in the rat brain. *The american journal of physiology*, **271**(4 Pt 2), R1096–100.

VAN LEIDEN, H A, DEKKER, J M, MOLL, A C, NIJPELS, G, HEINE, R J, BOUTER, L M, STEHOUWER, C D, & POLAK, B C. 2002. Blood pressure, lipids, and obesity are associated with retinopathy: the hoorn study. *Diabetes care*, **25**(8), 1320–1325.

VELLOSO, LICIO A, ARAUJO, ELIANA P, & DE SOUZA, CLAUDIO T. 2008. Diet-induced inflammation of the hypothalamus in obesity. *Neuroimmunomodulation*, **15**(3), 189–193.

WADA, S, SASAKI, Y, HORIMOTO, M, ITO, T, ITO, Y, TANAKA, Y, TOYAMA, T, KASAHARA, A, HAYASHI, N, & HORI, M. 1998. Involvement of growth factor receptor-bound protein-2 in rat hepatocyte growth. *Journal of gastroenterology and hepatology*, **13**(6), 635–642.

WANG, CHUANFENG, BOMBERG, ERIC, BILLINGTON, CHARLES J, LEVINE, ALLEN S, & KOTZ, CATHERINE M. 2010. Brain-derived neurotrophic factor (BDNF) in the hypothalamic ventromedial nucleus increases energy expenditure. *Brain research*, **1336**(June), 66–77.

WANG, LIXIN, SAINT-PIERRE, DAVID H, & TACHÉ, YVETTE. 2002. Peripheral ghrelin selectively increases Fos expression in neuropeptide Y - synthesizing neurons in mouse hypothalamic arcuate nucleus. *Neuroscience letters*, **325**(1), 47–51.

WELLEN, KATHRYN E, & HOTAMISLIGIL, GOKHAN S. 2005. Inflammation, stress, and diabetes. *Journal of clinical investigation*, **115**(5), 1111–1119.

WHITE, D W, KUROPATWINSKI, K K, DEVOS, R, BAUMANN, H, & TARTAGLIA, L A. 1997. Leptin receptor (OB-R) signaling. Cytoplasmic domain mutational analysis and evidence for receptor homo-oligomerization. *Journal of biological chemistry*, **272**(7), 4065–4071.

WHITE, M F, SHOELSON, S E, KEUTMANN, H, & KAHN, C R. 1988. A cascade of tyrosine autophosphorylation in the beta-subunit activates the phosphotransferase of the insulin receptor. *Journal of biological chemistry*, **263**(6), 2969–2980.

WHITMAN, M, DOWNES, C P, KEELER, M, KELLER, T, & CANTLEY, L. 1988. Type I phosphatidylinositol kinase makes a novel inositol phospholipid, phosphatidylinositol-3-phosphate. *Nature*, **332**(6165), 644–646.

WHO. 2012. Fact sheet N°311. *Who media center*.

WIRTH, M M, OLSZEWSKI, P K, YU, C, LEVINE, A S, & GIRAUDO, S Q. 2001. Paraventricular hypothalamic alpha-melanocyte-stimulating hormone and MTII reduce feeding without causing aversive effects. *Peptides*, **22**(1), 129–134.

WOODS, A J, & STOCK, M J. 1996. Leptin activation in hypothalamus. *Nature*, **381**(6585), 745.

WOODS, S C, LOTTER, E C, MCKAY, L D, & PORTE, D. 1979. Chronic intracerebroventricular infusion of insulin reduces food intake and body weight of baboons. *Nature*, **282**(5738), 503–505.

XU, ALLISON W, STE-MARIE, LINDA, KAELIN, CHRISTOPHER B, & BARSH, GREGORY S. 2007. Inactivation of signal transducer and activator of transcription 3 in proopiomelanocortin (Pomc) neurons causes decreased pomc expression, mild obesity, and defects in compensatory refeeding. *Endocrinology*, **148**(1), 72–80.

XU, AW, KAELIN, CB, TAKEDA, K, AKIRA, S, SCHWARTZ, MW, & BARSH, GS. 2005. PI3K integrates the action of insulin and leptin on hypothalamic neurons. *Journal of clinical investigation*, **115**(4), 951–958.

XU, B, GOULDING, EH, ZANG, K, CEPOI, D, CONE, RD, JONES, KR, TECOTT, LH, & REICHARDT, LF. 2003. Brain-derived neurotrophic factor regulates energy balance downstream of melanocortin-4 receptor. *Nature neuroscience*, **6**(7), 736–742.

YE, JIANG HONG, ZHANG, JINGLI, XIAO, CHENG, & KONG, JIAN-QIANG. 2006. Patch-clamp studies in the CNS illustrate a simple new method for obtaining viable neurons in rat brain slices: glycerol replacement of NaCl protects CNS neurons. *Journal of neuroscience methods*, **158**(2), 251–259.

YEO, G S, FAROOQI, I S, AMINIAN, S, HALSALL, D J, STANHOPE, R G, & O'RAHILLY, S. 1998. A frameshift mutation in MC4R associated with dominantly inherited human obesity. *Nature genetics*, **20**(2), 111–112.

ZHANG, R, DHILLON, H, YIN, H, YOSHIMURA, A, LOWELL, B B, MARATOS-FLIER, E, & FLIER, J S. 2008a. Selective Inactivation of Socs3 in SF1 Neurons Improves Glucose Homeostasis without Affecting Body Weight. *Endocrinology*, **149**(11), 5654–5661.

ZHANG, XIAOQING, ZHANG, GUO, ZHANG, HAI, KARIN, MICHAEL, BAI, HUA, & CAI, DONGSHENG. 2008b. Hypothalamic IKKbeta/NF-kappaB and ER stress link overnutrition to energy imbalance and obesity. *Cell*, **135**(1), 61–73.

ZHANG, Y, PROENCA, R, MAFFEI, M, BARONE, M, LEOPOLD, L, & FRIEDMAN, J M. 1994. Positional cloning of the mouse obese gene and its human homologue. *Nature*, **372**(6505), 425–432.

Danksagung

An dieser Stelle möchte ich die Gelegenheit nutzen, mich bei allen zu bedanken, die mich währen der letzten Jahre auf so vielfältige Weise bei meiner Promotion unterstützt haben, im Besonderen gilt mein Dank:

- **Prof. Dr. Jens C Brüning** für seine Unterstützung während meiner Doktorarbeit und die Möglichkeit an interessanten und vielversprechenden Projekten zu arbeiten.
- **PD. Dr. F. Thomas Wunderlich** für einfach Alles.
- **Prof. Dr. Peter Kloppenburg** für eine tolle Kooperation und viele interessante Diskussionen über sämtliche Projekte
- **Dr. Bengt F. Belgardt** für die Zusammenarbeit und die Unterstützung während der gesamten Doktorarbeit.
- **Dr. A. Christine Könner** für die tolle Hilfe in theoretischen und praktischen Angelegenheiten.
- **Dr. Simon Hess** und **Dipl. Biol. Lars Paeger** für eine richtig gute Zusammenarbeit und tolle Ergebnisse.
- **Dr. Linda A.W. Verhagen** für *in situ* Färbungen und sonstige Hilfe.
- **Brigitte Hampel** für viele tolle Färbungen.
- **Dr. Diana M. Willmes** für Diskussionen, Gespräche und Rückhalt während der gesamten Zeit im Labor.
- **Dipl. Biol. Sabine Gruber** für Rückhalt, Unterstützung, Aufmunterung, Motivation und vieles mehr.
- **Martin E. Hess, M.Sc.**, **Jesse L. Denson, M.Sc.** und **Julia Goldau** für eine unglaubliche tolle Zeit im Labor.

Erklärung

Ich versichere, dass ich die von mir vorgelegte Dissertation selbständig angefertigt, die benutzten Quellen und Hilfsmittel vollständig angegeben und die Stellen der Arbeit - einschließlich Tabellen, Karten und Abbildungen -, die anderen Werken im Wortlaut oder dem Sinn nach entnommen sind, in jedem Einzelfall als Entlehnung kenntlich gemacht habe; dass diese Dissertation noch keiner anderen Fakultät oder Universität zur Prüfung vorgelegen hat; dass sie - abgesehen von unten angegebenen Teilpublikationen - noch nicht veröffentlicht worden ist sowie, dass ich eine solche Veröffentlichung vor Abschluss des Promotionsverfahrens nicht vornehmen werde.

Die Bestimmungen der Promotionsordnung sind mir bekannt. Die von mir vorgelegte Dissertation ist von Prof. Dr. Jens C. Brüning betreut worden.

Köln, den 12.10.2012

_____

(Tim Klöckener)

Teilpublikationen

Artikel

KLÖCKENER, T; HESS, S; BELGARDT, BF; PAEGER, L; VERHAGEN, LAW; HUSCH, A; SOHN, JW; HAMPEL, B; DHILLON, H; ZIGMAN, JM; LOWELL, BB; WILLIAMS, KW; ELMQUIST, JK; HORVATH, TL; KLOPPENBURG, P; BRÜNING, JC. 2011. High-fat feeding promotes obesity via insulin receptor / PI3K-dependent inhibition of SF-1 VMH neurons. *Nature neuroscience*, **14**(7), 911-918.

Curriculum Vitae

Dipl. Biol. Tim Klöckener

Universität zu Köln
Institut für Genetik
Zülpicher Straße 47a
50674 Köln
Tel.: +49 (0)221 470-1580
Email: Tim.Kloeckener@uni-koeln.de
Geburtsdatum/ -ort: 13.08.1983 in Olpe
Staatsangehörigkeit: deutsch

AUSBILDUNG

2007 – 2008 **Universität zu Köln, Institut für Genetik**
Diplomarbeit im Labor von Prof. Dr. Jens C. Brüning. Thema: „Die Rolle des Insulin-Signalweges im Ventromedialen Hypothalamus in der Energie-Homöostase".

2008 – 2012 **Universität zu Köln, Institut für Genetik**
Doktorarbeit im Labor von Prof. Dr. Jens C. Brüning. Thema: „Insulin regulates Energy Homeostasis and Hypoglycemia in the Ventromedial Hypothalamus".

BERUFLICHE TÄTIGKEITEN

2003 – 2007 **FH Köln, Institut für Tropentechnologie**
Studentische Hilfskraft

Köln, den 12. Oktober 2012 _____
(Tim Klöckener)